

Technische Universität München

Lehrstuhl für organische Chemie II

**DESIGN AND APPLICATION OF
NATURAL PRODUCT DERIVED PROBES FOR
ACTIVITY BASED PROTEIN PROFILING**

Oliver Alexander Battenberg

Vollständiger Abdruck der von der Fakultät für Chemie

der Technischen Universität München zur Erlangung des akademischen Grades eines

Doktors der Naturwissenschaften

genehmigten Dissertation.

Vorsitzender: Univ.-Prof. Dr. Johannes Buchner

Prüfer der Dissertation:

1. Univ.-Prof. Dr. Stephan A. Sieber
2. TUM Junior Fellow Dr. Sabine Schneider

Die Dissertation wurde am 6. Februar 2013 bei der Technischen Universität München eingereicht und durch die Fakultät für Chemie am 5. März 2013 angenommen.

Diese Arbeit wurde an den Fachbereichen Chemie
der Ludwig Maximilian Universität und der Technische Universität München unter Leitung von
Herrn Prof. Dr. Stephan A. Sieber
in der Zeit von Oktober 2009 bis Februar 2013 durchgeführt.

Danksagung

Herrn Prof. Dr. Stephan A. Sieber danke ich für die Aufnahme in seinen Arbeitskreis, die ansprechende und herausfordernde Themenstellung sowie die hervorragende Förderung dieser Arbeit.

Bei den Mitgliedern der Prüfungskommission bedanke ich mich für die Bemühungen bei der Bewertung dieser Arbeit.

An Frau Dr. Sabine Schneider richtet sich mein Dank für die Bereitschaft sich für die Erstellung des Zweitgutachtens zur Verfügung zu stellen.

Mona Wolf und Katja Bäuml danke ich für ihre Hilfsbereitschaft und ihr unermüdliches Engagement für einen organisierten Laboralltag.

Für die zahlreichen wissenschaftlichen und persönlichen Unterredungen sowie die hauptanteilige Übernahme der angefallenen Korrekturarbeiten gilt mein außerordentlicher Dank Dr. Matthew Nodwell, der durch seine stete, motivierende Hilfestellung einen wichtigen Beitrag zu dieser Arbeit geleistet hat.

Besonderer Dank richtet sich auch an meine Laborkollegen Dr. Maximilian Pitscheider, Tanja Wirth, Dr. Thomas Menzel, Georg Rudolf und Franziska Mandl für die hervorragende Unterstützung, das aufgeschlossene Entgegenkommen und die anregenden Gespräche.

Abschließend gilt mein größter Dank Daniela Falkner, meiner Familie und meinem Freundeskreis für die besondere Unterstützung während der gesamten Promotionszeit.

TABLE OF CONTENTS

| | | |
|---|---|----|
| A | INTRODUCTION | 1 |
| | Activity-based protein profiling (ABPP) | 2 |
| | Protein-reactive natural products | 8 |
| | Ring-strained scaffolds | 8 |
| | Michael acceptor systems | 10 |
| | Other reactive moieties | 11 |
| | Photocrosslinking | 12 |
| | Aryl azides | 14 |
| | Aryl-diazirine | 15 |
| | Benzophenones | 17 |
| | Summary | 18 |
| B | SCOPE OF THIS WORK | 20 |
| C | RESULTS AND DISCUSSION | 21 |
| | Evaluation of α -pyrones and pyrimidones as photo affinity probes for activity based protein profiling | 22 |
| | Abstract | 22 |
| | Introduction | 23 |
| | Results and Discussion | 27 |
| | Conclusion | 40 |
| | Experimental | 41 |
| | Synthesis of a benzophenone-alkyne tag for reversible inhibitor-target profiling | 53 |
| | Introduction | 53 |
| | Results and Discussion | 55 |

| | |
|--|-----|
| Conclusion | 59 |
| Experimental Section | 60 |
| Target profiling of 4-hydroxyderricin in <i>S. aureus</i> reveals seryl-tRNA synthetase binding and inhibition by covalent modification..... | 63 |
| Abstract | 63 |
| Introduction | 64 |
| Results and Discussion..... | 67 |
| Conclusion | 76 |
| Experimental | 77 |
| D SUMMARY..... | 84 |
| α -Pyrone and pyrimidones as photoaffinity probes..... | 85 |
| Synthesis of a benzophenone-alkyne tag for affinity based protein profiling | 86 |
| Target profiling of 4-hydroxyderricin in <i>S. aureus</i> | 87 |
| E ZUSAMMENFASSUNG | 89 |
| α -Pyrone und Pyrimidone als Photoaffinitätssonden..... | 90 |
| Synthese eines Benzophenon-Alkin-Tags für das affinity based protein profiling..... | 91 |
| Target-Identifizierung von 4-Hydroxyderricin in <i>S. aureus</i> | 92 |
| F APENDIX 1 | 94 |
| G APENDIX 2 | 99 |
| H BIBLIOGRAPHY | 111 |
| I PUBLICATIONS..... | 119 |
| J CURRICULUM VITAE | 120 |

A INTRODUCTION

Activity-based protein profiling (ABPP)

Natural products are a unique class of organic molecules with distinct biological activities. The increasing knowledge about the molecular mechanism of biological processes identified this group of compounds as an almost unlimited source of bioactive molecules with a high therapeutic potential. In contrast to synthetic compound libraries natural products have co-evolved with biological systems and therefore show a remarkable selectivity for the interaction with biological structures.^[1-2] Since about 47% of the drugs that were approved from 1981 to 2006 are derived from natural products^[3] additional screening programs might be a starting point to face the increasing demand for novel therapeutic strategies.^[4]

The investigation and understanding of the complex interactions of a natural product in a biological system are challenging but a number of valuable methods are available to unravel the mechanism of natural product-protein interactions.^[5] Since the active cellular processes in living organisms are dominated by protein functions the proteome analysis of all natural product caused cellular changes is an important approach^[1]. Progress in the application of mass spectrometry within the last decade has paved the way for activity-based protein profiling (ABPP) experiments by protein directed small molecule probes capable of covalent protein modification.^[6] The design and application of these usually natural product derived probes with an appropriate reporter group enables a comprehensive proteome analysis and provides useful information about protein targets in complex biological systems.^[7]

The concept of ABPP is based on the design of a reactive probe that covalently modifies protein targets and subsequently offers a suitable readout mechanism for the identification of labeled enzymes. A typical ABPP probe therefore combines at least three functionalities (Figure 1):

- 1.) A binding group for affinity mediated target binding. These structure motives are responsible for the selective non-covalent interactions with a complementary protein structures. Because natural products are fine-tuned for the interaction with proteins these compounds are an ideal source for a binding group.

2.) A reactive group for the covalent modification of the target. These reactive groups might be part of the binding groups' structure (for example intrinsic reactivity of protein-reactive natural products) or have to be introduced by the addition of electrophilic or photo-reactive chemotypes for the covalent target binding.^[7]

3.) A reporter group for visualization or purification protocols usually fluorescence dyes and biotin-tags.

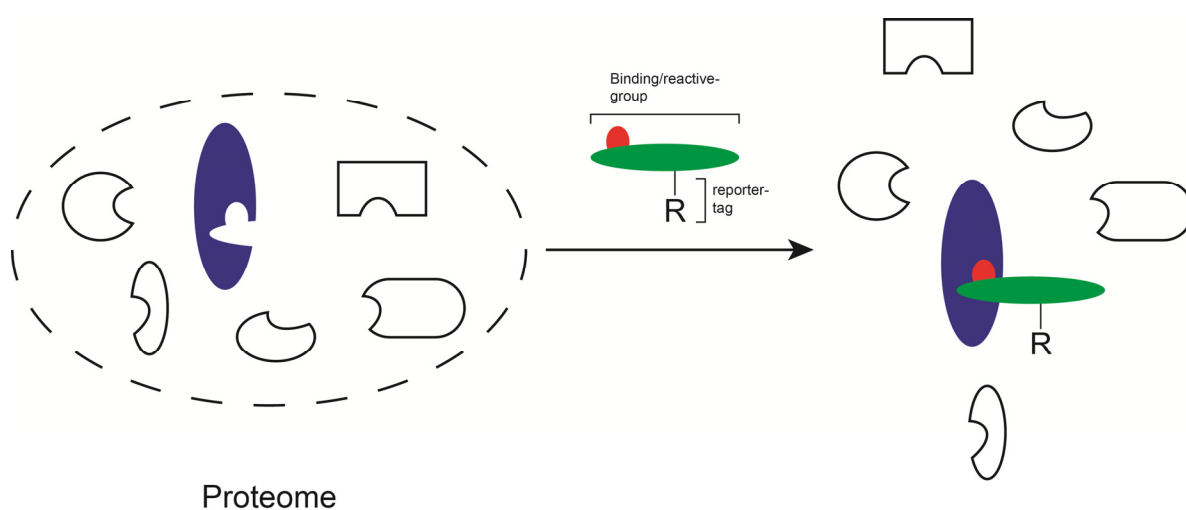
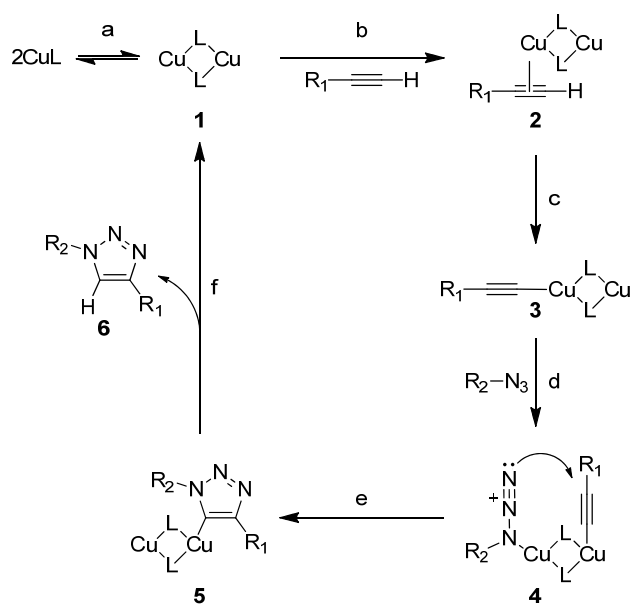


Figure 1. Schematic application and composition of an ABPP probe in covalent labeling of target-proteins.

A drawback of this approach is that the incorporation of these structure elements into the parent structure could change the natural products' biological profile as well as negatively affect the probes solubility and cell permeability. This is why an alternative strategy has been developed that avoids large tags in the natural product structure. A useful circumvention is the modification of bioactive molecules and reporter groups with click chemistry ligation handles. The Cu^{I} -catalyzed Huisgen [3+2] cycloaddition of azides and terminal alkynes forms 1,2,3-triazoles under physiological conditions. It is the most prominent example of a bioorthogonal ligation reaction and facilitates the probes connection with a tag after the initial labeling event (Scheme 1)^[8-10]



Scheme 1. Proposed mechanism for the copper catalyzed Huisgen [3+2] cycloaddition. (a) Formation of a Cu^{I} dimer. (b) π complexation of a Cu^{I} dimer to an terminal alkyne. (c) Deprotonation and formation of a Cu-acetylide complex. (d) Coordination and activation of an azide for nucleophilic attack at the alkyne. (e) Formation of the 1,2,3-triazole. (f) Release of the triazole product and reformation of the catalyst. ^[10-11]

Live cells or cell lysates are therefore incubated with a suitable alkyne-containing ABPP probe to covalently label the protein targets. The ligation reaction is then carried out by the addition of the complementary azide-tag e.g. a fluorescent dye, a Cu^{II} salt, a reducing agent such as sodium ascorbate or tris(2-carboxyethyl)phosphine (TCEP) for the *in situ* Cu-reduction and a suitable ligand such as tris-(5-benzyl-1H-triazol-4-yl)-methanamine (TBTA) to form the active Cu^{I} complex.^[11] Following the ligation reaction, separation of the proteins by SDS-PAGE and in-gel readout of the reporter-tag (fluorescence scanning) finally unravels probe modified proteins (Figure 2).^[12]

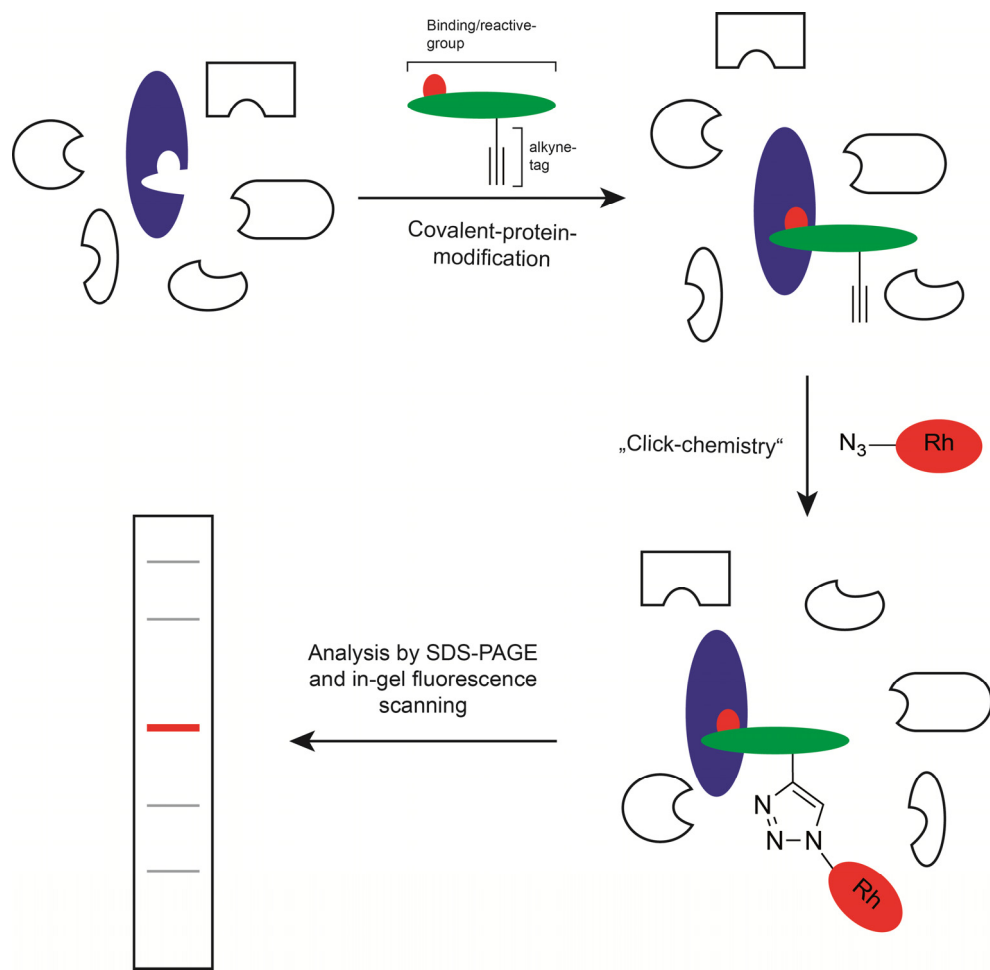


Figure 2. General workflow of a click chemistry based ABPP experiment (Rh: Rhodamine).

In order to identify the protein bands by a gel based approach the labeled proteins have to be selectively enriched for subsequent analysis to reduce the background of non-target proteins. An approach as outlined in Figure 3 is an avidin/biotin affinity purification protocol. Selective enzyme labeling by the protein reactive probe is followed by the click reaction with a tag that combines fluorescence readout and biotin enrichment capabilities for the visualization and purification. Affinity-enrichment on immobilized avidin yields potential protein targets that are subsequently separated by SDS-PAGE and analyzed by in-gel fluorescence scanning. Fluorescent bands are cut, tryptically digested and applied to LC-MS/MS analysis to unravel protein identities (Figure 3).

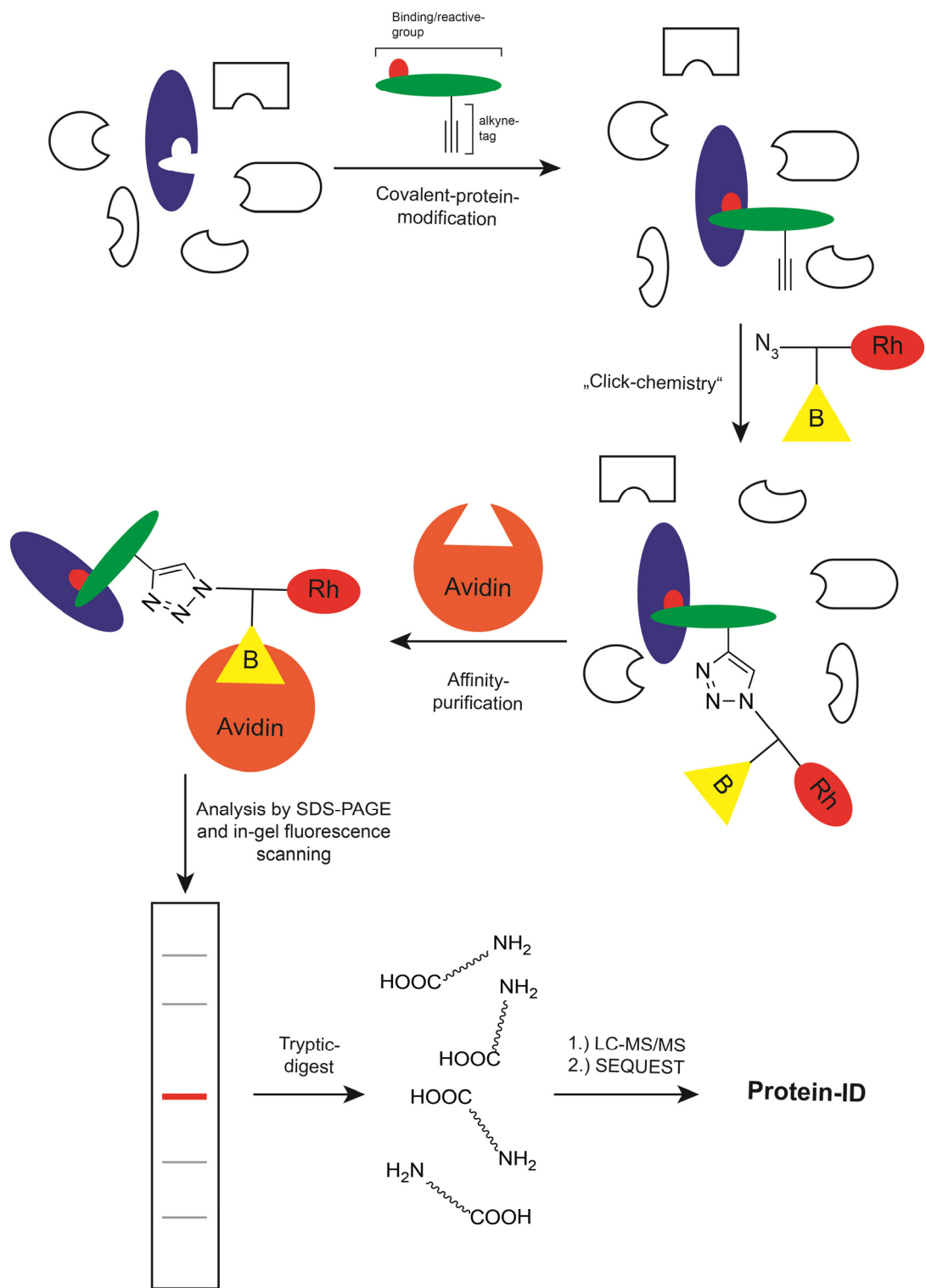


Figure 3. Identification of labeled proteins by avidin/biotin affinity purification and LC-MS/MS analysis (Rh: rhodamin, B: biotin).

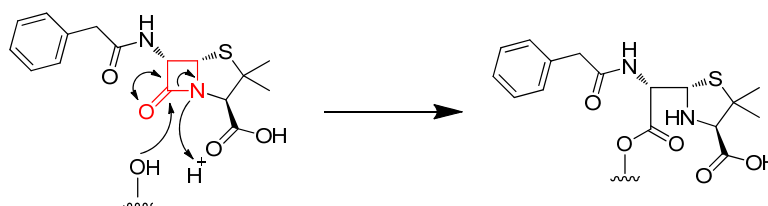
These gel based ABPP-platforms feature fast, simple and simultaneous analysis of different natural product proteome labeling experiments with an easy comparison of the obtained results. Although low resolution limits the universal application of this technique compared to gel-free methods ^[13-14] it is still is a very useful and frequently used analytical platform for protein target identification and therefore was exclusively applied in this work.

Protein-reactive natural products

Electrophilic natural products with a covalent target-binding mechanism are ideal compounds for mode of action studies by ABPP. The general reaction mechanism of these compounds is based on a covalent attack of nucleophilic protein-residues (e.g. lysine-, threonine-, serine- or cysteine-side-chains) on an electrophilic natural product center. This common electrophilicity facilitates the arrangement in subgroups due to similar chemical reactive moieties.^[2, 12, 15]

Ring-strained scaffolds

Because of its historical significance and its importance in antibacterial therapies the β -lactams probably are the most famous electrophilic natural products. The most prominent example are penicillins originally discovered by Alexander Fleming. These compounds exert their biological effects via covalent binding of enzymes involved in bacterial cell wall biosynthesis. A nucleophilic attack of an activated serine residue at the β -lactam functional group causes an irreversible enzyme inhibition (Scheme 2).^[16-17] The activities of these by definition called penicillin-binding proteins are essential for the cell-wall biosynthesis and therefore one of the most important antibacterial protein targets.^[18]



Scheme 2. Nucleophilic attack at the β -lactam core of penicillin G.

In addition to β -lactams β -lactones, aziridines and epoxides are important electrophilic centers whose reactivity is caused by ring strain. Attacks of suitable nucleophiles at natural products containing these reactive moieties are often the basis for the biological activity of these compounds.^[2, 15] A selection of representative molecules is shown in Figure 4.

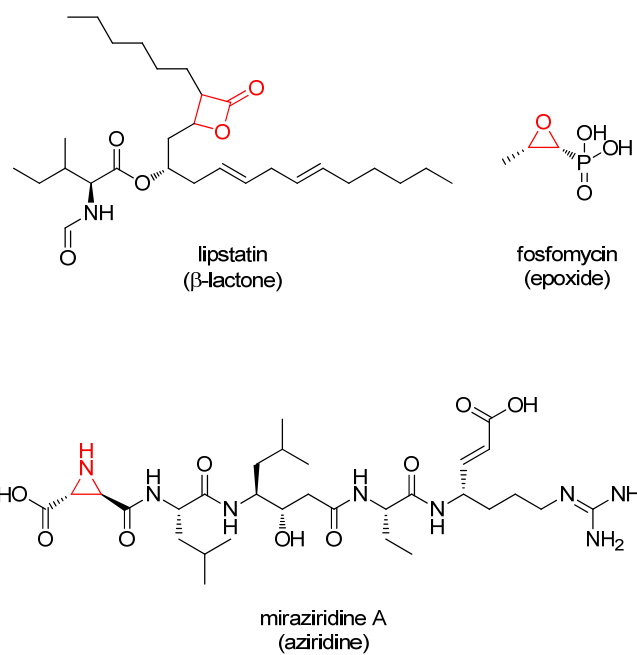
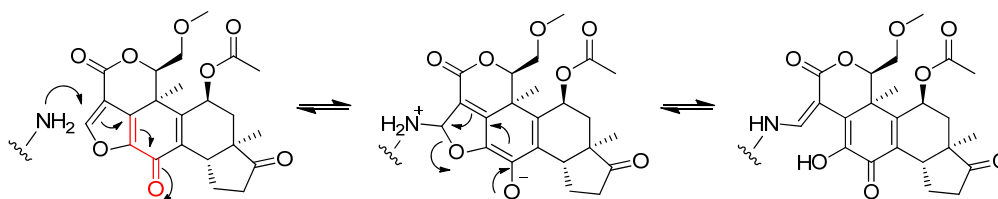


Figure 4. Selective representative natural products with ring strained reactive moieties.

Michael acceptor systems

Michael acceptor scaffolds are next to ring strained systems another important subgroup of electrophilic natural products. A variety of different α,β unsaturated systems induce their interesting bioactivities by a molecular mechanism based on the attack of nucleophilic amino acid side chains on the Michael acceptor scaffold.

A prominent example is the metabolite wortmannin isolated from the fungus *Penicillium wortmannii*. The antifungal and mainly antiproliferative activity of this natural product is based on a covalent modification of the lipid kinase phosphatidylinositol 3-kinase (PI3K). A nucleophilic PI3K-lysine attacks the furan of wortmannin and causes an irreversible inhibition of this important anti-cancer target (Scheme 3).^[12]



Scheme 3. Nucleophilic attack of Lys802 PI3-K at the Michael system of wortmannin.^[19]

Chalcones are another interesting group of Michael acceptor containing natural products. The chalcones have a general structure as shown in Figure 5. The substitution pattern of the two aromatic rings determines different bioactivities including anticancer, anti-inflammatory and antifungal activities. Particularly interesting are the antibacterial data for 4-hydroxyderricin (4HD, Figure7).^[20-21] Although no studies so far have investigated the molecular mechanisms for the antibacterial activity of this compound the reported reactivity of the 4-HD Michael system towards thiols is a strong indication for a covalent modification of its target structures.^[22-23] The proposed protein reactivity therefore makes this structure an ideal starting compound for the design of an APBB probe to unravel the antibacterial mode of action.

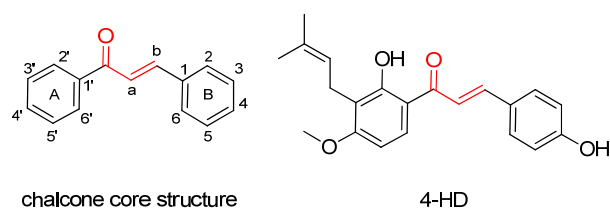


Figure 5. Structure and numbering of chalcone building blocks and 4-HD.

Other reactive moieties

Next to these two major groups of electrophilic natural products there is a variety of other electrophilic moieties for the covalent interaction with suitable biological nucleophiles. Carbamates, chlorodihydroisoxazoles, 4-hydroxycoumarins, isothiocyanates, disulfides and α -ketoamides are other interesting reactive scaffolds with reported protein reactivity as well as the diverse group of natural products with intracellular activation of the reactive electrophilic group. ^[15]

Photocrosslinking

ABPP using protein reactive probes is limited to investigate natural products that exert their biological effects via covalent inhibition. But many natural products exert their biological effect by reversible binding. The concept of proteome analysis by ABPP therefore needed to be expanded by the introduction of photo affinity labeling.^[24-25]

The design of a molecular photo-probe involves the addition of a photo-reactive group for the light induced covalent labeling of target structures (Figure 6). This concept is a very powerful approach to investigate the mechanism of natural products without intrinsic protein reactivity. Strictly speaking this approach has to be distinguished from activity based profiling by the introduction of the more general term of affinity based labeling but the transitions are fluid.^[26]

As shown in Figure 6 the general workflow of an ABPP experiment therefore consists of one additional step: After the incubation of the proteome with the photo reactive probe the covalent modification of the reversibly bound target is initiated by irradiation with light of a specific wavelength. This irradiation generates highly reactive species and causes the subsequent linkage between probe and target. This enables the further characterization of the labeled moieties as described above. In order to reliably and efficiently use photo crosslinking for target identification some important criteria have to be considered for the probe design.^[27-28]

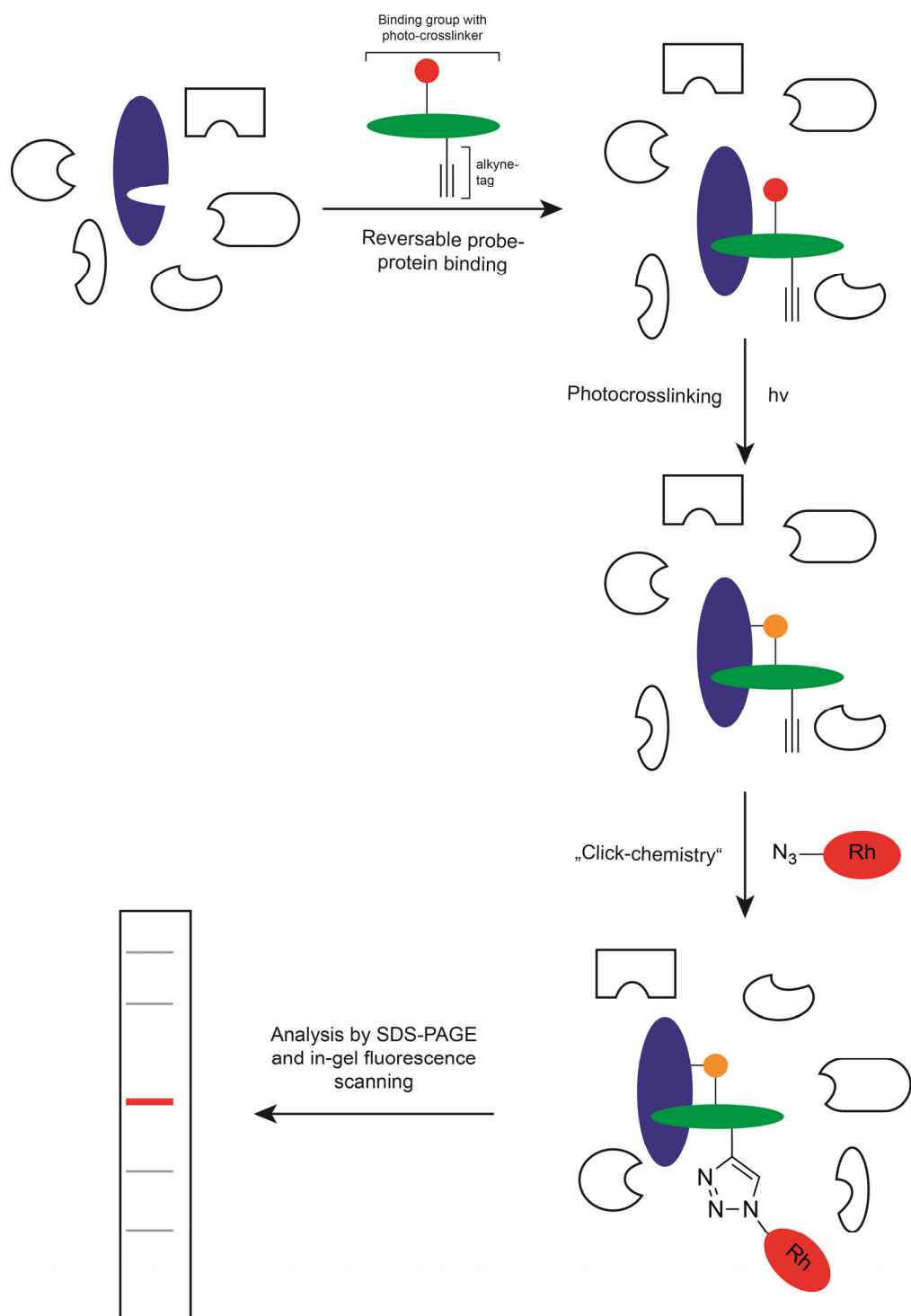


Figure 6. General workflow of a photo crosslinking experiment (Rh: Rhodamine).

1.) Sterically demanding crosslinking groups compared to the native structure have to be avoided. The modification of the native structure should minimize changes in the biological profile of the natural product.

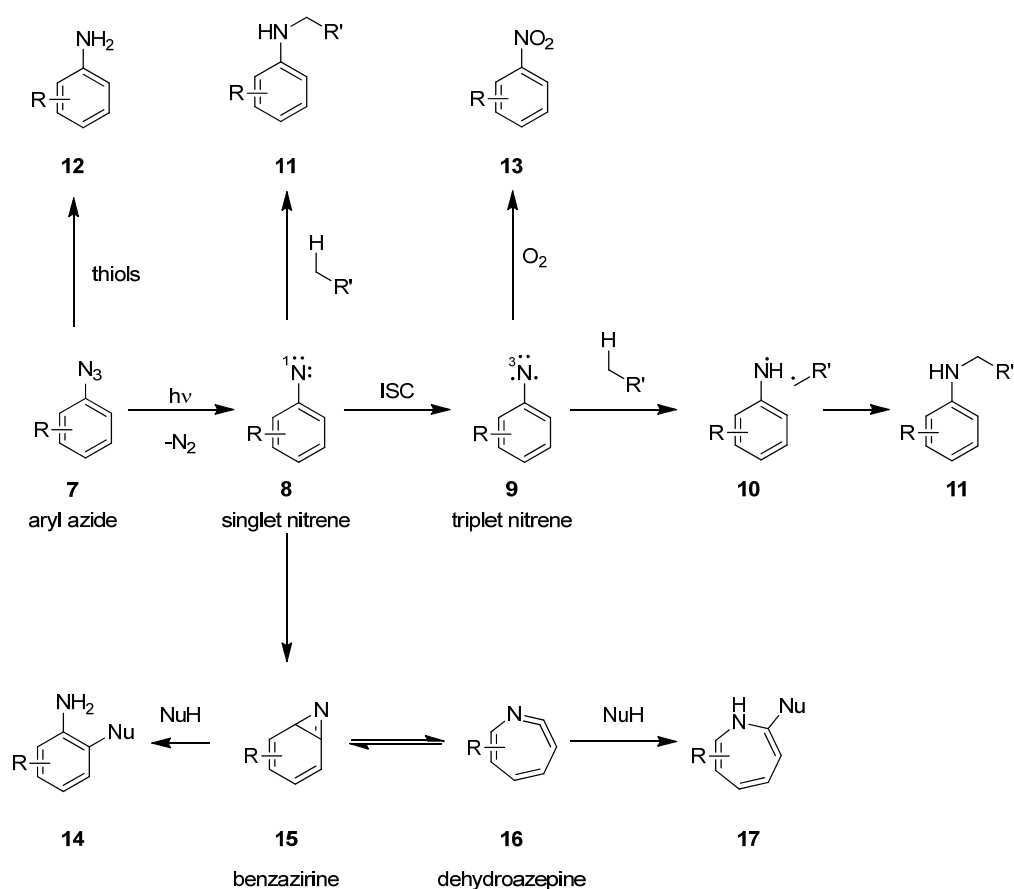
2.) The photo crosslinking moiety must not have light independent background reactivity and has to be stable in biological samples. Cross-reactivity before the actual irradiation step or the decomposition of the photo-probe either causes an increase in labeling of non-target structures or a reduction of the actual probe concentration.

3.) The moiety formed by the irradiation with a specific wavelength has to have a short lifetime and high reactivity. It is important that the activated species crosslinks to the target structure before the probe-target complex dissociates and undergoes a cross-linking reaction with non-target structures.

Due to these requirements in the design of a suitable photo-probe a manageable number of photo-reactive groups is available.^[29] These include aryl azides, diazirines and benzophenones.

Aryl azides^[24]

Although limited by a complex photochemistry aryl azides (**7**) are reactive small groups with an easy preparation and incorporation into natural biological compounds.^[30] Irradiation of aryl azides with UV light of 300 nm causes the elimination of molecular nitrogen and generates a highly reactive singlet nitrene **8** (Scheme 4).^[31-32] Direct insertion reactions with C-H bonds or deactivation by inter-system-crossing to form a triplet nitrene **9** followed by a radical based crosslinking with closely located C-H bonds is one mechanism for the photo induced reactivity of aryl azides to form crosslinks (**11**). The second mechanism of crosslinking is the rearrangement of singlet nitrenes into electrophilic benzazirines (**15**) and dehydroazepines (**16**) that themselves can react with suitable nucleophiles to form the covalent cross-links **14** and **17** respectively. Aerobic oxidations of the triplet nitrene **9** to the aromatic nitro-derivative **13**, reduction of the aryl azides by dithiols to the corresponding amine **12** as well as the deactivation of reactive intermediates by solvent (water) are all mechanisms that reduce the crosslinking efficiencies of this photoreactive group.^[33-34]

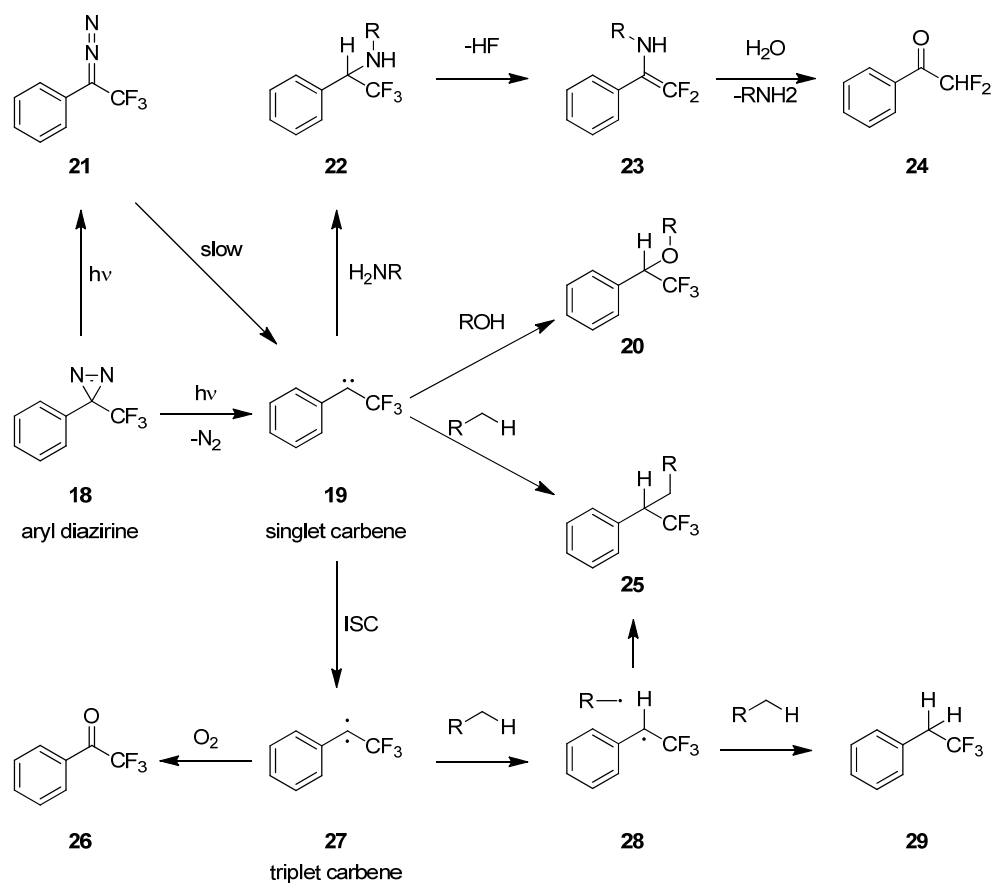


Scheme 4. Possible reaction mechanisms of the reactive intermediates formed after photolysis of aryl azides (7).^[24]

Aryl diazirine^[24]

An important advantage of aryl diazirines (**18**) compared to aryl azides is the chemical stability against acid and basic as well as oxidizing and reductive conditions.^[35] In addition the photo-reaction occurs at a wavelength of 350-380 nm. This is advantageous since irradiation with UV light above 300 nm usually does not damage protein structures. The mechanism for the photo-reactivity of diazirines is based on the elimination of molecular nitrogen to form a very reactive short-lived singlet carbene **19** (Scheme 5). This carbene can either react by insertion into O-H (\rightarrow **20**), C-H (\rightarrow **25**) and N-H (\rightarrow **22**) bonds or by the conversion into triplet carbenes (**27**) by inter system crossing. In accordance with triplet nitrenes, triplet carbenes tend to react on radical-based mechanism to form covalent cross-links (**25**). Oxidations of triplet carbenes by molecular

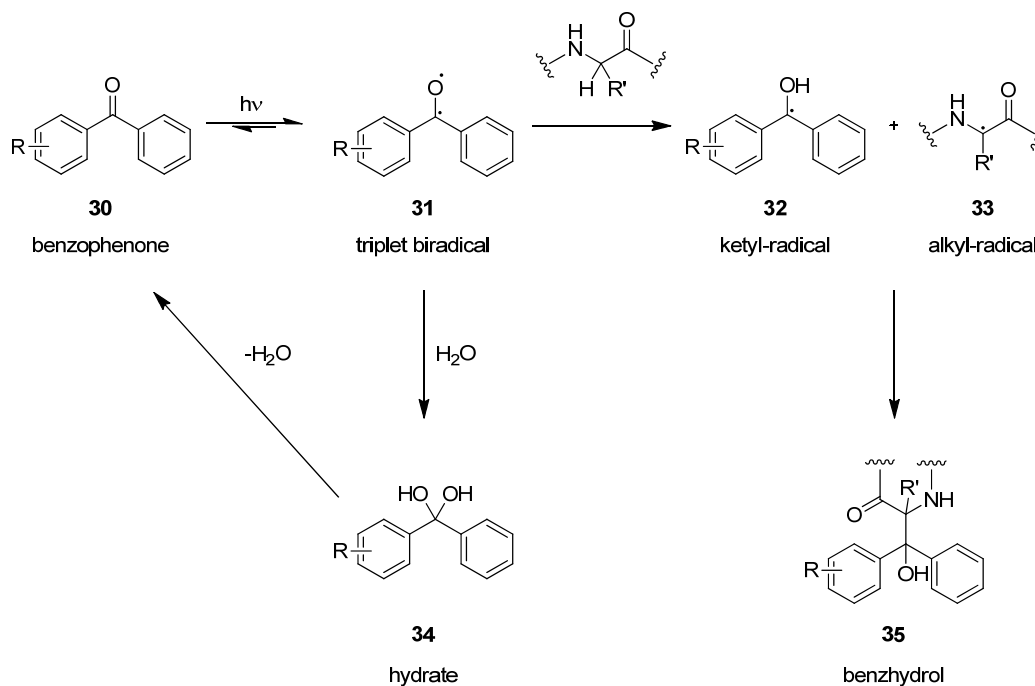
oxygen (\rightarrow **26**) and undesired radical recombination events (\rightarrow **29**) as well as the scavenging of singlet carbenes by water reduce photo-labeling efficacy. Additionally more than 30 % of the diazirines are transformed into a diazo species **21** upon irradiation with UV light. Although this diazo compound could eliminate to form the singlet carbene **19** as well, this reaction is slow. Unspecific labeling reaction by this species can be prevented by the introduction of a strong electron-withdrawing trifluoromethyl-group in close proximity to stabilize the diazo-isomer.^[36-37] Even with these limitations aryl diazirines are a very useful tool for the covalent labeling in target-identification-experiments.



Scheme 5. Possible reactions of the intermediates formed after photolysis of 3-aryl-3H-diazirines (**18**).^[24]

Benzophenones^[24]

UV light excitation of benzophenones (**30**) with wavelengths of 350-360 nm results in the reversible formation of a triplet benzhydryl biradical **31** for the cross-linking reaction with biological compounds.^[38] If no suitable reaction partner is trapped by the reactive moiety the excited state relaxes to its ground state within 120 μ s. As in the case of diazirines the UV light irradiation is limited to energies above 300 nm and therefore makes benzophenones suitable reactive groups for non-disruptive investigations of biological samples. Reaction partners are preferentially C-H bonds over O-H bonds.^[39] The first step is hydrogen abstraction that is especially favored for benzylic positions, amino acid α -positions, tertiary carbon centers and heteroatom-stabilized positions because of suitable stabilization of the generated carbon radical. The hydrogen abstraction causes the formation of a ketyl (**32**) and alkyl radical (**33**) that in the next reaction step combine quickly to form a stable cross-linked benzhydryl **35**. Although benzophenones are the most sterically demanding photo reactive groups that frequently interfere with the biological activities of the underlying natural product they do not suffer from as many undesirable side reactions as the other reported cross linkers. In contrast: The reaction of the triplet diradical with water forms the corresponding hydrate **34** that quickly eliminates to restore the initial ketone **30**. This mechanism reduces unspecific labeling events by unbound photo-probes and facilitates the crosslinking of affinity bound target structures.



Scheme 6. Chemistry of benzophenones after photolysis.^[24]

Summary

The design and application of natural product based photo-reactive probes is a very useful additional methodology to investigate target-structures in biological samples. Many examples confirm the ability of this approach to unravel reversible binding partners of interesting biological active small molecules and contributed to the understanding of mode of action. Nevertheless the selection of a suitable cross-linking moiety to address a specific biological question is not an uncomplicated procedure. The results of a carefully designed experiment are highly dependent from the selection of the crosslinking group. Every reactive group has its advantages and disadvantages that have to be considered and unfortunately there is no universally applicable guideline available for the right design of a suitable photo-reactive-probe.^[40-42]

A major drawback of all these systems for the photo induced irreversible labeling of target structures is the actual change of a natural products structure by the introduction of a photo-cross-linker. This change could be neglected for probes that arise from the modification of relatively big biomolecules compared to the crosslinking group. But especially in cases of

natural-products that are in the molecular range of the photo-reactive groups a suitable design of an adequate probe without changing the biological profile could be challenging or even impossible.

A promising approach to avoid additional chemical alterations is the use of intrinsic photo-reactivity. Although this method is limited to structures that already contain light inducible reactivity a number of natural products are composed of functional groups that are known to form reactive species upon irradiation with light. In the same way that intrinsic electrophilicity has to be confirmed for each protein reactive natural product the validation of intrinsic photo-inducible protein-reactivity is an even more challenging task. Light induced formation of derived reactive species has to be evaluated to proof the predicted covalent labeling of target structures for identification experiments.

B SCOPE OF THIS WORK

Mechanistic studies of the interaction of antibacterial natural products with their protein targets rely on the design of chemical probes. These probes are derived from the parent structure by the incorporation of tags for covalent labeling of target proteins. Identification and characterization of these targets contributes to the development of new antibacterial approaches to face the increasing emergence of resistant bacteria.

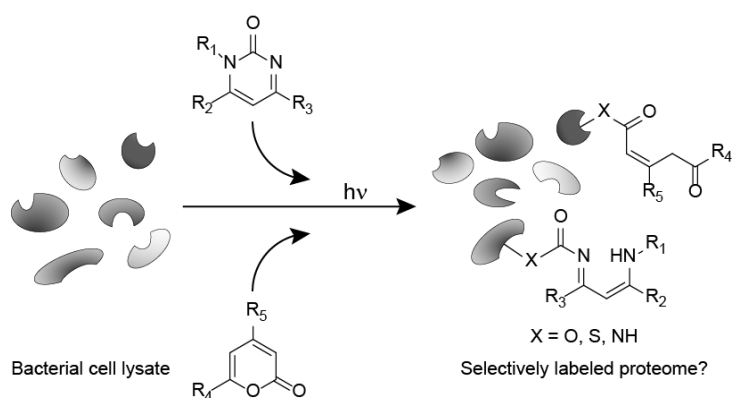
The scope of this work focuses on three new strategies for the covalent labeling and identification of natural product protein targets by activity based protein profiling:

1. Evaluation of the intrinsic photo-reactivity of α -pyrones and pyrimidones for use as photolabels.
2. Synthesis of a benzophenone-based tag that combines photo-crosslinking capabilities with an alkyne handle for the one step synthesis of probes derived from reversible inhibitors.
3. Design, synthesis and application of a 4-hydroxyderricin-probe to unravel the antibacterial mechanism of this compound against *Staphylococcus aureus*.

C RESULTS AND DISCUSSION

Evaluation of α -pyrones and pyrimidones as photo affinity probes for activity based protein profiling.

This chapter was published in: O. A. Battenberg, M. B. Nodwell, S. A. Sieber, *The Journal of Organic Chemistry* **2011**, 76, 6075-6087.



Abstract

α -pyrones and pyrimidones are common structural motifs in natural products and bioactive compounds. They also display photochemistry that generates high-energy intermediates that may be capable of protein reactivity. A library of pyrones and pyrimidones was synthesized and their potential to act as photoaffinity probes for nondirected affinity-based protein profiling in several crude cell lysates was evaluated. Further “proof-of-principle” experiments demonstrate that a pyrimidone tag on an appropriate scaffold is equally capable of proteome labeling as a benzophenone.

Introduction

Many disease states arise from aberrant protein function, and it is thus a major goal to determine the molecular, cellular and physiological functions for the multitude of proteins encoded by eukaryotic and prokaryotic genomes – a goal that cannot be accomplished by analysis of genome sequences alone. Because proteins do not function in isolation, but rather as parts of complex regulatory networks, a method to examine proteins in their natural state has been developed. Termed activity based protein profiling (ABPP), this chemical-proteomic approach involves the interrogation of an entire native proteome with carefully designed probes.^[43-46] These probes typically contain an active-site directed group for binding and covalent modification of the target protein, a linker and a tag that allows for visualization or enrichment of the labelled proteins.

Typically, ABPP probes achieve covalent protein modification of enzyme active sites either by electrophilic labeling of complimentary protein nucleophilic sites, or by photocrosslinking, which is the strategy of choice for probes that lack an electrophilic function. Photo-cross-linking does not necessarily represent a mechanism-based labeling of target proteins and therefore can also be referred to as “affinity-based protein profiling”.

Common examples of photocrosslinking groups^[28, 47] are aryl azides,^[48] diazirines,^[49] and benzophenones.^[50] Each group has its disadvantages and advantages; however, each involves the incorporation of a non-natural moiety into a probe structure that can drastically perturb probe-protein interaction. This limitation can be circumvented by the application of intrinsically photoreactive probes – ie probes whose natural structures generate highly reactive intermediates upon irradiation. Examples of intrinsic photoreactivity include steroid enones,^[51-52] some aryl chlorides^[53] and some thioethers.^[54-55]

α -pyrones and pyrimidones are structural motifs found in many natural products and bioactive molecules. Examples include citreoviridin,^[56] bufadienolides,^[57] aureothins,^[58] fusapyrone,^[59] pyrimidone-thiazolidinediones^[60] and Zebularine^[61] (Figure 1).

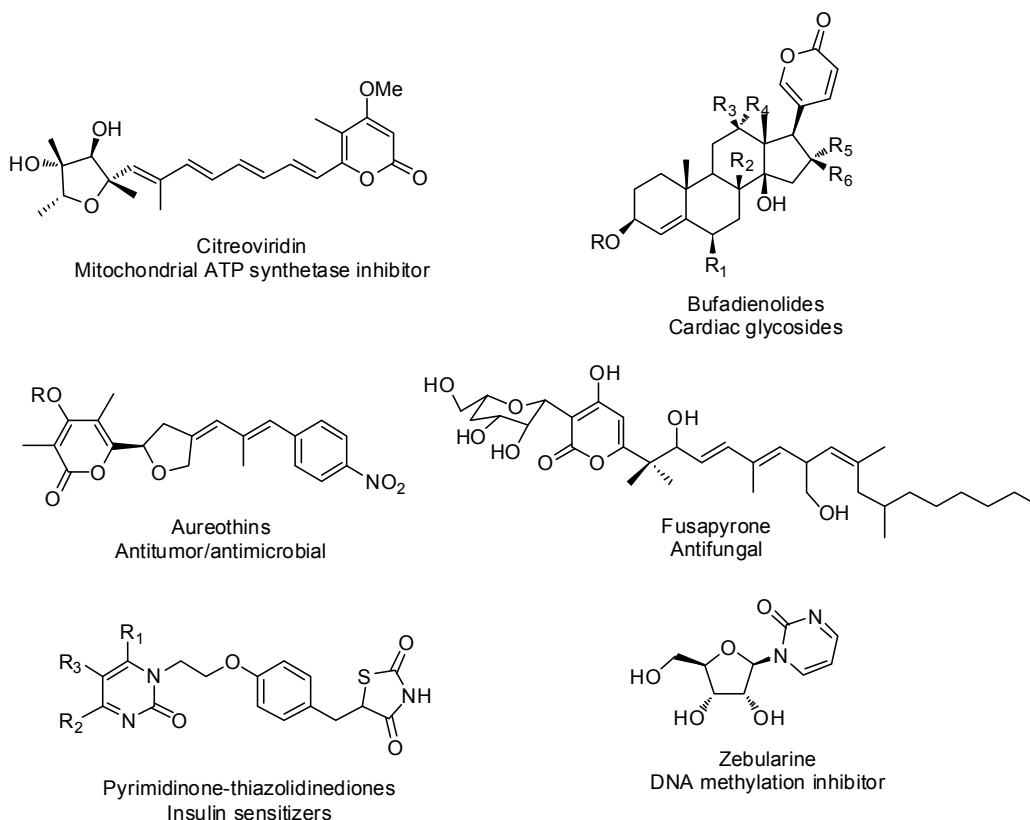
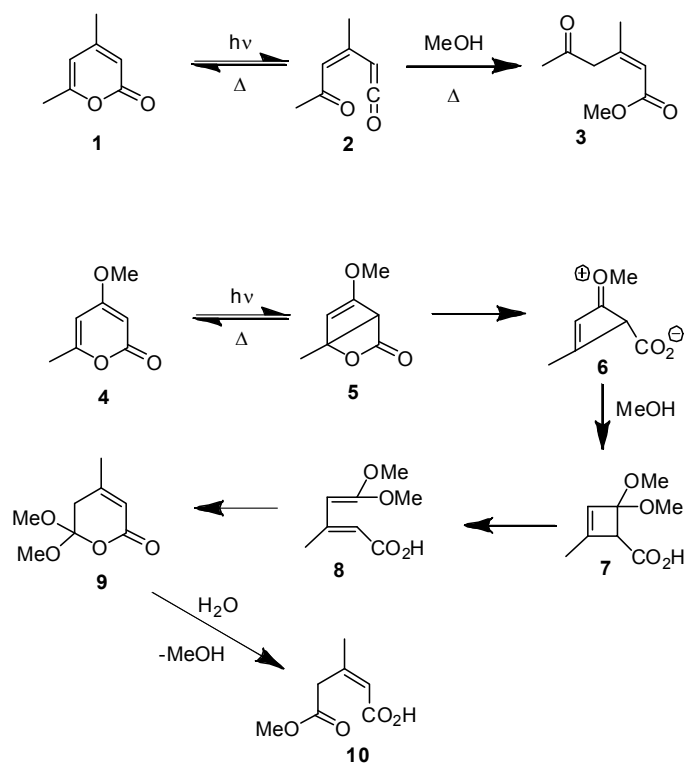


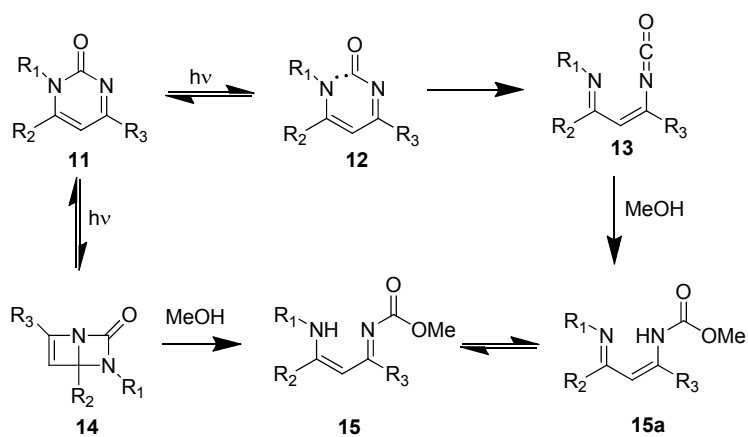
Figure 1. Pyrone and pyrimidone-containing bioactive compounds.

In addition to their presence in bioactive compounds, pyrones and pyrimidones also display well-documented photoreactivities. α -pyrones (**1** or **4**), upon irradiation with UV light, undergo an isomerization to either ketene **2** or a bicyclic β -lactone **5**, depending on the nature of the substituents on the pyrone ring.^[62-64] These isomerised forms can then undergo reactions with nucleophiles. In the case of 4-alkyl substituted pyrone **1**, simple attack of the nucleophile – in this example, methanol – on ketene **2** leads to methyl β -acetylacrylate **3**. In the case of 4-alkoxy substituted pyrone, which initially forms bicyclic lactone **5** upon irradiation, the reaction pathway involves zwitterionic intermediate **6**.^[65] MeOH addition to **6** followed by thermal conrotatory ring opening of **7** forms intermediate **8**, which can undergo ring closure to orthoester product **9**. Hydrolysis of **9** in aqueous media results in formation of β -carbomethoxymethylacrylate **10** (Scheme 1).



Scheme 1.^[64]

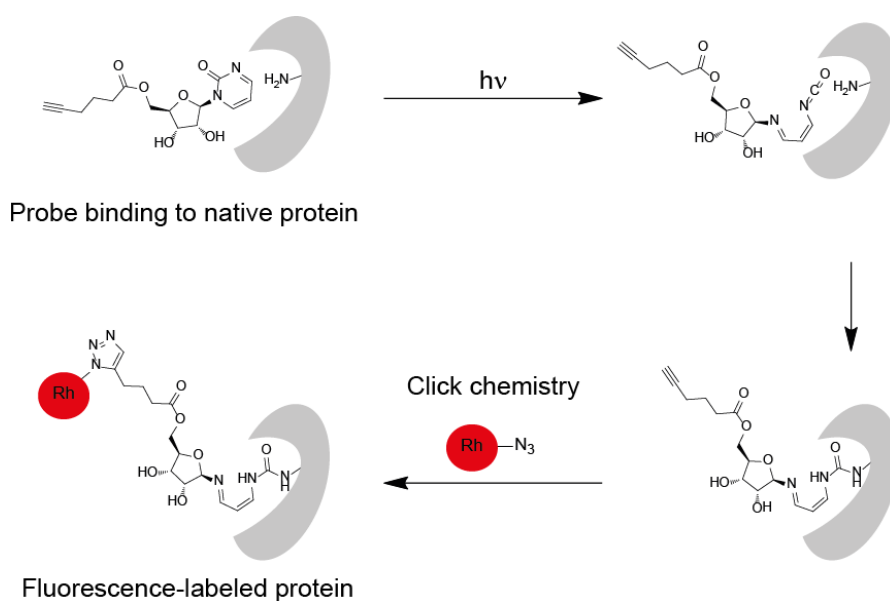
Pyrimidones (**11**), upon irradiation undergo a Norrish type I reaction (**11** to **12**) to form either an isocyanate **13** or bicyclic intermediate **14** which can then react with nucleophiles to form the tautomeric products **15** and **15a** as shown in Scheme 2.^[66-67]



Scheme 2.^[67]

Kinetics of photoisomerization and reaction of the intermediates with nucleophiles has been the subject of several studies.^[68-72] Whereas the above photoisomerizations to active species are fast, the reaction of these species with nucleophiles is relatively slow. However, given that the formation of the active species is largely reversible and in a proteinsubstrate complex, the nucleophile concentration is high, and a protein-labeling event is likely to occur.

We found this photoreactivity, coupled with the occurrence of α -pyrones and pyrimidones in various natural product and bioactive compounds to be an intriguing approach to intrinsic photoreactivity. Natural products and other bioactive compounds with α -pyrones or pyrimidones in their structures could be photo-activated to a reactive species as illustrated in Schemes 1 and 2. This reactive species could then react with a nearby nucleophilic amino acid to covalently modify the binding protein (Scheme 3).



Scheme 3.

In this report, we outline syntheses of α -pyrone- and pyrimidone- containing compounds and attempts to use these as non-directed photoactivatable affinity probes.

Results and Discussion

The design of the probes required careful consideration for their structural elements. We sought to have a wide variety of probe structures in order to maximize the opportunities for specific biological interactivity – in this case with bacterial proteomes. In addition to the α -pyrone or pyrimidone, within each structure is a sterically benign alkyne tag suitable for the Cu(I)-catalyzed Huisgen [3+2]-azide-alkyne cycloaddition^[73-75] which would allow the attachment of a fluorescent or a biotin tag for visualization and enrichment, respectively. Figure 2 shows the probes used in our proteome labeling experiments. These probes can be broadly divided in two classes – those that are inspired by compounds with known bioactivity (biology-inspired probes), and those that are not (diversity-oriented probes).

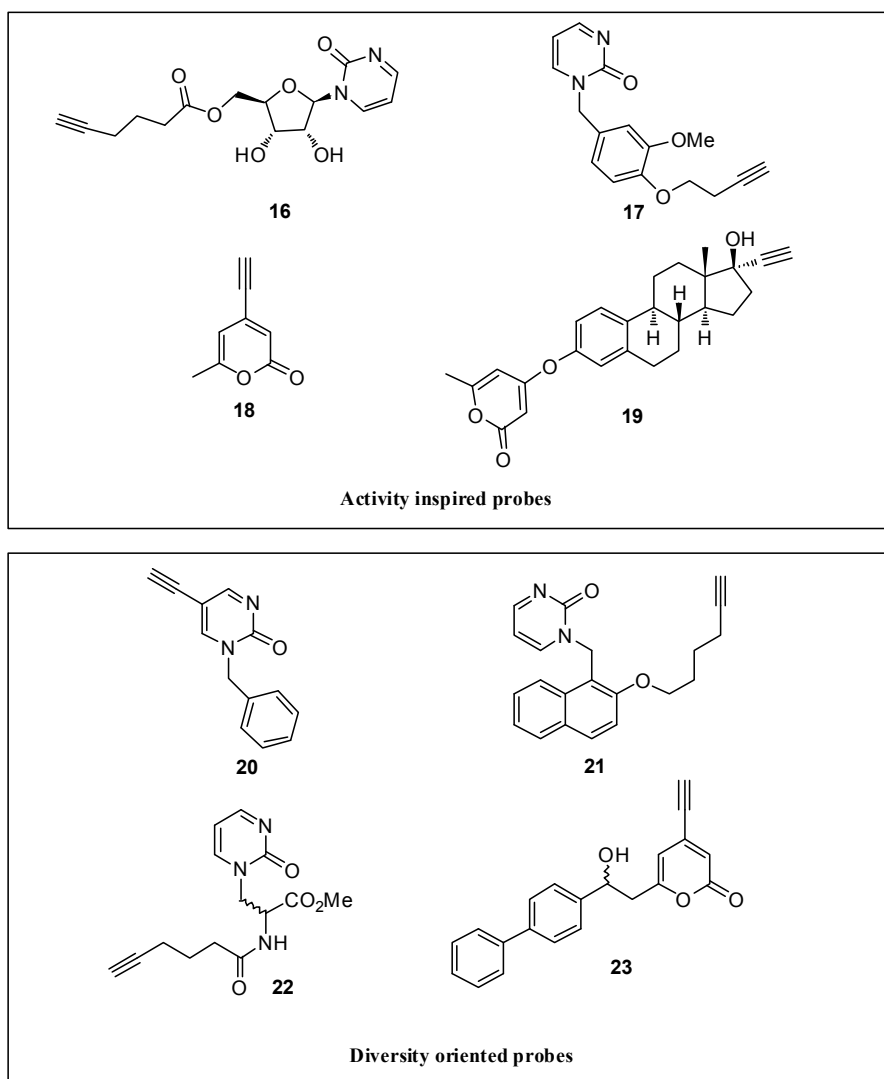


Figure 2. Biology- and diversity-inspired probes.

16 was designed as a mimic of the DNA methylation inhibitor Zebularine^[61] (Figure 3).

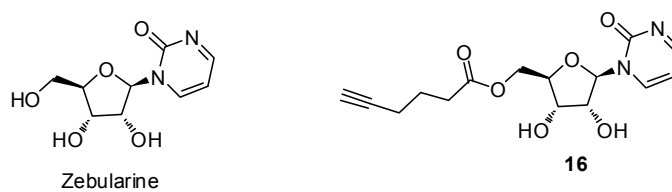
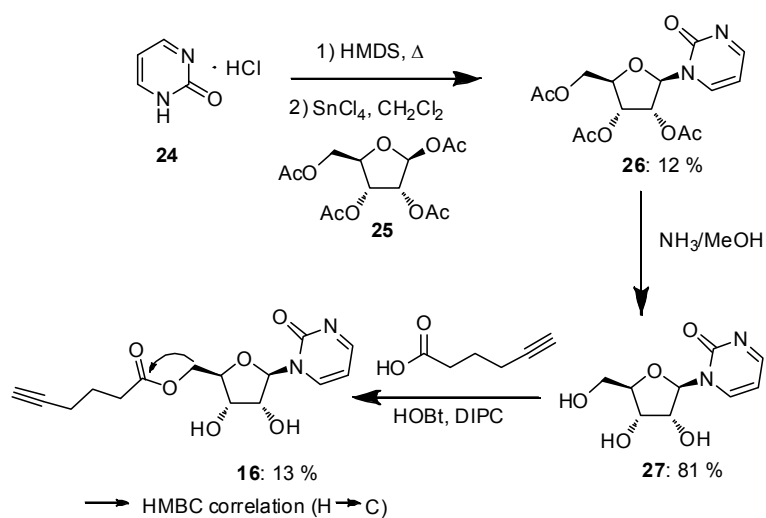


Figure 3. Zebularine and probe **16**.

Formation of the glycosidic bond was accomplished by utilizing a one-pot procedure as outlined by Vorbrüggen *et al* [76-77] between pyrimidine **24** and peracetylated ribofuranose **25** to give **26** in 12 % yield. Deprotection of the acetyl groups by ammonia in MeOH gives nucleoside **27** in 81 % yield.^[78] At this point, the alkyne tag was installed by coupling of 5-hexynoic acid to nucleoside **27** in DMF. Probe **16** was isolated from a mixture of isomers and its regiochemistry was confirmed by HMBC correlations between the 5' ribofuranose methylene and the ester carbonyl (Scheme 4).



Scheme 4.

Probe **17** was designed to resemble the dihydrofolate reductase inhibitor trimethoprim.^[79] (Figure 4)

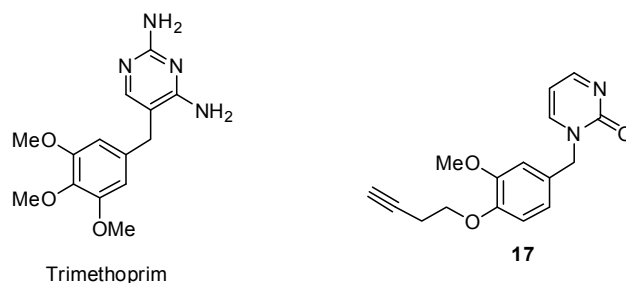
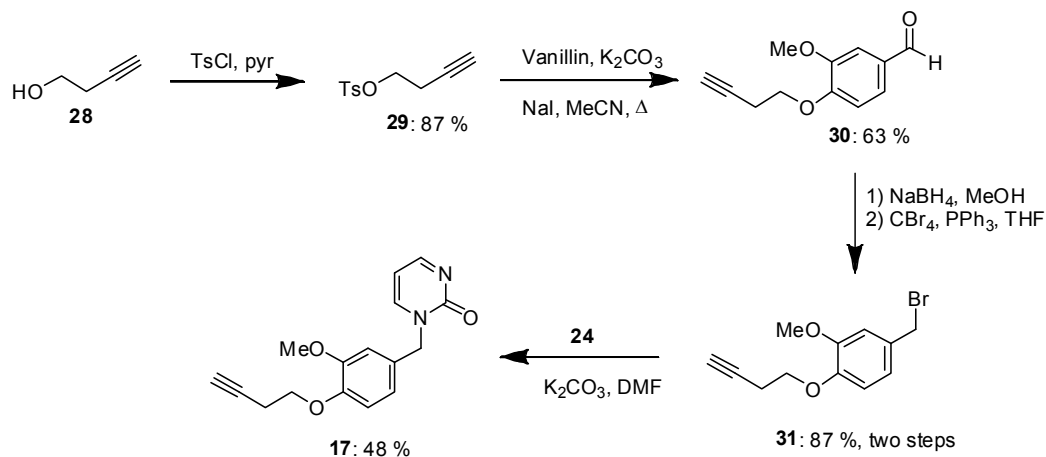


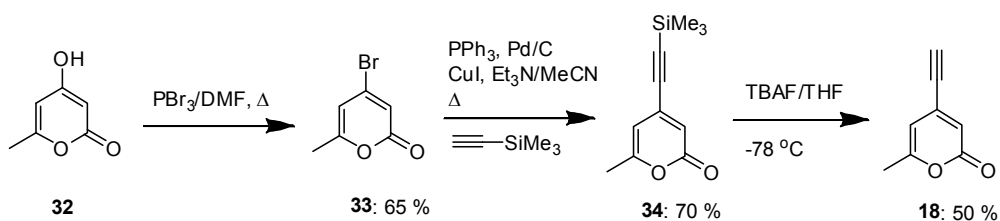
Figure 4. Trimethoprim and probe **17**.

Therefore, vanillin was alkylated by tosylate **29** to yield aldehyde **30**.^[80] Functional group interchanges^[81-82] yielded bromide **31** which was then substituted with pyrimidone **24** to yield probe **17**. (Scheme 5)



Scheme 5.

α -pyrone* probe **18** has been reported to possess broad-spectrum antibacterial activity,^[83] and was prepared via bromination and subsequent sonogashira reaction with trimethylsilylacetylene of the commercially available triacetic acid lactone **32**.^[84] (Scheme 6)

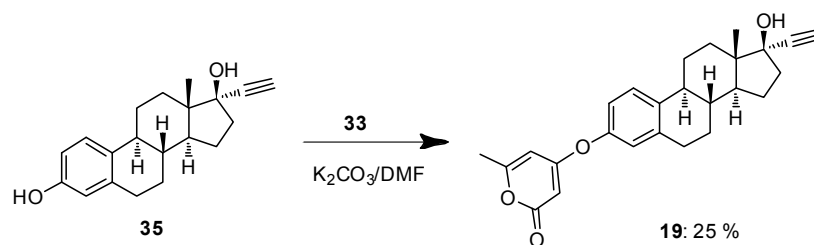


Scheme 6.

Probe **19** is based upon 17α -ethynylestradiol (**35**) – a common estrogenic component in oral contraceptives that conveniently has a terminal alkyne in its structure. While 17α -ethynylestradiol will in all probability display no appreciable biological activity towards bacterial proteins, the core steroid structure is a common one and may impart specific protein binding in

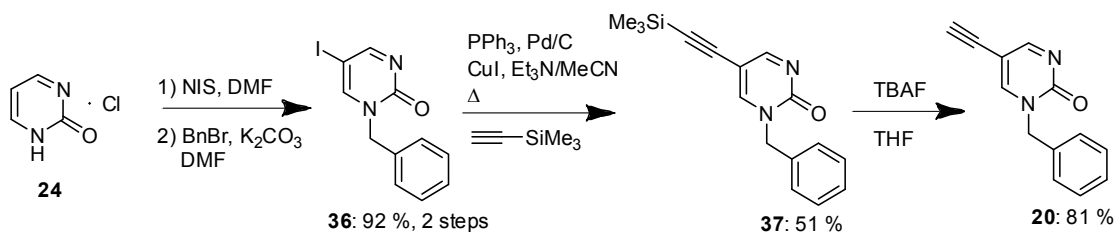
* α -Pyrone-based probes have been synthesized and characterized by the co-author M. B. Nodwell.

the bacterial proteome. Reaction of 17 α -ethynylestradiol with bromide **33** under basic conditions results in a Michael addition- β -elimination to yield probe **19**.^[85] (Scheme 7)



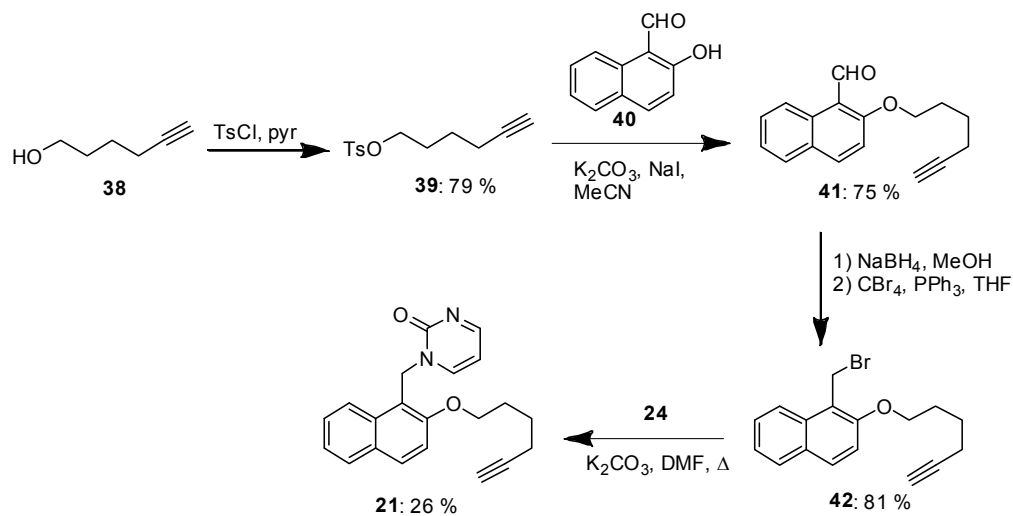
Scheme 7.

The diversity-oriented class of probes were not based upon bioactive scaffolds, but were chosen to present a variety of structural elements to the proteome. Probe **20** was synthesized by iodination of pyrimidone **24** with N-iodosuccinimide,^[86] followed by installation of a benzyl group to yield **36**. Sonogashira reaction between iodide **36** and trimethylsilylacetylene yields **37**. Standard deprotection (TBAF/THF) then yields probe **20**. (Scheme 8)



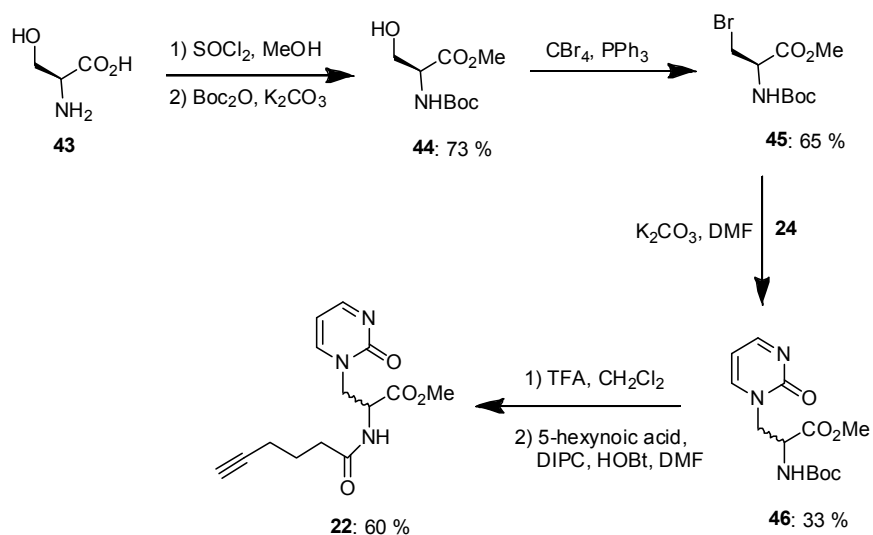
Scheme 8.

Probe **21** was based on a naphelene core and was synthesized in a manner analogous to probe **17** starting with 2-hydroxy-1-naphthaldehyde (**40**). (Scheme 9)



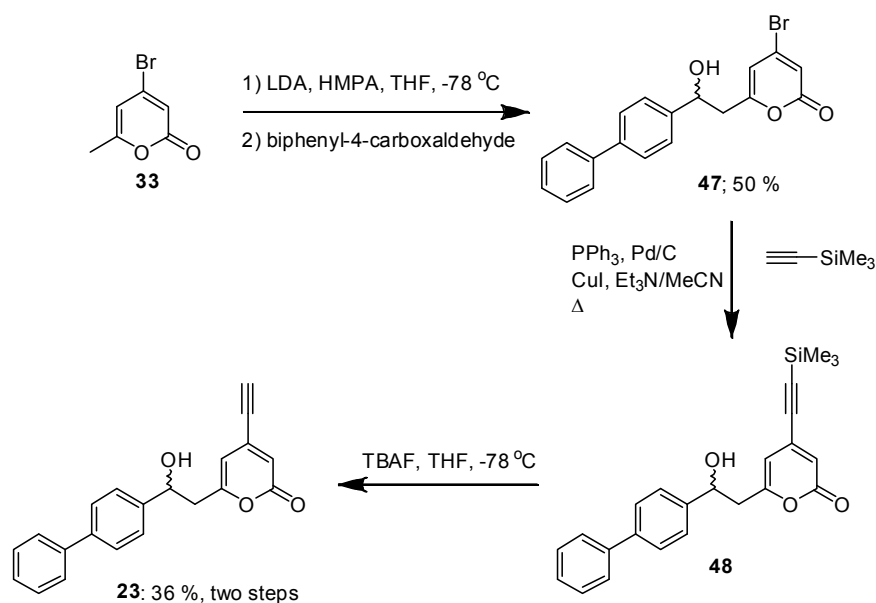
Scheme 9.

Probe **22** was based on an amino acid scaffold, in this case, serine. Protection of the C and N terminals of serine as a methyl ester and t-butyl carbamate respectively gives **44**.^[87] Bromination^[88] of the 1° alcohol to yield **45** followed by substitution with pyrimidone **24** gives **46**, albeit with racemization of the chiral centre. Deprotection of the Boc group under standard conditions, followed by amide formation with 5-hexynoic acid yields probe **22**. (Scheme 10)



Scheme 10.

The final pyrone probe **23**, was synthesized via deprotonation of bromide **33** at C7, followed by quenching of the anion with biphenyl-4-carboxaldehyde to yield **47**.^[89-90] Sonogashira reaction with trimethylsilylacetylene and **47**, followed by standard deprotection yields probe **23**. (Scheme 11)



Scheme 11.

With probes **16-23** in hand, we wanted to verify their light-induced reactivity with nucleophiles. We picked two probes, **18** and **20** as test compounds.

Irradiation of a methanolic solution of **18** at 350 nm resulted in the loss of starting material and the formation of a peak that corresponds to the expected ester photoproduct **49**. (Figure 5) As LC-MS was problematic for this compound, it was isolated and the ¹H and ¹³C NMR spectra of **49** were recorded. This reaction was complete after less than 10 min.

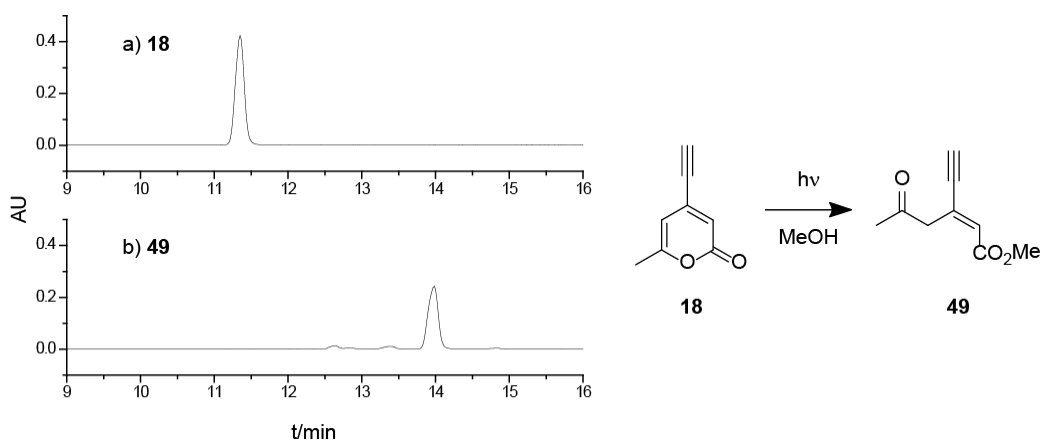


Figure 5. UV-dependent conversion of **18** to **49**.

Irradiation of **20** in MeOH at 350 nm results in almost complete conversion after 30 min, accompanied by the formation of a peak that corresponds to the proposed photoproduct **50** as determined by LC-MS. (Figure 6)

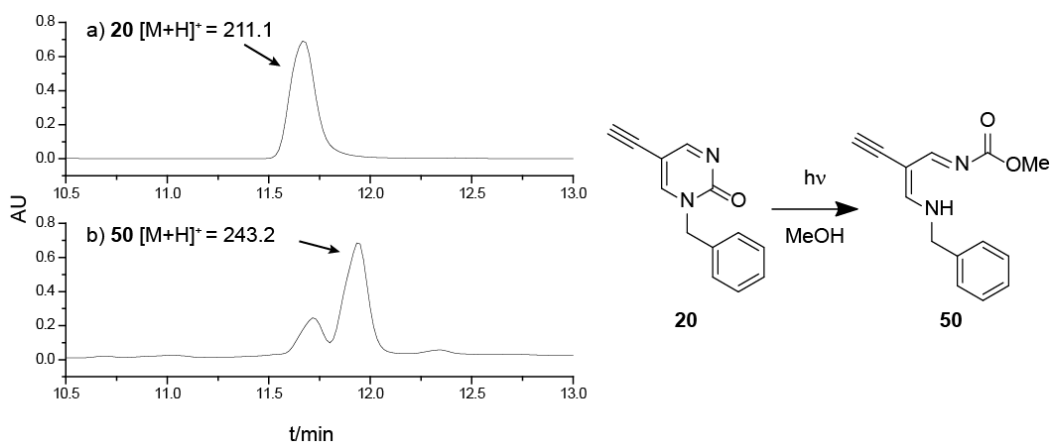


Figure 6. UV-dependent conversion of **20** to **50**

Once we were satisfied that our probes were reacting sufficiently with weak nucleophiles, we set labeling parameters for optimal probe reaction with crude cell lysate preparations. Using either *E. coli* or *S. aureus* Mu50 cytosol preparations as our standard proteome preparations, we screened representative probes for time and concentration dependence with respect to photolabeling. In a typical experiment, a crude cell lysate (proteome) is diluted with PBS to give 43 μ L 1 mg/mL protein concentration. 1 μ L of the desired probe is then added in DMSO to give

the final probe concentration. Irradiation is carried out over ice cooling in a 96-well plate. The irradiated solutions are then transferred back to a reaction vessel, and [3+2]-azide-alkyne “click chemistry” is performed on the solution with rhodamine azide for 1h at rt. Figure 7 shows that for probe **19**, 100 μM and 1h yields saturated protein labeling .

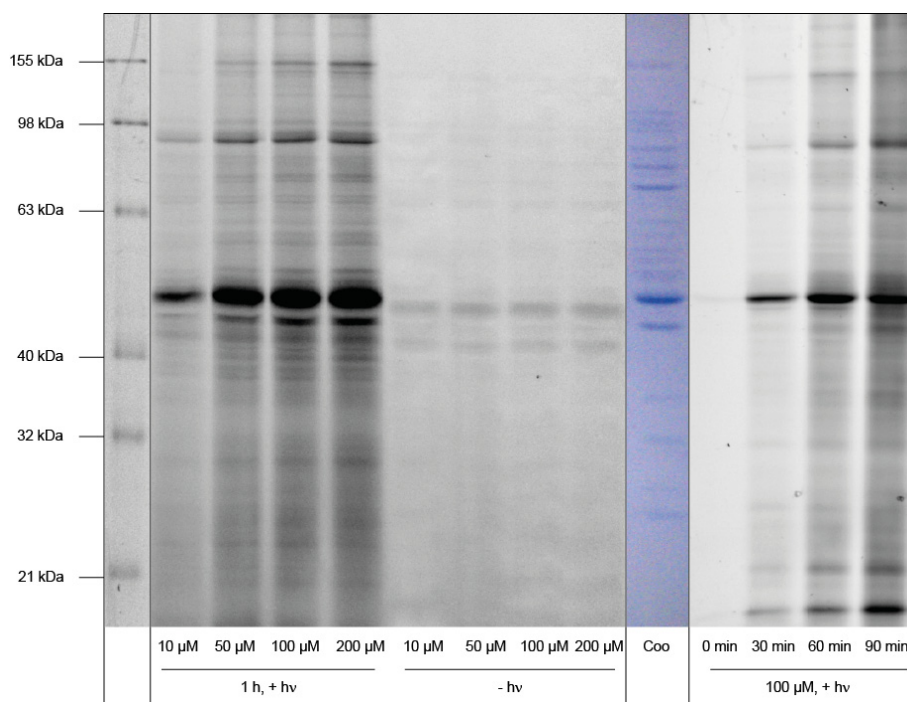


Figure 7. Time and concentration dependent labeling of *E. coli*. crude cellular lysate with **19**

These conditions also result in saturated labeling for **17**, however for **20**, while 100 μM remains an optimal concentration, only 20 min is necessary for saturated labeling (Supporting Figures 1 and 2, Appendix 1). Increases in irradiation time only increase background signal, while probe concentrations over 100 μM do not result in significantly increased signal to noise ratios. Non-irradiated controls demonstrate a clear light-dependent labeling for some protein bands (Figure 7, lanes 5-8), emphasizing that photoinduced reactivity leads to protein labeling .

With the key parameters set, we then compared all probes for labeling patterns in both *L. welshimerii* and *E. coli* crude cell lysates using the optimized labeling parameters as described above. A variety of structures as shown in Figure 2 should, by virtue of their differing non-

covalent interactions, show a wide variety of labeling patterns as well. However Figure 8 demonstrates that while a variety of structural types are displayed to the bacterial proteomes, the labeling patterns show only a few differences. (see also Supporting Figure 3, Appendix 1)

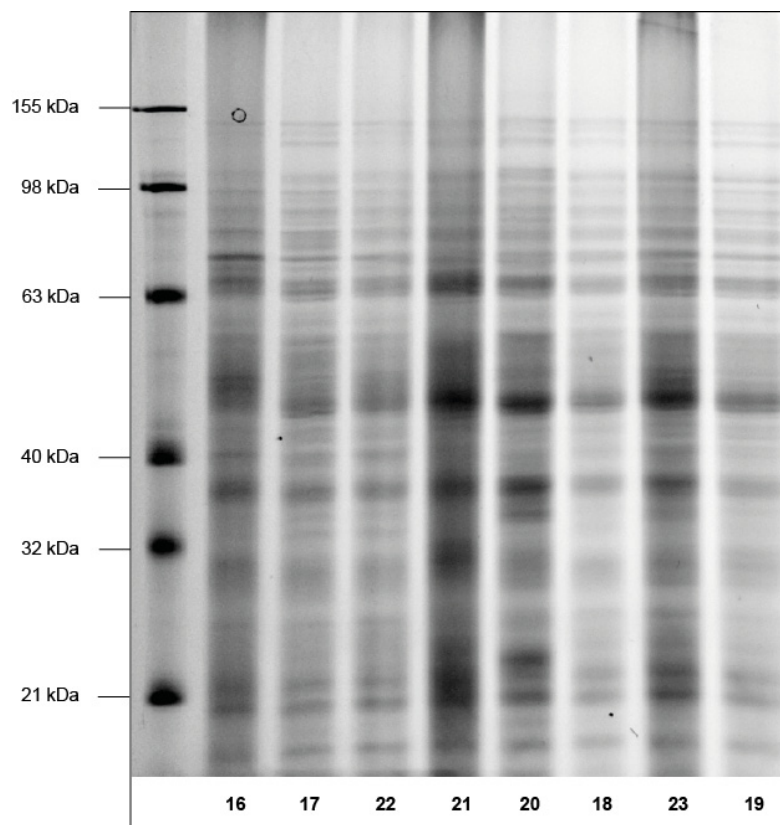


Figure 8. Labeling of *L. welshimerii* crude cell lysate with probes **16-23**.

The similarity in labeling patterns may be due to the relatively long lifespan of the photogenerated intermediates of the α -pyrones or pyrimidones (Schemes 1 and 2) that allows for mobility from the probes original binding site. This mobile intermediate can then equilibrate amongst the reaction medium and then react with available protein nucleophiles, and hence the probes designed herein reflect a preference for type of reactant instead of type of binding site. However, a striking feature of cell lysate labeling with probes **16-23** is the moderate reactivity of the photogenerated species with respect to the native proteomes emphasizing that the photoinduced electrophiles display a certain selectivity for available protein nucleophiles.

Concerned with this apparent lack of selectivity that probes **16-23** demonstrate towards bacterial lysates, we sought a more comparative approach towards demonstrating the feasibility of our hypothesis. Realizing that biology-based probes **16-19** display significant structural deviations from their original inspirations that may drastically reduce their target binding,^[91-93] and that diversity based probes **20-23** may not possess enough structural elements to prevent diffusion after photoactivation, we chose to modify a substrate whereby the additional elements (photolabel and alkyne tag) would constitute a minimal structural change. A recent account from our group details the synthesis of vancomycin-based photoaffinity probes that selectively label autolysin (ATLam) and an ABC transporter protein (pABC) in *S. aureus* and *E. faecalis* respectively (Figure 9).

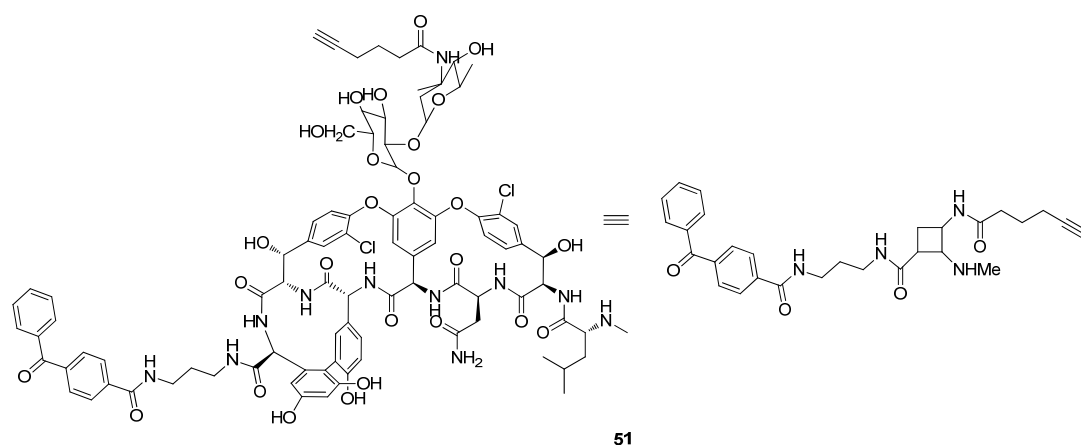
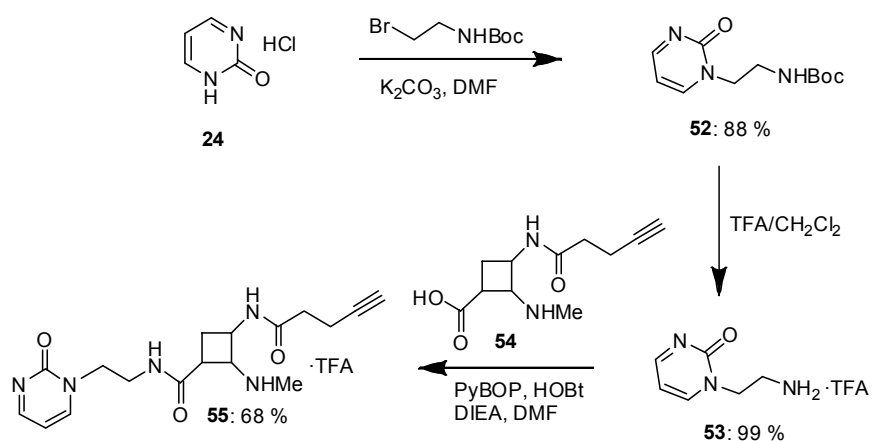


Figure 9. Full and shorthand illustrations of probe **51**.

We reasoned that by substituting the benzophenone in probe **51** for a pyrone or pyrimidone, we could directly compare the labeling efficacy of a well-established photocrosslinking moiety with a novel crosslinking group. For synthetic ease, we chose to examine a pyrimidone in this position. Compound **55** was prepared according to Scheme 12 by a coupling of primary amine **53** with modified vancomycin **54**:



Scheme 12.

With probe **55** in hand, we then compared the labeling patterns of **51** and **55** in BL21 *E. coli* recombinant clone cell lysates overexpressing both ATLam and pABP. To our gratification, the labeling patterns for both **51** and **55** were identical at 1 and 10 μM respectively, while non-irradiated controls demonstrated little to no labeling at 100 μM **55**. Furthermore, attempts to photolabel the overexpressed *E. coli* cell lysates with 100 μM **22** gave no appreciable labeling, showing patterns similar to Figure 8, demonstrating the key role of the vancomycin scaffold in the proteome labeling of **55** (Figure 10).

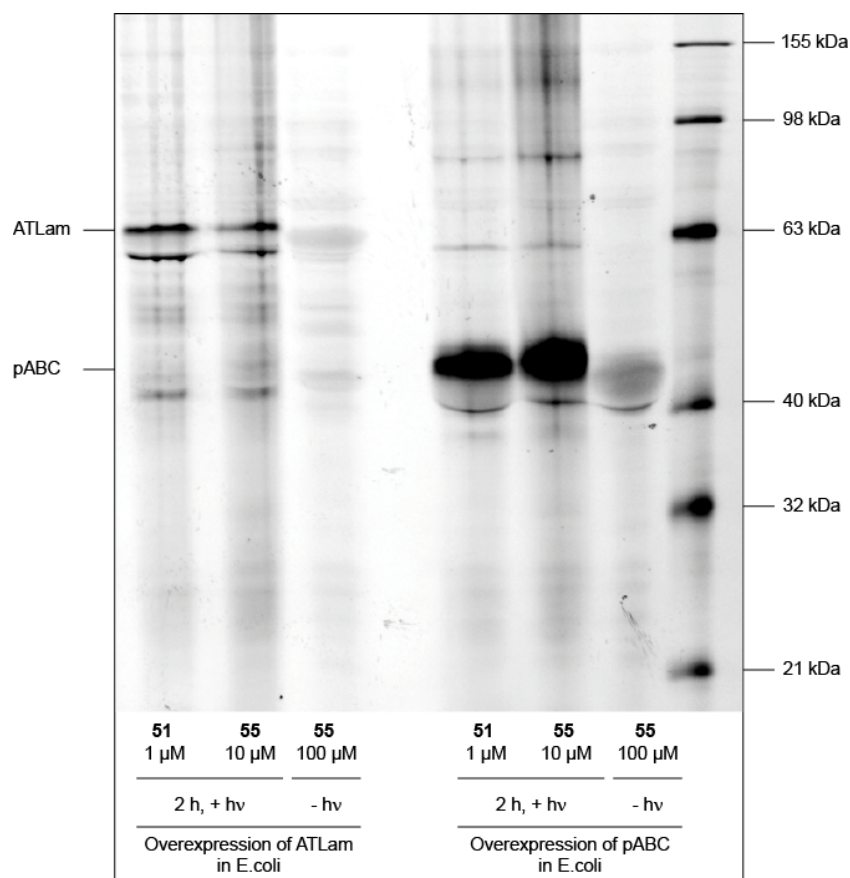


Figure 10. Labeling of *E. coli* overexpressing ATLam and pABC with **51** and

55.

While **51** appears to label more effectively than **55**, both probes show identical selectivity towards the bacterial proteome. This result represents an important validation of the hypothesis that pyrimidones can be used as photocrosslinkers. The selectivity of probe **55** relative to probes **16-23** can be explained by the much greater molecular complexity of vancomycin, which results in greater non-covalent protein binding, allowing the photoactivated species to remain target-bound while the isocyanate reacts with the protein. Given the results displayed in Figure 10, we are confident that a high affinity natural product or bioactive compound containing a native pyrone or pyrimidone, appropriately modified with an alkyne tag will display selective photolabeling of complex proteomes. Work is currently underway to adapt this approach to affinity labeling of proteomes with natural structures.

Conclusion

Using intrinsic photoreactivity represents a powerful approach to photoaffinity labeling that precludes the necessity of additional photoreactive groups which can perturb native substrate-target interaction. We have attempted to use non-directed α -pyrone and pyrimidone probes to demonstrate the feasibility of these groups as intrinsic photolabels. We synthesized a series of biology- and diversity-inspired probes **16-23** and demonstrated that representative samples of these probes displayed light-induced reaction with MeOH and also displayed light-dependent labeling of crude bacterial lysates. However, these probes displayed little to no selectivity in bacterial proteomes, prompting us to attempt a secondary “proof of principle” strategy. In this strategy, vancomycin-based probe **55** displays selective labeling of ATLam and pABC proteins in *E. coli* in a manner identical to that for the similar benzophenone containing vancomycin probe **51**. This result validates our hypothesis and encourages us to attempt this approach with natural product structures already containing a pyrone or pyrimidone.

Acknowledgements

We thank Mona Wolff for excellent scientific support, and Jurgen Eirich for *E. coli* clones and a sample of probe **51**. S.A.S. was supported by the Deutsche Forschungsgemeinschaft (Emmy Noether), SFB749, FOR1406, an ERC starting grant and the Center for Integrated Protein Science Munich CIPSM. M.B.N thanks the Alexander von Humboldt foundation for financial support. O.A.B. thanks the TUM graduate school for project funding.

Experimental

General Methods - All non-aqueous reactions were carried out in flame-dried glassware unless otherwise noted. Air and moisture sensitive liquid reagents were manipulated via a dry syringe. Anhydrous tetrahydrofuran (THF) was obtained from distillation over sodium. All other solvents and reagents were used as obtained from commercial sources without further purification. Flash chromatography was performed using Merck Silica Gel 60 (40-63 μm). HPLC analysis was accomplished with a C18 column 5 μm (4.6x100 mm) and a PDA detector. Mobile phase (HPLC grade): A: 0.1% (v/v) TFA in H_2O ; B: 0.1% TFA in Acetonitrile. Flow: 0.5 ml/min.

2', 3', 5'-Tri-O-acetyl-zebularine (26) - Pyrimidine **24** (8.9 g, 67 mmol) and a catalytic amount of $(\text{NH}_4)_2\text{SO}_4$ were refluxed for 4 h in HMDS (25 mL) under an inert atmosphere. Excessive HMDS was removed under reduced pressure and the residue was dissolved in dry CH_2Cl_2 (10 mL). A solution of **25** (7.2 g, 23 mmol) and SnCl_4 (4 mL, 34 mmol) were then combined in 5 mL dry CH_2Cl_2 and the solution was stirred at rt for 16 h. The mixture was washed with saturated NaHCO_3 solution and the resulting emulsion was filtered over silica. The aqueous layer was extracted into CH_2Cl_2 . The organic layer was dried over MgSO_4 , filtered and concentrated. The crude product was purified by column chromatography to yield **26** (2.9 g, 8 mmol, 12%) as a colorless solid. ^1H NMR (400 MHz, CDCl_3) δ 1.91 (s, 3H), 1.96 (s, 6H), 4.23 (d, $J = 3.4$ Hz, 2H), 4.26 – 4.32 (m, 1H), 5.12 – 5.18 (m, 1H), 5.32 (dd, $J = 3.4, 5.5$ Hz, 1H), 5.88 (d, $J = 3.3$ Hz, 1H), 6.29 (dd, $J = 4.1, 6.8$ Hz, 1H), 7.94 (dd, $J = 2.8, 6.8$ Hz, 1H), 8.45 (dd, $J = 2.9, 4.0$ Hz, 1H); ^{13}C NMR (100 MHz, CDCl_3) δ 20.3, 20.3, 20.6, 62.4, 69.2, 73.6, 79.6, 90.1, 104.3, 143.4, 155.0, 166.6, 169.3, 169.3, 170.0. HRMS (ESI): $[\text{M} + \text{Na}]^+$ $\text{C}_{15}\text{H}_{18}\text{O}_8\text{N}_2\text{Na}$ calcd 377.0955, found 377.0954. R_f (10% MeOH/ CH_2Cl_2) = 0.6.

Zebularine (27) - This compound **27** was prepared by the removal of the acetyl groups in **26** with NH_3/MeOH to yield **27** (603 mg, 2.6 mmol, 81%) as a colorless solid. The spectral data matched with those reported in the literature.^[61] ^1H NMR (400 MHz, CD_3CD) δ 3.81 (dd, $J = 2.4, 12.5$ Hz, 1H), 3.99 (dd, $J = 2.1, 12.5$ Hz, 1H), 4.09 – 4.19 (m, 3H), 5.87 (s, 1H), 6.59 (dd, $J = 4.3, 6.7$ Hz, 1H), 8.58 (dd, $J = 2.7, 4.2$ Hz, 1H), 8.79 (dd, $J = 2.7, 6.7$ Hz, 1H); ^{13}C NMR

(100 MHz, CD₃OD) δ 59.5, 68.2, 75.2, 84.4, 92.2, 104.6, 145.3, 156.1, 165.9. HRMS (ESI): [2M + Na]⁺ C₁₈H₂₄N₄NaO₁₀ calcd 479.1385, found 479.1382.

5'-O-Hex-5-ynoyl-zebularine (16) - HOBt (432 mg, 3.2 mmol) and 5-Hexynoic acid (353 μ L, 3.2 mmol) were dissolved in DMF (5 mL) and N,N'-diisopropylcarbodiimide (496 μ L, 3.2 mmol) was added. The reaction mixture was stirred for 30 min at rt. A solution of **27** (1.1 g, 3.2 mmol) in DMF (5 mL) was added. The mixture was stirred for 16 h at 50 °C. The reaction mixture was concentrated to dryness and purified by column chromatography (CH₂Cl₂/MeOH) to yield **16** (121 mg, 0.4 mmol, 13%) as a colorless solid. ¹H NMR (500 MHz, CD₃OD) δ 1.79 – 1.88 (m, 2H), 2.24 – 2.30 (m, 3H), 2.54 (t, *J* = 7.4 Hz, 2H), 4.05 (dd, *J* = 5.0, 7.9 Hz, 1H), 4.21 (dd, *J* = 1.5, 4.9 Hz, 1H), 4.29 – 4.34 (m, 1H), 4.40 – 4.51 (m, 2H), 5.83 (d, *J* = 1.2 Hz, 1H), 6.64 (dd, *J* = 4.2, 6.7 Hz, 1H), 8.40 (dd, *J* = 2.7, 6.7 Hz, 1H), 8.61 (dd, *J* = 2.9, 4.1 Hz, 1H); ¹³C NMR (90 MHz, CD₃OD) δ 17.0, 23.4, 32.2, 62.6, 69.0, 69.1, 74.6, 81.4, 82.6, 93.0, 104.7, 144.4, 156.0, 166.2, 172.8. HRMS (ESI): [M + H]⁺ C₁₆H₁₈N₂O₆ calcd 323.1238, found 323.1220. *R_f* (10% MeOH/CH₂Cl₂) = 0.5.

But-3-yn-1-yl 4-methylbenzenesulfonate (29).^[80] - 4-Methylbenzenesulfonyl chloride (20.4 g, 110 mmol) was added to a solution of **28** (5.4 mL, 70 mmol) and pyridine (11.5 mL, 140 mmol) in CH₂Cl₂ at 0 °C, warmed to rt and stirred for 16 h. The reaction mixture was treated with water and extracted with CH₂Cl₂. The combined organic layers were washed with 1 M HCl, saturated NaHCO₃, H₂O and brine. The solution was dried over MgSO₄ and concentrated to dryness. The crude product was purified by column chromatography to yield **29** (13.6 g, 61 mmol, 87%) as a colorless oil. ¹H NMR (360 MHz, CDCl₃) δ 1.98 (t, *J* = 2.7 Hz, 1H), 2.46 (s, 3H), 2.56 (td, *J* = 2.7, 7.0 Hz, 1H), 4.11 (t, *J* = 7.0 Hz, 2H), 7.36 (d, *J* = 8.0 Hz, 2H), 7.81 (d, *J* = 8.3 Hz, 2H); ¹³C NMR (90 MHz, CDCl₃) δ 19.4, 21.6, 67.5, 70.8, 78.4, 127.9, 129.9, 132.8, 145.0. HRMS (EI): [M]⁺ C₁₁H₁₂O₃³²S calcd 224.0502, found 224.0504. *R_f* (hexanes) = 0.7.

4-(But-3-yn-1-yloxy)-3-methoxybenzaldehyde (30).^[80] - A suspension of vanillin (5.1 g, 34 mmol), **29** (7.5 g, 33 mmol), K₂CO₃ (13.9, 101 mmol) and NaI (510 mg, 3.4 mmol) in CH₃CN was refluxed for 16 h. The solution was concentrated, treated with EtOAc/H₂O and the aqueous layer was extracted with EtOAc. The combined organic layers were washed with H₂O and brine, dried

over MgSO₄ and concentrated to dryness to yield **30** (4.2 g, 21 mmol, 63%) as a colorless solid. ¹H NMR (500 MHz, CDCl₃) δ 2.07 (t, *J* = 2.6 Hz, 1H), 2.76 (td, *J* = 2.6, 7.3 Hz, 2H), 3.90 (s, 3H), 4.21 (t, *J* = 7.3 Hz, 2H), 6.98 (d, *J* = 8.2 Hz, 1H), 7.37 – 7.45 (m, 2H), 9.83 (s, 1H); ¹³C NMR (90 MHz, CDCl₃) δ 19.3, 56.0, 66.9, 70.5, 79.6, 109.6, 111.9, 126.5, 130.5, 149.9, 153.3, 190.8. HRMS (ESI): [M + H]⁺ C₁₂H₁₃O₃ calcd 205.0856, found 205.0854. *R_f* (50% EtOAc/hexanes) = 0.3.

4-(Bromomethyl)-1-(but-3-yn-1-yloxy)-2-methoxybenzene (31). - At 0 °C NaBH₄ (445 mg, 12 mmol) was slowly added to a cooled solution of **30** (1.2 g, 6 mmol) in dry THF. After 30 min the reaction mixture was treated with H₂O and extracted with EtOAc. The combined organic layers were washed with H₂O and brine, dried over MgSO₄ and concentrated. The crude product was used without further purification. The alcohol was added to a solution of CBr₄ (2.8 g, 8.5 mmol) and PPh₃ (2.2 g, 8.5 mmol) in THF and stirred for 16 h. The precipitate was removed by filtration and the filtrate was concentrated to dryness. The crude product was purified by column chromatography to yield **31** (1.4 g, 5.2 mmol, 87%) as a yellow solid. ¹H NMR (360 MHz, CDCl₃) δ 2.06 (t, *J* = 2.7 Hz, 1H), 2.74 (td, *J* = 2.7, 7.4 Hz, 2H), 3.89 (s, *J* = 2.0 Hz, 3H), 4.16 (t, *J* = 7.4 Hz, 2H), 4.50 (s, *J* = 5.5 Hz, 2H), 6.81 – 6.98 (m, 3H); ¹³C NMR (90 MHz, CDCl₃) δ 19.4, 34.2, 56.0, 67.2, 70.2, 80.1, 112.9, 113.6, 121.6, 131.1, 148.0, 149.7. HRMS (EI): [M]⁺ C₁₂H₁₃⁷⁹BrO₂ calcd 268.0093, found 268.0085. *R_f* (50% EtOAc/hexanes) = 0.4.

1-(4-(But-3-yn-1-yloxy)-3-methoxybenzyl)pyrimidin-2(1H)-one (17) - Bromide **31** (675 mg, 2.5 mmol) was added to a suspension of K₂CO₃ (1.0 g, 7.5 mmol) and pyrimidine **24** (398 mg, 3.0 mmol) in DMF (25 mL). The reaction mixture was stirred for 16 h at 70 °C and concentrated to dryness. The crude product was purified by column chromatography (CH₂Cl₂/MeOH) to yield **17** (336 mg, 1.2 mmol, 48%) as a yellow solid. ¹H NMR (500 MHz, CD₃OD) δ 2.33 (t, *J* = 2.7 Hz, 1H), 2.66 (td, *J* = 2.7, 6.9 Hz, 2H), 3.86 (s, 3H), 4.11 (t, *J* = 6.9 Hz, 2H), 5.15 (s, 2H), 6.64 – 6.71 (m, 1H), 6.99 (d, *J* = 0.9 Hz, 2H), 7.10 (s, 1H), 8.45 – 8.50 (m, 1H), 8.63 – 8.68 (m, 1H); ¹³C NMR (125 MHz, CD₃OD) δ 18.7, 54.2, 55.2, 67.2, 69.6, 79.9, 104.6, 112.9, 114.0, 121.4, 127.6, 148.5, 150.0, 153.2, 153.6, 163.3. HRMS (ESI): [M + H]⁺ C₁₆H₁₇N₂O₃ calcd 285.1234, found 285.1228. *R_f* (10% MeOH/CH₂Cl₂) = 0.4

4-ethynyl-6-methyl-2H-pyran-2-one (18) - This compound was prepared according to Fairlamb *et al.*^[84] The characterization data for this compound matched with those reported in the literature.

3-(6-methyl-2H-pyran-2-one)-17 α -ethynylestradiol (19) - 17 α -ethynylestradiol **35** (45.9 mg, 0.16 mmol), bromide **33** (30 mg, 0.16 mmol) and K₂CO₃ (21.4 mg, 0.16 mmol) were stirred in 1 mL DMF at rt for 24 h. EtOAc was added and the resulting suspension was extracted with 3 x H₂O. The organic phase was dried over Na₂SO₄, filtered and concentrated to dryness. The crude product was purified by column chromatography to yield **19** (16.8 mg, 0.04 mmol, 25%) as a colorless solid. ¹H NMR (360 MHz, CDCl₃) δ 0.93 (s, 3H), 1.35-1.62 (m, 4H), 1.63-1.86 (m, 4H), 1.87 - 1.98 (m, 1H), 2.00 - 2.14 (m, 2H), 2.27 (s, 3H), 2.34 - 2.45 (m, 2H), 2.62 (s, 1H), 2.88 (m, 2H), 5.24 (s, 1H), 5.99 (s, 1H), 6.79 (s, 1H), 6.84, (dd, J = 2.2, 8.1 Hz, 1H), 7.34 (d, J = 8.1 Hz, 1H); ¹³C NMR (90 MHz, CDCl₃) δ 12.7, 20.0, 22.8, 26.3, 26.9, 29.6, 32.7, 38.9, 39.0, 43.7, 47.1, 49.5, 74.1, 79.8, 87.5, 90.9, 100.4, 118.0, 120.1, 127.1, 138.7, 139.2, 150.1, 163.1, 164.9, 171.1. HRMS (EI): [M]⁺ C₂₆H₂₈O₄ calcd 404.1982, found 404.1971. R_f (40% EtOAc/hexanes) = 0.5.

1-Benzyl-5-iodopyrimidin-2(1H)-one (36) - Pyrimidine **24** (304 mg, 2.3 mmol) and N-iodosuccinimide (541 mg, 2.4 mmol) in dry DMF (5 mL) were stirred at rt for 48 h. The reaction mixture was treated with Et₂O and the resulting precipitate was collected by filtration. The crude product was washed with MeOH and used without further purification. The crude iodide, K₂CO₃ (934 mg, 6.7 mmol) and benzyl bromide (321 μ L, 2.7 mmol) were dissolved in DMF (10 mL). The reaction mixture was stirred for 16 h at rt and concentrated to dryness. The crude product was purified by column chromatography (CH₂Cl₂/MeOH) to yield **36** (647 mg, 2.1 mmol, 92%, 2 steps) as a yellow solid. ¹H NMR (360 MHz, CDCl₃) δ 5.06 (s, 2H), 7.31 - 7.43 (m, 5H), 7.75 (d, J = 3.1 Hz, 1H), 8.59 (d, J = 3.1 Hz, 1H); ¹³C NMR (90 MHz, CDCl₃) δ 54.3, 63.9, 128.8, 129.0, 129.3, 134.2, 151.2, 154.3, 170.3. HRMS (ESI): [M + H]⁺ C₁₁H₁₀ON₂I calcd 312.9832, found 312.9825. R_f (5% MeOH/CH₂Cl₂) = 0.5.

1-Benzyl-5-((trimethylsilyl)ethynyl)pyrimidin-2(1H)-one (37) - A solution of **36** (298 mg, 1.0 mmol), Ethynyltrimethylsilane (675 μ L, 4.8 mmol), 10% Pd/C (2 mol% based on Pd), PPh₃ (2.5 mol%) and CuI (4 mol%) in 1:1 Et₃N/CH₃CN (10 mL) was refluxed for 4 h under an inert atmosphere. Solids were removed by centrifugation and the remaining mixture was concentrated to dryness. The crude product was purified by column chromatography (CH₂Cl₂/MeOH) to yield **37** (134 mg, 0.5 mmol, 51%) as a yellow solid. ¹H NMR (500 MHz, CDCl₃) δ 0.23 (s, 9H), 5.10 (s, 2H), 7.34 – 7.44 (m, 5H), 7.78 (d, *J* = 3.1 Hz, 1H), 8.62 (s, 1H); ¹³C NMR (125 MHz, CDCl₃) δ -0.3, 54.3, 96.4, 98.8, 102.2, 128.8, 128.9, 129.3, 134.2, 149.7, 154.6, 167.7. HRMS (ESI): [M + H]⁺ C₁₆H₁₉N₂OSi calcd 283.1261, found 283.1256. *R*_f (50% EtOAc/hexanes) = 0.5.

1-Benzyl-5-ethynylpyrimidin-2(1H)-one (20) - **37** (124 mg, 0.4 mmol) was added to a solution of TBAF 3 H₂O (274 mg, 0.8 mmol) and AcOH (48 μ L, 0.8 mmol) in THF (5 mL). The reaction mixture was stirred for 1 h at rt, concentrated to dryness and purified by column chromatography (CH₂Cl₂/MeOH) to yield **20** (68 mg, 0.3 mmol, 81%) as a slightly yellow solid. ¹H NMR (500 MHz, CDCl₃) δ 3.16 (s, 1H), 5.11 (s, 2H), 7.34 – 7.47 (m, 5H), 7.79 (d, *J* = 3.0 Hz, 1H), 8.65 (s, 1H); ¹³C NMR (125 MHz, CDCl₃) δ 54.3, 75.7, 81.2, 101.0, 128.9, 129.1, 129.4, 134.0, 150.1, 154.6, 167.6. HRMS (ESI): [M + H]⁺ C₁₃H₁₁ON₂ calcd 211.0866, found 211.0862. *R*_f (10% MeOH/CH₂Cl₂) = 0.5.

Hex-5-yn-1-yl 4-methylbenzenesulfonate (39).^[80] - 4-Methylbenzenesulfonyl chloride (20.0 g, 105 mmol) was added to a solution of **38** (7.7 mL, 70 mmol) and pyridine (11.3 mL, 140 mmol) in CH₂Cl₂ (150 mL) at 0 °C, warmed to rt and stirred for 16 h. The reaction mixture was treated with water and extracted with CH₂Cl₂. The combined organic layers were washed with 1 M HCl, saturated NaHCO₃, H₂O and brine. The solution was dried over MgSO₄ and concentrated to dryness. The crude product was purified by column chromatography (hexane/EtOAc) to yield **39** (14.0 g, 55 mmol, 79%) as a colorless oil. ¹H NMR (360 MHz, CDCl₃) δ 1.53 – 1.63 (m, 2H), 1.75 – 1.86 (m, 2H), 1.94 (t, *J* = 2.7 Hz, 1H), 2.19 (td, *J* = 2.7, 6.9 Hz, 2H), 2.47 (s, 3H), 4.08 (t, *J* = 6.3 Hz, 2H), 7.34 – 7.40 (m, 2H), 7.78 – 7.84 (m, 2H); ¹³C NMR (90 MHz, CDCl₃) δ 17.7, 21.6, 24.2, 27.8, 69.0, 69.9, 83.4, 127.9, 129.8, 133.1, 144.7. HRMS (EI): [M]⁺ C₁₃H₁₆O₃³²S calcd 252.0815, found 252.0808. *R*_f (20% EtOAc/hexanes) = 0.4

2-(Hex-5-yn-1-yloxy)-1-naphthaldehyde (41) - A suspension of aldehyde **40** (1.4 g, 8 mmol), **39** (3.0 g, 12 mmol), K₂CO₃ (3.3, 24 mmol) and NaI (120 mg, 0.8 mmol) in CH₃CN was refluxed for 16 h. The solution was concentrated, treated with EtOAc/H₂O and the aqueous layer was extracted with EtOAc. The combined organic layers were washed with H₂O and brine, dried over MgSO₄ and concentrated to dryness. The crude product was purified by column chromatography (hexane/EtOAc) to yield **41** (1.49 g, 6 mmol, 75%) as a slightly yellow solid. ¹H NMR (500 MHz, CDCl₃) δ 1.75 – 1.82 (m, 2H), 1.99 – 2.07 (m, 3H), 2.29 – 2.36 (m, 2H), 4.24 (t, *J* = 6.2 Hz, 2H), 7.25 (d, *J* = 9.1 Hz, 1H), 7.43 (ddd, *J* = 1.1, 6.9, 8.0 Hz, 1H), 7.63 (ddd, *J* = 1.4, 6.9, 8.5 Hz, 1H), 7.77 (d, *J* = 8.1 Hz, 1H), 8.03 (d, *J* = 9.1 Hz, 1H), 9.30 (d, *J* = 8.7 Hz, 1H), 10.93 (s, 1H); ¹³C NMR (125 MHz, CDCl₃) δ 18.1, 25.0, 28.3, 68.8, 69.0, 83.8, 113.4, 116.6, 124.7, 124.9, 128.2, 128.4, 129.9, 131.5, 137.6, 163.5, 192.0. HRMS (EI): [M]⁺ C₁₇H₁₆O₂ calcd 252.1145, found 252.1131. *R_f* (25% EtOAc/hexanes) = 0.5.

1-(Bromomethyl)-2-(hex-5-yn-1-yloxy)naphthalene (42) - At 0 °C NaBH₄ (151 mg, 4.0 mmol) was slowly added to a cooled solution of **41** (504 mg, 2.0 mmol) in dry MeOH (5 mL). After 30 min the reaction mixture was treated with H₂O and extracted with EtOAc. The combined organic layers were washed with H₂O and brine, dried over MgSO₄ and concentrated. The crude product was used without further purification. The alcohol was added to a solution of CBr₄ (975 mg, 2.9 mmol) and PPh₃ (772 mg, 2.9 mmol) in THF (20 mL) and stirred for 16 h. The precipitate was removed by filtration and the filtrate was concentrated to dryness. The crude product was purified by column chromatography (hexane/EtOAc) to yield the bromide **42** (515 mg, 1.6 mmol, 81%) as a yellow solid. ¹H NMR (500 MHz, CDCl₃) δ 1.83 – 1.88 (m, 2H), 2.03 – 2.07 (m, 3H), 2.34 – 2.40 (m, 2H), 4.22 (t, *J* = 6.2 Hz, 2H), 5.13 (s, 2H), 7.23 (d, *J* = 9.1 Hz, 1H), 7.36 (d, *J* = 8.1 Hz, 1H), 7.42 (t, *J* = 7.5 Hz, 1H), 7.62 (t, *J* = 7.5 Hz, 1H), 7.81 – 7.87 (m, 1H), 8.06 (d, *J* = 8.6 Hz, 1H); ¹³C NMR (125 MHz, CDCl₃) δ 18.3, 25.1, 25.5, 28.5, 68.6, 69.0, 84.2, 114.0, 118.3, 122.7, 123.9, 127.3, 128.7, 129.1, 129.9, 132.3, 154.6. HRMS (EI): [M]⁺ C₁₇H₁₇O⁷⁹Br calcd 316.0457, found 316.0447. *R_f* (25% EtOAc/hexanes) = 0.6.

1-((2-(Hex-5-yn-1-yloxy)naphthalen-1-yl)methyl)pyrimidin-2(1H)-one (21) - Bromide **46** (201 mg, 0.63 mmol) was added to a suspension of K₂CO₃ (249 mg, 1.80 mmol) and pyrimidine **24**

(100 mg, 0.75 mmol) in DMF (5 mL). The reaction mixture was stirred for 16 h at 70 °C and concentrated to dryness. The crude product was purified by column chromatography (CH₂Cl₂/MeOH) to yield **21** (52 mg, 0.17 mmol, 26%) as a yellow solid. ¹H NMR (500 MHz, CDCl₃) δ 1.67 – 1.76 (m, 2H), 1.94 – 2.03 (m, 3H), 2.25 – 2.32 (m, 2H), 4.24 (t, *J* = 6.3 Hz, 2H), 5.64 (s, 2H), 6.12 (dd, *J* = 4.1, 6.5 Hz, 1H), 7.35 (d, *J* = 9.1 Hz, 1H), 7.38 – 7.43 (m, 2H), 7.53 (t, *J* = 7.3 Hz, 1H), 7.84 (d, *J* = 8.1 Hz, 1H), 7.90 – 7.97 (m, 2H), 8.52 (s, 1H); ¹³C NMR (125 MHz, CDCl₃) δ 18.1, 24.9, 28.4, 43.1, 68.7, 69.0, 83.7, 104.2, 113.5, 114.3, 122.7, 124.3, 128.2, 128.7, 129.1, 131.8, 133.0, 146.4, 155.8, 156.8, 165.1. HRMS (ESI): [M + H]⁺ C₂₁H₂₁N₂O₂ calcd 333.1598, found 333.1594. *R_f* (10% MeOH/CH₂Cl₂) = 0.5.

(S)-Methyl 2-((tert-butoxycarbonyl)amino)-3-hydroxypropanoate (44) - Compound **44** was prepared according to the method of Chamberlain *et al*^[87] to yield **44** (7.2 g, 33 mmol, 73%) as a colorless oil. The spectral data matched with those reported in the literature. ¹H NMR (360 MHz, DMSO) δ 1.39 (s, 9H), 3.56 – 3.71 (m, 4H), 4.01 – 4.14 (m, 1H), 4.88 (t, *J* = 6.1 Hz, 1H), 6.92 (d, *J* = 8.0 Hz, 1H); ¹³C NMR (90 MHz, DMSO) δ 28.6, 52.2, 56.7, 61.8, 78.8, 155.7, 171.9. HRMS (ESI): [M + H]⁺ C₉H₁₈NO₅ calcd 220.1180, found 220.1170.

(R)-Methyl 3-bromo-2-((tert-butoxycarbonyl)amino)propanoate (45) - Alcohol **44** (4.0 g, 18.3 mmol), PPh₃ (7.2 g, 27.5 mmol) and CBr₄ (9.1 g, 27.5 mmol) were dissolved in CH₂Cl₂ (100 mL). The reaction mixture was stirred for 48 h at rt. Et₂O was added and the resulting precipitate was removed by filtration. The organic layer was washed with saturated NaHCO₃ and brine, dried over MgSO₄ and concentrated to dryness. The crude product was purified by column chromatography to yield **45** (3.3 g, 12 mmol, 65%) as a yellow solid. ¹H NMR (250 MHz, CDCl₃) δ 1.40 (s, 9H), 3.59 – 3.87 (m, 4H), 4.62 – 4.80 (m, 1H), 5.36 – 5.54 (m, 1H); ¹³C NMR (63 MHz, CDCl₃) δ 28.2, 34.0, 52.9, 53.9, 80.4, 154.9, 169.6. HRMS (ESI): [M + H]⁺ C₉H₁₇BrNO₄ calcd 282.0336, found 282.0336. *R_f* (30% EtOAc/hexanes) = 0.5.

(S)-Methyl 2-((tert-butoxycarbonyl)amino)-3-(2-oxopyrimidin-1(2H)-yl)propanoate (46) - A suspension of Bromide **45** (2.3 g, 8.3 mmol), pyrimidine **24** (1.3 g, 10 mmol) and K₂CO₃ (3.5 g, 25 mmol) in DMF (50 mL) was stirred for 16 h at rt. The reaction mixture was concentrated to dryness and the crude product was purified by column chromatography (CH₂Cl₂/MeOH) to yield

46 (0.8 g, 2.8 mmol, 33%) as a slightly brown solid. Optical rotation measurements demonstrated that racemization of the chiral centre had occurred during the reaction. ^1H NMR (360 MHz, CDCl_3) δ 1.35 (s, 9H), 3.74 (s, 3H), 4.15 – 4.29 (m, 1H), 4.38 – 4.51 (m, 1H), 4.56 – 4.68 (m, 1H), 5.89 (d, J = 6.8 Hz, 1H), 6.29 (dd, J = 4.2, 6.4 Hz, 1H), 7.69 – 7.80 (m, 1H), 8.53 – 8.58 (m, 1H); ^{13}C NMR (90 MHz, CDCl_3) δ 28.2, 52.1, 52.8, 80.3, 104.1, 149.2, 155.4, 156.5, 162.5, 166.4, 170.2. HRMS (ESI): $[\text{M} + \text{H}]^+$ $\text{C}_{13}\text{H}_{20}\text{N}_3\text{O}_5$ calcd 298.1398, found 298.1393. R_f (10% MeOH/ CH_2Cl_2) = 0.6.

(S)-Methyl 2-(hex-5-ynamido)-3-(2-oxopyrimidin-1(2H)-yl)propanoate (22) - A solution of pyrimidone **46** (298 mg, 1.0 mmol) in 1:1 TFA/ CH_2Cl_2 (2 mL) was stirred for 5 h (0 °C-rt). The reaction mixture was treated with saturated NaHCO_3 and the aqueous phase was extracted with CH_2Cl_2 . The organic phase was dried over MgSO_4 and concentrated. The crude product was used without further purification. HOBt (270 mg, 2.0 mmol) and 5-Hexynoic acid (220 μL , 2.0 mmol) were dissolved in DMF (1 mL) and DIC (309 μL , 2.0 mmol) was added. The reaction mixture was stirred for 30 min at rt. A solution of the amine in DMF (1 mL) was added. The mixture was stirred for 2 h at rt. The reaction mixture was concentrated to dryness and purified by column chromatography ($\text{CH}_2\text{Cl}_2/\text{MeOH}$) to yield **22** (175 mg, 0.6 mmol, 60%) as a yellow solid. ^1H NMR (500 MHz, CD_3OD) δ 1.72 – 1.80 (m, 2H), 2.17 – 2.22 (m, 2H), 2.28 (t, J = 2.7 Hz, 1H), 2.32 – 2.36 (m, 2H), 3.78 (s, 3H), 4.13 (dd, J = 8.8, 13.3 Hz, 1H), 4.60 (dd, J = 5.2, 13.3 Hz, 1H), 4.93 (dd, J = 5.2, 8.8 Hz, 1H), 6.54 (dd, J = 4.3, 6.5 Hz, 1H), 8.02 (dd, J = 2.8, 6.5 Hz, 1H), 8.61 (dd, J = 2.8, 4.3 Hz, 1H); ^{13}C NMR (90 MHz, CD_3OD) δ 18.5, 25.6, 35.2, 51.6, 53.2, 53.2, 70.4, 84.0, 106.1, 151.9, 158.3, 168.0, 171.1, 175.6. HRMS (ESI): $[\text{M} + \text{H}]^+$ $\text{C}_{14}\text{H}_{18}\text{O}_3\text{N}_4$ calcd 292.1292, found 292.1287. R_f (10% MeOH/ CH_2Cl_2) = 0.5.

6-(2-([1,1'-biphenyl]-4-yl)-2-hydroxyethyl)-4-bromo-2H-pyran-2-one (47) - Diisopropylamine (90.4 μL , 0.64 mmol) was dissolved under Ar in 5 mL dry THF. $n\text{BuLi}$ (0.27 mL, 2.4 M in hexanes, 0.64 mmol) was then added and the solution was stirred at rt for 15 min. The reaction mixture was then cooled to -78 °C and 100 μL HMPA was added. After stirring at -78 °C for 30 min, a solution of bromide **33** (100 mg, 0.53 mmol) in 1 mL dry THF was slowly added. The reaction mixture was stirred cold for an additional 40 min, then a solution of biphenyl-4-

carboxaldehyde (116 mg, 0.64 mmol) in 1 mL dry THF was slowly added. The reaction mixture was stirred at $-78\text{ }^{\circ}\text{C}$ for 1 h, then water was added to the cold solution, and the mixture was allowed to warm to rt. EtOAc was added and the organic phase was washed with 2 x 1 M HCl and 1 x satd NaHCO_3 . The organic phase was dried over Na_2SO_4 , filtered and concentrated to dryness. The crude product was purified by flash chromatography to yield **47** (100 mg, 0.27 mmol, 50%) as a white solid. ^1H NMR (360 MHz, CDCl_3) δ 2.79 - 2.99 (m, 3H), 5.20 (m, 1H), 6.32 (s, 1H), 6.48 (s, 1H), 7.32 – 7.52 (m, 5H), 7.55 – 7.66 (m, 4H); ^{13}C NMR (90 MHz, CDCl_3) δ 43.5, 71.0, 110.0, 115.4, 126.0, 127.1, 127.5, 128.9, 140.5, 141.1, 141.4, 141.9, 160.8, 162.0. HRMS (EI): $[\text{M}]^+$ $\text{C}_{19}\text{H}_{15}\text{O}_3^{79}\text{Br}_1$ calcd 370.0199, found 370.0181. R_f (20% EtOAc/hexanes) = 0.2.

6-(2-([1,1'-biphenyl]-4-yl)-2-hydroxyethyl)-4-ethynyl-2H-pyran-2-one (23) - Bromide **47** (100 mg, 0.27 mmol), 10 % Pd/C (5.73 mg), PPh_3 (17.5, 0.067 mmol) and CuI (2.1 mg, 0.011 mmol) were combined in 1.5 mL dry CH_3CN / 2.2 mL dry Et_3N . Trimethylsilylacetylene (64.5 mL, 0.46 mmol) was then added and the solution was heated to $80\text{ }^{\circ}\text{C}$ for 16 h. The reaction mixture was then cooled to rt, the solids filtered off and washed with EtOAc. The resulting organic solution was then washed with 2 x 1 M HCl, and 1 x satd NaHCO_3 . The organic phase was dried over Na_2SO_4 , filtered and concentrated to dryness. The crude product was then passed through a silica plug and was used in the next step without further purification. Crude **48** was dissolved in 2 mL THF and cooled to $-78\text{ }^{\circ}\text{C}$. A solution of TBAF (300 μL , 1.0M in THF, 300 mmol) was slowly added and the solution was stirred for 1.5 h at $-78\text{ }^{\circ}\text{C}$. The cold reaction was quenched by the addition of water and the resulting solution was allowed to warm to rt. EtOAc was added and the organic phase was washed with 1 x satd NaHCO_3 . The organic phase was then dried over Na_2SO_4 , filtered and concentrated to dryness. The crude product was purified by column chromatography to yield **23** (31 mg, 0.097mmol, 36%, 2 steps) as a yellow solid. ^1H NMR (360 MHz, CDCl_3) δ 2.57 (s, br, 1H), 2.81 - 2.98 (m, 2H), 3.50 (s, 1H), 5.20 (m, 1H), 6.11 (s, 1H), 6.33 (s, 1H), 7.32 – 7.56 (m, 5H), 7.55 – 7.66 (m, 4H); ^{13}C NMR (90 MHz, CDCl_3) δ 43.5, 71.1, 79.3, 86.6, 106.9, 116.9, 126.0, 127.0, 127.5, 128.9, 137.8, 140.6, 141.1, 141.9, 161.9, 162.1. HRMS (EI): $[\text{M}]^+$ $\text{C}_{21}\text{H}_{16}\text{O}_3$ calcd 316.1094, found 316.1087. R_f (20% EtOAc/hexanes) = 0.3.

E)-methyl 3-ethynyl-5-oxohex-2-enoate (49) - 18 (16.2 mg, 0.12 mmol) was dissolved in 6 mL MeOH and irradiated at 350 nm at a distance of 1 cm for 30 min. The solvent was then removed and the resulting residue was purified by flash chromatography. The major product was **49** (9.9 mg, 0.060 mmol, 50%). ¹H NMR (360 MHz, CDCl₃) δ 1.62 (s, 3H), 2.71 (m, 2H), 3.39 (s, 3H), 3.53 (s, 1H), 6.26 (s, 1H); ¹³C NMR (90 MHz, CDCl₃) δ 22.9, 39.3, 50.1, 80.4, 87.7, 103.7, 124.2, 135.4, 162.5. MS (EI): [M]⁺ C₉H₁₀O₃ calcd 166.06, found 166.1. R_f (20% EtOAc/hexanes) = 0.35.

tert-butyl (2-(2-oxopyrimidin-1(2H)-yl)ethyl)carbamate (52) - A suspension of 2-(Boc-amino)ethyl-bromide (200 mg, 0.9 mmol), **24** (108 mg, 0.8 mmol) and K₂CO₃ (340 mg, 2.5 mmol) in DMF (5 mL) was stirred for 48 h at rt. The reaction mixture was concentrated to dryness and the crude product was purified by column chromatography (CH₂Cl₂ /MeOH) to yield **52** (186 mg, 0.7 mmol, 88%) as a colorless solid. ¹H NMR (360 MHz, CDCl₃) δ 1.33 (s, 9H), 3.46 (t, J = 5.5 Hz, 2H), 4.01 (t, J = 5.5 Hz, 2H), 6.25 (dd, J = 4.2, 6.4 Hz, 1H), 7.65 – 7.75 (m, J = 3.9 Hz, 1H), 8.45 – 8.55 (m, 1H). ¹³C NMR (90 MHz, CDCl₃) δ 28.3, 38.9, 51.2, 79.5, 104.0, 149.0, 156.2, 156.5, 166.0. HRMS (ESI): [M + H]⁺ C₁₁H₁₈O₃N₃ calcd 240.1343, found 240.1344. R_f (10% MeOH/CH₂Cl₂) = 0.3.

1-(2-aminoethyl)pyrimidin-2(1H)-one (53) - A solution of pyrimidone **52** (97 mg, 0.4 mmol) in 1:1 TFA/CH₂Cl₂ (2 mL) was stirred for 5 h (0 °C-rt). The reaction mixture was poured into ice cold Et₂O. The precipitate was collected by centrifugation and dried under reduced pressure. The crude product **53** (101 mg, 0.4 mmol, quant.) was used without further purification. ¹H NMR (500 MHz, CD₃OD) δ 3.48 (s, br, 2H), 4.40 (s, br, 2H), 6.74 (s, br, 1H), 8.50 (s, br, 1H), 8.74 (s, br, 1H). ¹³C NMR (125 MHz, CD₃OD) δ 38.2, 49.5, 105.3, 153.3, 155.1, 164.9. HRMS (ESI): [M + H]⁺ C₆H₁₀ON₃ calcd 140.0818, found 140.0819.

N'-(hex-5-ynamide)-vancomycin (54) - This compound was prepared according to Eirich *et al.* The characterization data for this compound matched with those reported in the literature.

N'-(hex-5-ynamide)-C-[1-(2-aminoethyl)pyrimidin-2(1H)-one]-vancomycin (55) - N'-(hex-5-ynamide)-vancomycin (**54**) (30 mg, 19 μmol), pyrimidone **53** (10 mg, 39 μmol) and DIPEA (16 μL, 95 μmol) were dissolved in DMF. PyBOP (11 mg, 21 μmol) and HOBT (4 mg, 21 μmol) were

added and the reaction mixture was stirred for 16 h at rt. The solution was poured into cold Et₂O and the precipitate was collected by centrifugation and dried under reduced pressure. The crude product was purified by HPLC to yield **55** (22 mg, 13 μmol, 68%) as a colorless solid. HRMS (ESI): [M + H]⁺ C₇₈H₈₉O₂₅N₁₂Cl³⁷Cl calcd 1665.5404, found 1665.5488.

Preparation of proteome for photolabeling experiments - The proteomes of the bacterial strains *Staphylococcus aureus* Mu50, *E. coli* K12 and *Listeria welshimeri* SLCC 5334 were prepared from 1 L liquid cultures in BHB or LB medium, harvested 1 h after transition in the stationary phase by centrifugation at 9000 rpm. The bacterial cell pellet was washed with PBS, resuspended in PBS, and lysed by sonication with a Bandelin Sonopuls instrument under ice cooling. Membrane and cytosol were separated by centrifugation at 9000 rpm for 45 min.

Recombinant expression - ATlam and pABC were recombinantly expressed in BL21 *E. coli* as described by Eirich *et al.*^[94] For overexpression labeling, recombinant clones were grown in ampicillin LB medium and target gene expression was induced with anhydrotetracyclin or IPTG depending on the expression vector used.

Proteome photolabeling experiments - Proteome samples were adjusted to a final concentration of 1 mg protein/mL by dilution with PBS prior to probe addition. Experiments were carried out in 43 μL total volume, such that once click chemistry reagents were added, the total volume was 50 μL. Probes were added at various concentrations in 1 μL DMSO to achieve the desired final concentration. Photolysis was carried out over ice cooling in 96 well plates with either 2 x 8 W Hitachi FL8BL-B lamps centred at 350 nm, or 1 x 15 W Herolab lamp at 312 nm. The distance from lamp to sample was approximately 2 cm. For heat controls, the proteome was denatured with 2 % SDS (4 mL of 21.5 % SDS) at 95 °C for 6 min and cooled to room temperature before the probe was applied. Following incubation, reporter-tagged azide reagents 13 μM rhodamine-azide (1 μL) were added, followed by 1 mM TCEP (1 μL) and 100 μM ligand (3 μL). Samples were gently vortexed, and the cycloaddition was initiated by the addition of 1 mM CuSO₄ (1 μL). The reactions were incubated at room temperature for 1 h. For analytical gel electrophoresis, 50 μL of 2 × SDS loading buffer was added and 50 μL applied on the gel.

Fluorescence was recorded in a Fujifilm Las-4000 luminescent image analyzer with a Fujinon VRF43LMD3 lens and a 575DF20 filter.

Synthesis of a benzophenone-alkyne tag for reversible inhibitor-target profiling

Introduction

Natural product isolates are an important source for new biomedical lead structures. Especially compounds extracted from marine organism's exhibit a broad range of bioactivities. *Pseudopterogorgia elisabethae* is a soft coral abundant in the Caribbean region and a rich source of biological active natural products.^[95] One of these compounds is Pseudopterosin A (PsA, **1**, Figure 1A), a tricyclic diterpene with a reported antibacterial activity against *Streptococcus pyogenes*, *Enterococcus faecalis* and *Staphylococcus aureus* with MIC values of 1.9 μM/4.9 μM/7.9 μM, respectively.^[96]

The investigation of the molecular targets of PsA to unravel the mode of action by a derived probe is complicated by two limitations: the biological activities of this compound rely on a reversible binding mechanism and the design of a derived probe is complicated by a limited number of chemically tolerated modifications. We therefore were inspired to develop a universal applicable tag that combines a photo reactive group for UV-light induced crosslinking of target proteins, an alkyne handle for downstream target identification using click chemistry and an activated linker for the connection to reversible binding natural products like PsA (Figure 1A).

The advantage of this tool is the modification of non-covalent inhibitors by the linked introduction of a crosslinking- and reporter group by one single substitution reaction: synthetic efforts and changes of the bioactive structure could be minimized.

In this report we present the synthesis of the alkyne modified benzophenone tool **2** and its application in the synthesis of a PsA ABPP probe (**3**) (Figure 1B).

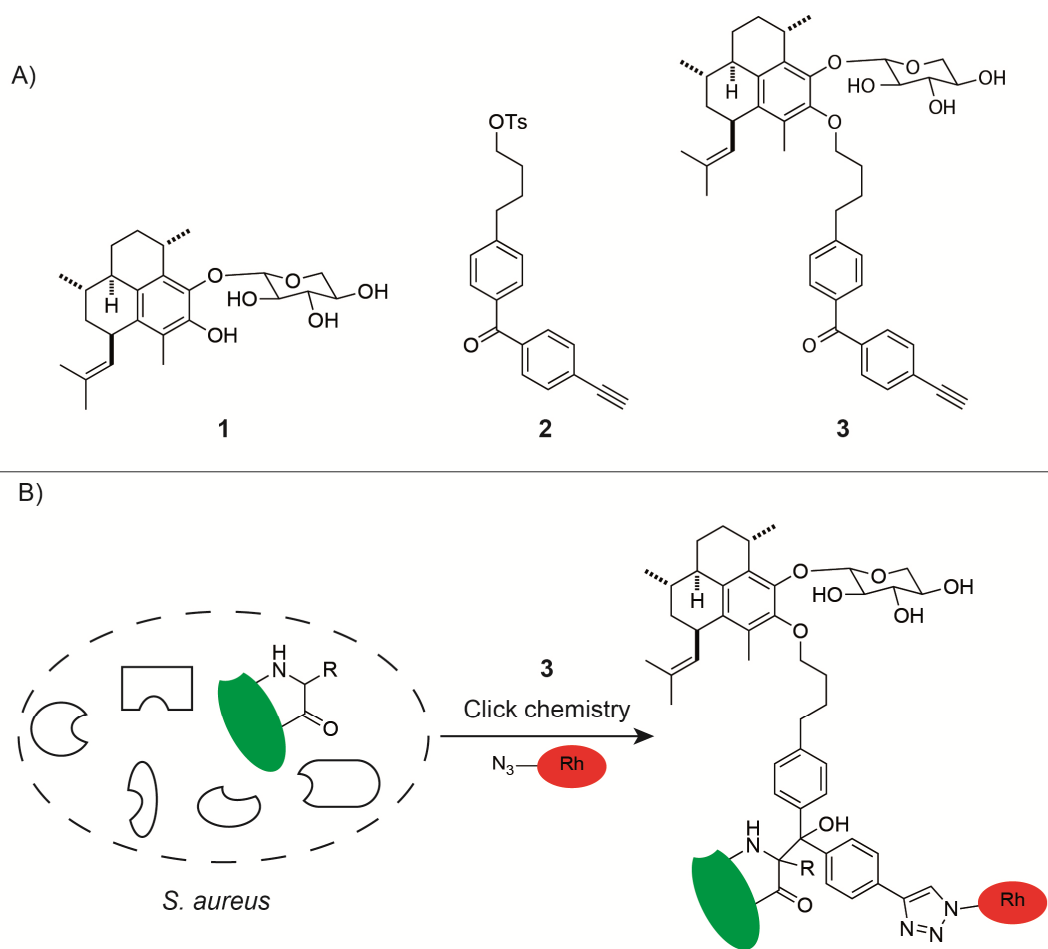
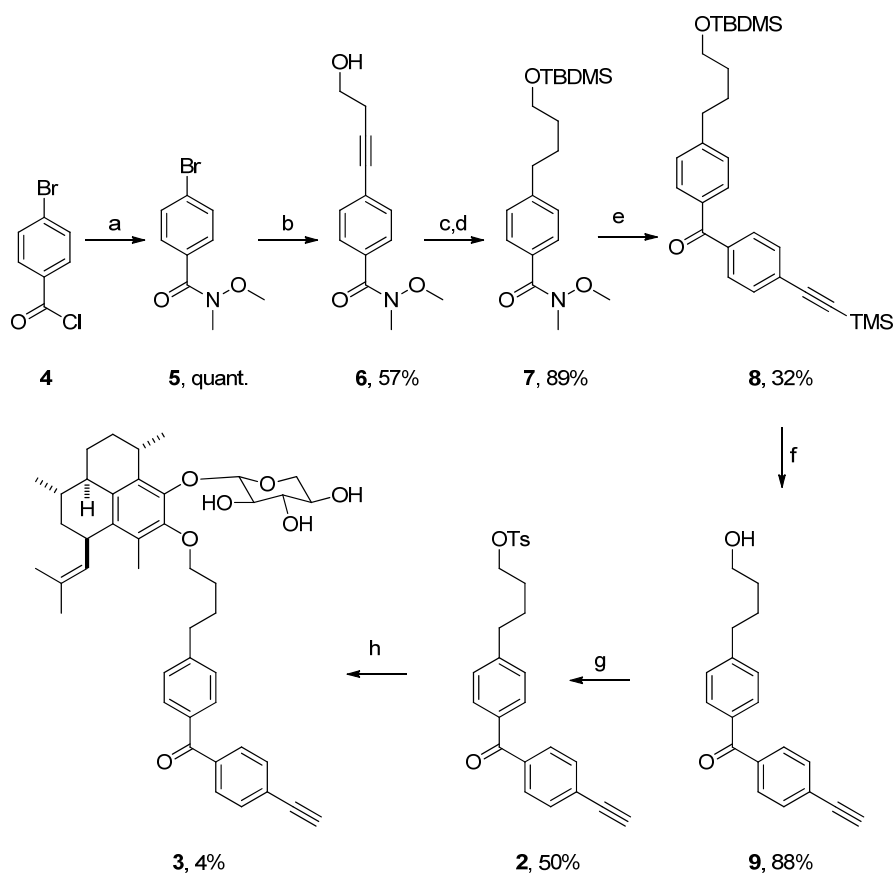


Figure 1. A) Structure of PsA (1), photocrosslinker 2 and probe 3. B) Conjugation of a rhodamine tag to probe modified proteins by click chemistry.

Results and Discussion

The central reaction for the synthesis of the benzophenone moiety is the Grignard reaction between the TBDMS protected Weinreb amide **7** and commercial available (4-Bromophenylethynyl)-trimethylsilane (Scheme 1). **7** was synthesized from 4-bromobenzoyl chloride (**4**). Introduction of the amide by treatment of **4** with *N,O*-Dimethylhydroxylamin^[97] followed by a Sonogashira cross-coupling with 3-Butyn-1-ol yielded precursor **6** in a good yield of 57%. The four-carbon chain was implemented as a spacer to retain conformational flexibility for the photocrosslinking reaction with target-protein-residues. Subsequent hydrogenation of **6** and TBDMS-protection of the free hydroxyl group gave building block **7** with 89% yield.

The Grignard reagent for the synthesis of the benzophenone derivative **8** was formed by treatment of (4-bromophenylethynyl)trimethylsilane with pre-activated Mg. The reaction with **7** and the subsequent simultaneous deprotection of the hydroxyl-group and the alkyne with TBAF completed the benzophenone photocrosslinker **9** supplemented with a universal linker and an alkyne as a multifunctional reporter group. With the aim to modify PsA by a substitution reaction at the phenolic PsA-hydroxyl group **9** was transformed to the corresponding toluenesulfonate ester **2** which was then reacted with the natural product **1** to finally yield the ABPP-probe **3** (Scheme 1). Moderate yields for this step are probably due to low reactivity of the PsA-hydroxyl group towards the activated linker. PsA starting material could be recovered by HPLC separation.



Scheme 1. Synthesis of photocrosslinker **2**. a) *N,O*-Dimethylhydroxylamin, pyridine, CH_2Cl_2 , $0\text{ }^\circ\text{C}$ -rt; b) 3-Butyn-1-ol, PdCl_2 , CuI , PPh_3 , NEt_3 , Δ ; c) H_2 , Pd/C , EtOH , rt; d) TBDMSCl , imidazole, DMF , rt; e) Mg , (4-Bromophenylethynyl)trimethylsilane, THF , Δ ; f) TBAF , AcOH , THF , rt; g) TsCl , pyridine, CH_2Cl_2 , $0\text{ }^\circ\text{C}$ -rt; h) **1**, K_2CO_3 , NaI , DMF , $70\text{ }^\circ\text{C}$.

The most important concern about changing a natural product with a tag is the impact of the modification on the biological activity. We addressed this question in our case by measuring and comparing the minimal inhibitory concentrations (MICs) of PsA and the derived probe **3** against *S. aureus* NCTC 8325 (Figure 2). As reported in the literature^[96] the MIC for the natural product was in the range of 5-10 μM however, probe **3** did not show any growth inhibition up to concentrations of 500 μM . This result demonstrates that the introduction of our photocrosslinker at the phenolic hydroxyl group is not tolerated concerning the antibacterial activities of PsA against *S. aureus*. Although previous studies show that alkylation of the phenolic hydroxyl group

on the pseudopterosin aglycone retains at least some activity^[98] the molecular weight ratio of natural product to photocrosslinker in this case might be inappropriate to generate a bioactive probe.

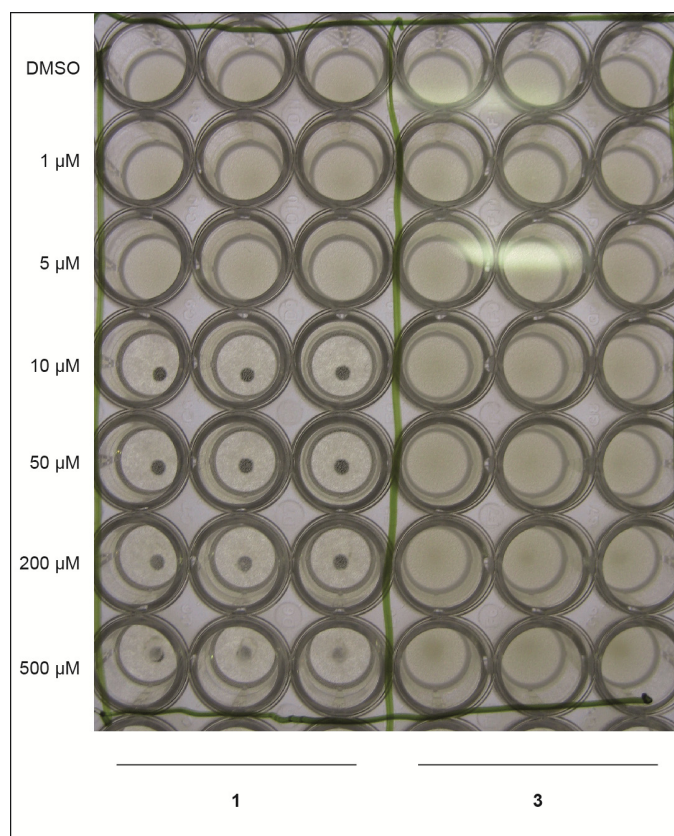


Figure 2. Comparative MIC of **1** and **3** in *S. aureus* NCTC 8325.

Relying on the initial results, that **3** is not a suitable probe to investigate the molecular functions of PsA in a biological system we were encouraged to use **3** as a biological inspired probe in a general ABPP “fishing” experiment to validate the benefits of our photocrosslinker system.

Soluble fractions of *S. aureus* cell lysate were pre-incubated for 20 min with different concentrations of **3** ranging from 50-500 μM. One hour irradiation with 366 nm UV light was then carried out over ice cooling in a 96-well plate. The reaction mixtures were then reacted with a fluorescent dye (RhN₃) through an alkyne-azide cycloaddition protocol (click chemistry) and proteins subsequently analysed by SDS-gel electrophoresis and in-gel fluorescence scanning.

Figure 3 compares irradiated and non-irradiated samples with different probe concentrations and a DMSO negative control. The gel shows that our strategy does not cause a strong and specific protein labeling pattern. The similarities between the coomassie (coo.) staining and the obtained labeling patterns with the highest probe concentrations show that interactions with most abundant proteins cause a negligible fluorescence signal. Unspecific and only light labeling illustrated **3** as insufficient ABPP probe for downstream mass spectrometric target identification experiments.

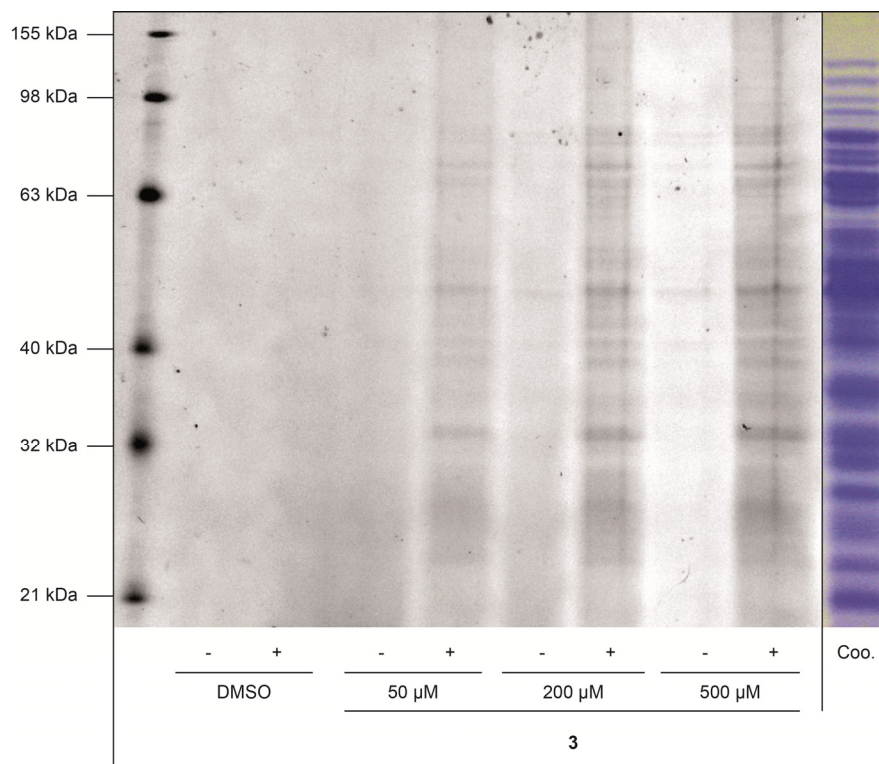


Figure 3. Concentration dependent labeling experiments of *S. aureus* proteome with probe **3**. (-: no irradiation control; +: irradiation with 366 nm UV light)

Conclusion

Identification of non-covalent interactions between reversible inhibitors and their targets relies on the design of derived probes with intrinsic crosslinking reactivity. To simplify the modification of the underlying natural product we designed and successfully synthesized a new benzophenone based reporter group with a linker and an alkyne for the application of click chemistry based target identification protocols.

Pseudopterosin A is an interesting compound with promising antibacterial bioactivity. Since its mode of action is most likely based on non-covalent target interactions we chose this molecule for proof of principle studies with our new tag. To our surprise the exemplary introduction of our tool into the PsA structure caused a loss of the antibacterial activity against *S. aureus* and did not result in a specific labeling pattern in soluble *S. aureus* cell fractions.

On the basis of these results two potential limitations of this approach have to be considered: The first one addresses the general application of benzophenones in conjugation with an alkyne as a photocrosslinker. So far no reported data confirm our hypothesis that the extension of the conjugated system by an alkyne does not change the well known photo chemistry of bezophenones. The second one addresses the application of our tool to design a PsA-photo probe. Changes of the biological PsA-profile by the introduction of our crosslinker exclude this compound as an adequate test system. Further experiments will be needed to validate and maybe tune the photo reactivity of our cross linker and to select other natural products for the implementation of this tool.

Experimental Section

Reagents and solvents were of reagent grade and used without further purification as obtained from commercial sources. PsA was a kind gift from Prof. Brück, Fachgebiet Industrielle Biokatalyse, Technische Universität München and Russell G. Kerr, Department of Chemistry, and Department of Biomedical Sciences, Atlantic Veterinary College - University of Prince Edward Island. Reactions sensitive to air and moisture were carried out under an inert atmosphere. Column chromatography was performed on Merck silica gel (Geduran Si 60, 0.040-0.063 mm). HPLC analysis was performed on a Waters 2695 separation module, a Waters PAD 2996 and a Waters XBridge C18 column (4.6 x 100 mm). For preparative scale HPLC separation, a Waters 2545 quaternary gradient module in combination with a Waters PAD 2998 and a Waters XBridge C18 (30 x 150 mm) or a YMC Triart C18 (10 x 250 mm) column was used. Mobile phase: water, 0.1% (v/v) TFA and acetonitrile, 0.1% (v/v) TFA unless otherwise noted. ^1H NMR and ^{13}C NMR spectra were recorded at rt on Bruker Avance 360, Avance 500 and Avance III 500 spectrometers and were calibrated to the residual proton and carbon signal of the deuterated solvent. Mass spectra were obtained on a Thermo Scientific DFS High Resolution GC/MS (EI) and a LTQ FT Ultra (ESI). *S. aureus* labeling experiments and MICs have been performed as described previously.^[99-100]

4-Bromo-N-methoxy-N-methylbenzamide (5) - Compound **5** was prepared according to the method of Uehara et al. The spectral data matched with those reported in the literature.^[97]

4-(4-Hydroxybut-1-yn-1-yl)-N-methoxy-N-methylbenzamide (6) - To a solution of **5** (4.0 g, 16.4 mmol) in triethylamine (40 mL) was added PPh_3 (52 mg, 0.2 mmol), CuI (38 mg, 0.2 mmol) and 3-Butyn-1-ol (5 mL, 64.2 mmol) under inert atmosphere. The solution was degassed and PdCl_2 (142 mg, 0.8 mmol) was added. The mixture was refluxed for 3 h, concentrated to dryness and purified by column chromatography to yield **6** (2.2 g, 9.4 mmol, 57%) as a colorless oil. ^1H NMR (360 MHz, CDCl_3) δ 2.72 (t, J = 6.3 Hz, 2H), 3.37 (s, 3H), 3.55 (s, 3H), 3.84 (q, J = 6.2 Hz, 2H), 7.38 – 7.54 (m, 2H), 7.58 – 7.70 (m, 2H). ^{13}C NMR (125 MHz, CDCl_3) δ 23.9, 61.1,

61.1, 76.8, 81.8, 88.5, 125.8, 128.3, 131.3, 133.2, 169.2. HRMS (EI): $[M]^+$ $C_{13}H_{13}NO_3$ calcd 233.1046, found 233.1046. R_f (EtOAc) = 0.5.

4-(4-((Tert-butyldimethylsilyl)oxy)butyl)-N-methoxy-N-methylbenzamide (7) - A suspension of **6** (2.2 g, 9.4 mmol) and 10% Pd/C (220 mg) in ethanol was stirred under hydrogen atmosphere (1 atm) for 3 d. The catalyst was removed by filtration and the filtrate was concentrated to dryness. The crude product was dissolved in DMF. Imidazole (1.1 g, 15.8 mmol) and TBDMS-Cl (2.4 g, 15.8 mmol) were added and the solution was stirred for 2 h at rt. The reaction was diluted with EtOAc and washed with 1x water and 1x saturated $NaHCO_3$. The organic phase was dried over $MgSO_4$, filtered and concentrated to dryness. The crude product was purified by flash chromatography to yield **7** (2.9 g, 8.2 mmol, 89%) as a colorless oil. 1H NMR (360 MHz, $CDCl_3$) δ 0.02 – 0.09 (m, 6H), 0.86 – 0.97 (m, 9H), 1.49 – 1.61 (m, 2H), 1.63 – 1.78 (m, 2H), 2.68 (t, J = 7.6 Hz, 2H), 3.37 (s, 3H), 3.59 (s, 3H), 3.65 (t, J = 6.3 Hz, 2H), 7.23 (d, J = 8.2 Hz, 2H), 7.63 (d, J = 8.2 Hz, 2H). ^{13}C NMR (125 MHz, $CDCl_3$) δ -5.3, 18.4, 26.0, 27.4, 32.3, 33.9, 35.6, 61.0, 62.9, 128.0, 128.3, 131.4, 145.6, 170.0. HRMS (ESI): $[M+Na]^+$ $C_{19}H_{33}O_3N^28SiNa$ calcd 374.2122, found 374.2122. R_f (20% EtOAc/hexanes) = 0.3.

(4-(4-((tert-butyldimethylsilyl)oxy)butyl)phenyl)(4-((trimethylsilyl)-

ethynyl)phenyl)methanone (8)- Magnesium turnings (180 mg, 7.9 mmol) were activated with iodine and MeI in dry THF under a inert atmosphere. A solution of (4-Bromophenylethynyl)trimethylsilane (1.0 g, 3.9 mmol) in dry THF was added drop wise and the mixture was refluxed for 4 h. **7** (1.0 g, 2.8 mmol) dissolved in THF was added and the suspension was refluxed for additional 16 h. The reaction was treated with ice and saturated NH_4Cl and extracted with Et_2O . The combined organic layers were washed with saturated $NaHCO_3$ and H_2O . The solution was dried over $MgSO_4$ and concentrated to dryness. The crude product was purified by flash chromatography to yield **8** (419 mg, 0.9 mmol, 32%) as a yellow solid. 1H NMR (360 MHz, $CDCl_3$) δ 0.07 (s, J = 3.9 Hz, 6H), 0.29 (s, J = 3.5 Hz, 9H), 0.92 (s, J = 3.0 Hz, 9H), 1.55 – 1.65 (m, 2H), 1.69 – 1.79 (m, 2H), 2.74 (t, J = 7.6 Hz, 2H), 3.66 (t, J = 6.3 Hz, 2H), 7.29 – 7.34 (m, 2H), 7.55 – 7.60 (m, 2H), 7.70 – 7.78 (m, 4H). ^{13}C NMR (125 MHz, $CDCl_3$) δ -5.3, -0.1, 18.4, 26.0, 27.4, 32.3, 35.7, 62.9, 97.6, 104.1, 127.0, 128.4, 129.8, 130.3,

131.7, 134.9, 137.3, 148.1, 195.7. HRMS (ESI): $[M+H]^+$ $C_{28}H_{41}O_2^{28}Si_2$ calcd 465.2640, found 465.2644. R_f (10% EtOAc/hexanes) = 0.6.

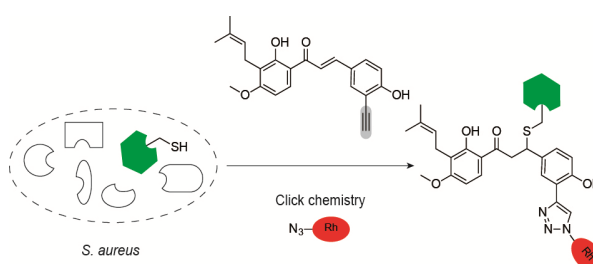
(4-ethynylphenyl)(4-(4-hydroxybutyl)phenyl)methanone (9) - A solution of **8** (419 mg, 0.9 mmol), TBAF·3 H₂O (1.1 g, 3.6 mmol) and AcOH (216 μ L, 3.6 mmol) in THF was stirred at rt for 1 h. The mixture was concentrated to dryness and purified by column chromatography to yield **9** (217 mg, 0.8 mmol, 88%) as a yellow solid. ¹H NMR (360 MHz, CDCl₃) δ 1.60 – 1.70 (m, 2H), 1.73 – 1.84 (m, 2H), 2.76 (t, J = 7.6 Hz, 2H), 3.26 (s, 1H), 3.71 (t, J = 6.4 Hz, 2H), 7.31 (t, J = 7.5 Hz, 2H), 7.59 – 7.64 (m, 2H), 7.72 – 7.79 (m, 4H). ¹³C NMR (125 MHz, CDCl₃) δ 27.3, 32.2, 35.7, 62.7, 80.0, 82.9, 126.0, 128.5, 129.9, 130.3, 132.0, 134.9, 137.7, 147.8, 195.6. HRMS (ESI): $[M+H]^+$ $C_{19}H_{19}O_2^{28}$ calcd 279.1379, found 279.1381. R_f (50% EtOAc/hexanes) = 0.5.

4-(4-(4-ethynylbenzoyl)phenyl)butyl 4-methylbenzenesulfonate (2) - TsCl (228 mg, 1.2 mmol) and pyridine (128 μ L, 1.6 mmol) were added to a solution of **9** (111 mg, 0.4 mmol) in CH₂Cl₂ at 0 °C. The mixture was stirred at rt for 16 h. The solution was diluted with CH₂Cl₂, washed with 1 N HCl, dried over MgSO₄ and concentrated to dryness. The crude product was purified by flash chromatography to yield **2** (107 mg, 0.2 mmol, 50%) as a yellow solid. ¹H NMR (360 MHz, CDCl₃) δ 1.67 – 1.81 (m, 4H), 2.46 (s, 3H), 2.69 (s, 2H), 3.26 (s, 1H), 4.08 (s, 2H), 7.25 (d, J = 8.2 Hz, 2H), 7.36 (d, J = 8.2 Hz, 2H), 7.61 (d, J = 8.4 Hz, 2H), 7.70 – 7.84 (m, 6H). ¹³C NMR (125 MHz, CDCl₃) δ ¹³C NMR (126 MHz, CDCl₃) δ 21.7, 26.8, 28.3, 35.2, 70.2, 80.0, 82.8, 126.1, 127.9, 128.4, 129.9, 130.3, 132.0, 133.0, 135.1, 137.6, 144.8, 147.0, 195.6. HRMS (ESI): $[M+H]^+$ $C_{26}H_{25}O_4S$ calcd 433.1468, found 433.1461. R_f (33% EtOAc/hexanes) = 0.5.

PsA-probe 8 - A solution of PsA (8 mg, 18 μ M), **7** (7 mg, 16 μ M) K₂CO₃ (10 mg, 72 μ M) and NaI (kat) in DMF was stirred for 16 h at 70 °C. The mixture was concentrated to dryness. The solvent was removed under reduced pressure and the crude product was purified by HPLC to yield **8** (0.5 mg, 0.7 μ M, 4%) as a yellow solid. HRMS (ESI): $[M+Na]^+$ $C_{44}H_{52}O_7Na$ calcd 715.3605, found 715.3575.

Target profiling of 4-hydroxyderricin in *S. aureus* reveals seryl-tRNA synthetase binding and inhibition by covalent modification

This chapter was published in: O. A. Battenberg, Y. Yang, S. H. L. Verhelst, S. A. Sieber,
Molecular BioSystems **2013**, 9, 343-351.



Abstract

4-Hydroxyderricin is a heat labile bioactive chalcone isolated from the plant *Angelica keiskei*. It received attention due to its antibiotic potency against several strains of bacteria including pathogens such as *Staphylococcus aureus*. Despite these promising pharmacological properties, the exact mode of action or the biological targets are still unknown. Here we report the synthesis and the application of a 4-hydroxyderricin probe for activity-based protein profiling (ABPP) in *S. aureus*. Due to the heat sensitivity of the natural product we utilize a chemical tool for the mild and selective enrichment of labile probe-protein conjugates and report seryl-tRNA synthetase (STS) to be covalently modified by our probe. This modification results in inhibition of the amino acylation of tRNAs catalyzed by *S. aureus* STS which is an essential enzymatic pathway for bacterial viability.

Introduction

Amino-acyl-tRNA synthetases (AARS) are essential enzymes for the biosynthesis of proteins by catalyzing the specific condensation of a single amino acid (AA) with its corresponding tRNA. This conjugation reaction proceeds by a reaction sequence that is mandatory for all ribosomal peptide synthesis: recognition of the correct AA, activation by ATP-hydrolysis (formation of an aminoacyl-adenylate) and transfer to the 3' end of the cognate tRNA (Figure 1).^[101]

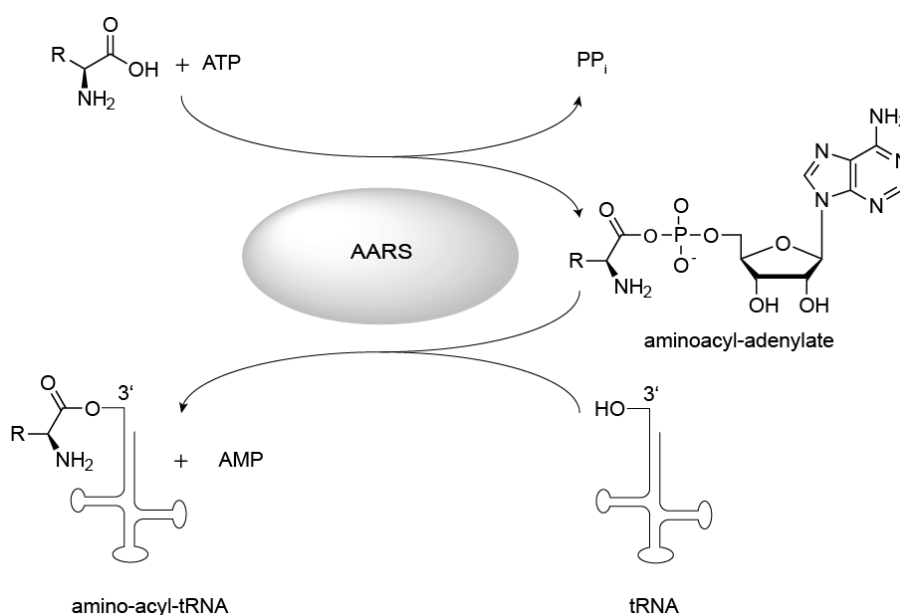


Figure 1. Enzymatic mechanism of AARS.

Inhibition of this important cellular function leads to the accumulation of uncharged tRNAs at the ribosome and finally results in the interruption of protein biosynthesis.^[102] Although a variety of reported inhibitors for AARS (Figure 2) in different organisms demonstrate the potential of these enzymes as interesting antimicrobial targets, so far just one compound has found general application in clinical practice.^[101-107] This compound, Mupirocin, is the only approved topical antibacterial agent with potent activity against gram-positive pathogens including MRSA by the selective inhibition of bacterial isoleucyl-tRNA synthetase. However, the widespread clinical use of Mupirocin is accompanied by the emergence of resistance mechanisms and accentuates the

need for the identification of new natural or synthetic compounds that inhibit amino-acyl-tRNA synthetases as validated antibacterial targets. ^[108]

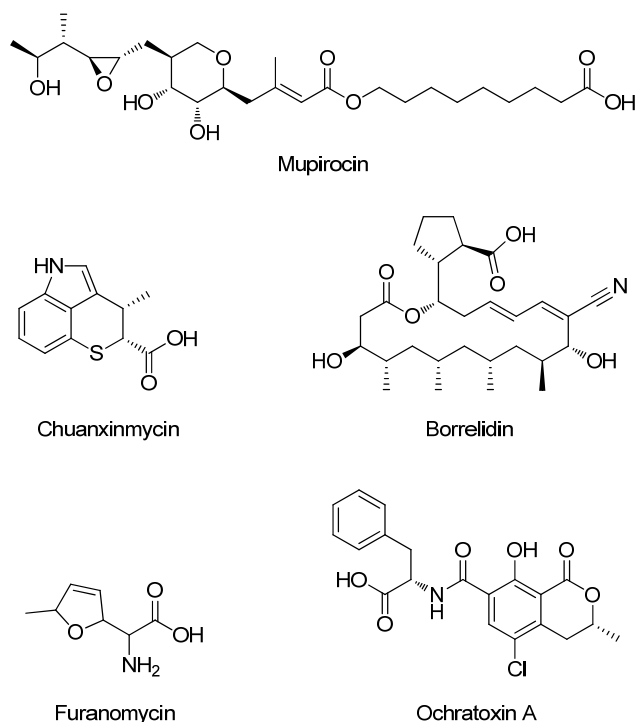


Figure 2. Molecular structures of selected AARS-inhibitors. ^[101-102]

4-Hydroxyderricin (**1**, 4-HD, Figure 3A) is an antibacterial chalcone that was isolated as a main component from *Angelica keiskei*, a hardy perennial herb from the Pacific coast of Japan. ^[109] Since the publication of its total synthesis in 2008, the interest in the antibacterial potential of this compound is growing. ^[110-111] Structure-activity relationship (SAR) studies of 31 antibacterial chalcones revealed that compound **1** exhibits the highest activity against *S. aureus* with an MIC of 23 μ M and a cytotoxicity against human cancer cell lines with an IC_{50} 5.5 μ M. ^[20-21] However, as with many natural products the biological targets and mode of action in bacterial systems of **1** is still unknown. The electrophilic character of the central Michael acceptor and the reported reactivity of **1** towards free thiols led us to believe that the biological activities of **1** might arise from the covalent modification of its target-structures. ^[22-23] In order to elucidate the binding mode as well as corresponding bacterial targets we designed molecular probe **2** bearing an alkyne handle for downstream target identification via activity based protein profiling (ABPP) and

MS identification (Figure 3B).^[8-9] The position of the alkyne was selected based on the available SAR data for the individual building blocks of **1**.^[112]

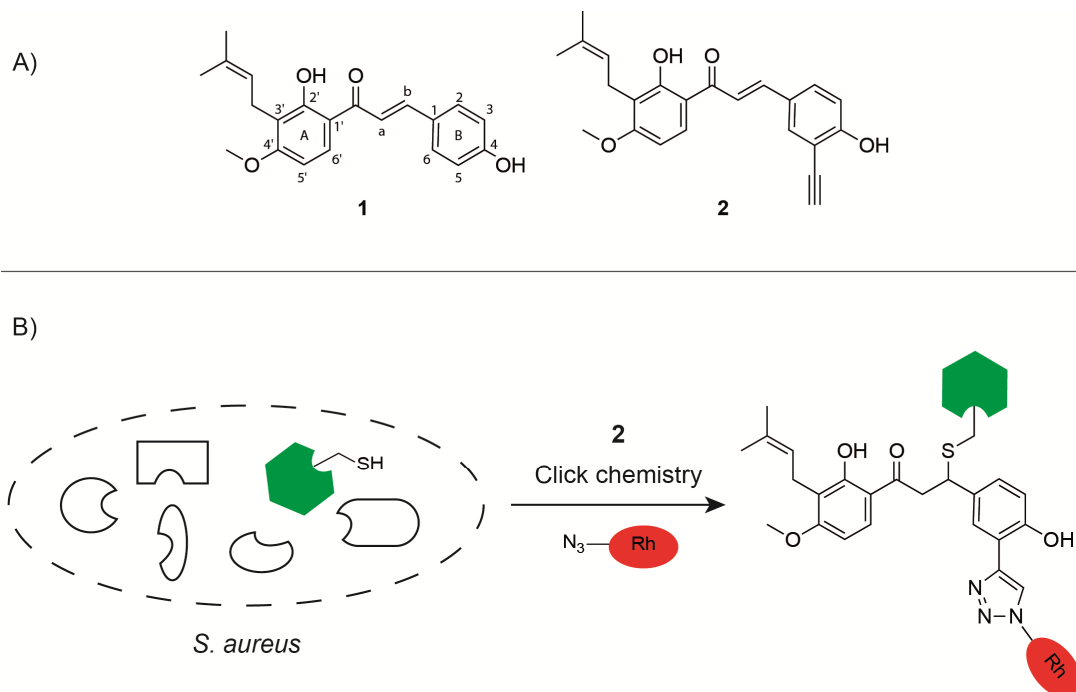
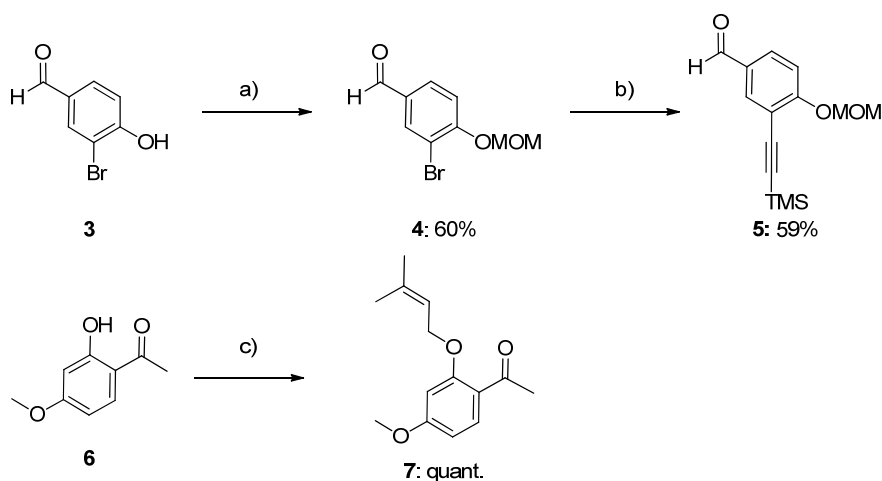


Figure 3. A) Structure and numbering of 4-HD (**1**) and probe **2**. B) Conjugation of a rhodamine tag to probe modified proteins by click chemistry.

In this paper we characterize 4-HD and its derived probe **2** for target interactions by an in-depth chemical biology approach in the bacterial pathogen *S. aureus*. Our studies show that seryl-tRNA synthetase (STS) is inhibited by **2** and provide first insights into a possible antibiotic mode of action. Moreover, we introduce a novel chemical tool for the mild and selective detachment of labile compound-protein conjugates off solid support - a critical step in proteome target applications.

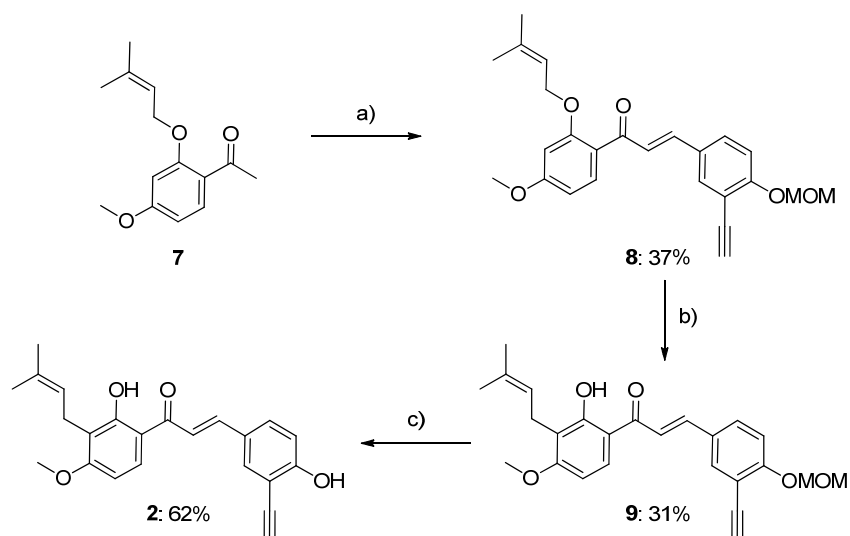
Results and Discussion

In order to investigate the target preferences of 4-HD in proteome studies we applied synthetic protocols derived from published procedures and prepared the natural product as well as a probe derivative.^[111, 113] The synthesis of probe **2** represents a modification of the total synthesis of 4-HD (**1**) with the introduction of an alkyne in the 5-position (Figure 3). The central reaction step for the synthesis of the chalcone **2** was a Claisen-Schmidt condensation of the intermediates **5** and **7**. Aldehyde **5** was prepared by the MOM protection of the commercial available alcohol **3**^[114] followed by a Sonogashira cross-coupling with trimethylsilylacetylene (Scheme 1).



Scheme 1. Synthesis of chalcone building blocks **5** and **7**. a) MOMCl, K₂CO₃, acetone, Δ; b) Trimethylsilylacetylene, PdCl₂, CuI, PPh₃, piperidine, Δ; c) prenyl chloride, K₂CO₃, acetone, Δ.

The reaction of alcohol **6** with prenyl chloride yielded ketone **7** for use in the subsequent condensation reaction.^[113] An aldol condensation of both building blocks with 3 M NaOH in EtOH gave chalcone **8** with the simultaneous removal of the TMS alkyne protecting group (Scheme 2). Rearrangement of the prenyl group in the presence of the solid acid catalyst montmorillonite K10 followed by MOM deprotection with *p*-toluenesulfonic acid finally yielded the 4-HD-probe **2** (Scheme 2).



Scheme 2. Synthesis of 4-HD probe **2**. A) **5**, NaOH, EtOH; b) Montmorillonit K10, CH₂Cl₂, 0 °C; c) p-TsOH, MeOH, 30 °C.

Our intention with the design of **2** was to keep the final probe structurally as similar to the natural product as possible without changing the biological activity. To confirm that the slight modification retained the biological effect we compared the antibacterial potential of the natural product **1** with probe **2** by measuring the growth inhibition of *S. aureus* NCTC 8325 (Supporting Figure 1, Appendix 2). To our satisfaction both compounds exhibited a minimal inhibitory concentration (MIC) below 5 μ M demonstrating that the modification of **1** by addition of an alkyne tag did not change the antibacterial properties in *S. aureus*. The reported value is even slightly lower than reported in literature (5 vs. 23 μ M) and confirms the potent antibacterial effect of 4-HD. ^[21]

Based on the hypothesis that the antibacterial activities of **1** and **2** might rely on a covalent modification of the cellular target we applied probe **2** in a *S. aureus* NCTC 8325 proteome labeling experiment. Soluble fractions of cell lysate were incubated with different concentrations of **2** ranging from 5-100 μ M. After 1 h, probe modified proteins were reacted with a fluorescent dye (RhN₃, Supporting Figure 2, Appendix 2) through an alkyne-azide cycloaddition protocol (click chemistry)^[115-117], separated based on their molecular weight via SDS-gel electrophoresis and analyzed by in-gel fluorescence scanning. Labeling of *S. aureus* lysate with probe **2**

revealed several protein bands in the region of about 50 kDa which exhibited stronger labeling intensities with increasing probe concentrations (Figure 4A, Supporting Figure 3, Appendix 2). Heat denaturation of the proteome prior to probe labeling resulted in an attenuation of the labeling pattern which shows the selectivity of the probe for correctly folded protein structures (Figure 4A). In order to confirm that the natural product and the probe share the same protein binding preferences the *S. aureus* proteome was pre-treated with a 1x, 5x, 10x and 50x excess of unmodified **1** for 20 minutes, and subsequently incubated with 100 μ M of probe **2**. Fluorescent SDS analysis of this sample revealed a strong reduction of protein labeling at 5-fold excess emphasizing a direct competition between probe and natural product for the same binding sites (Figure 4B).

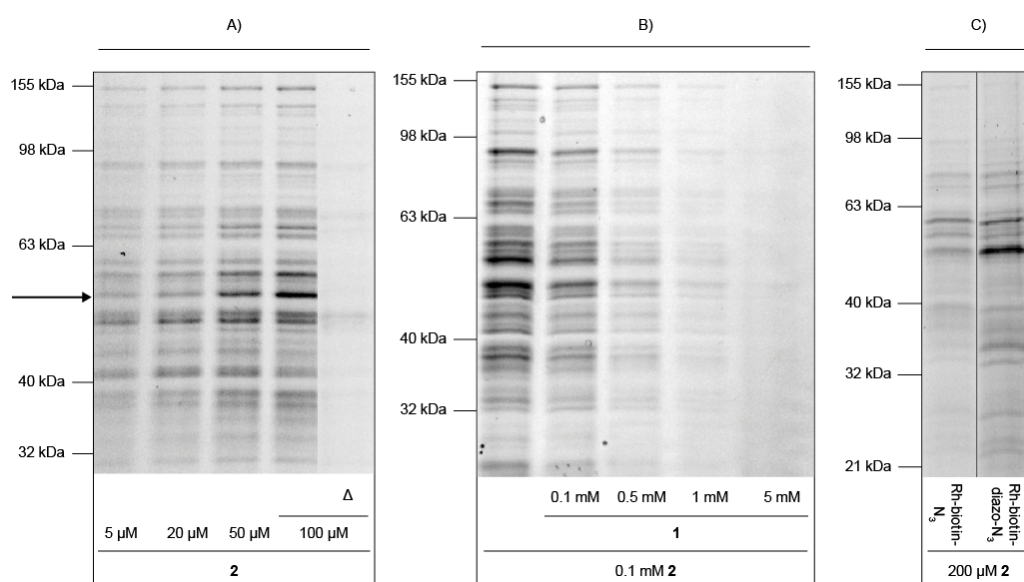


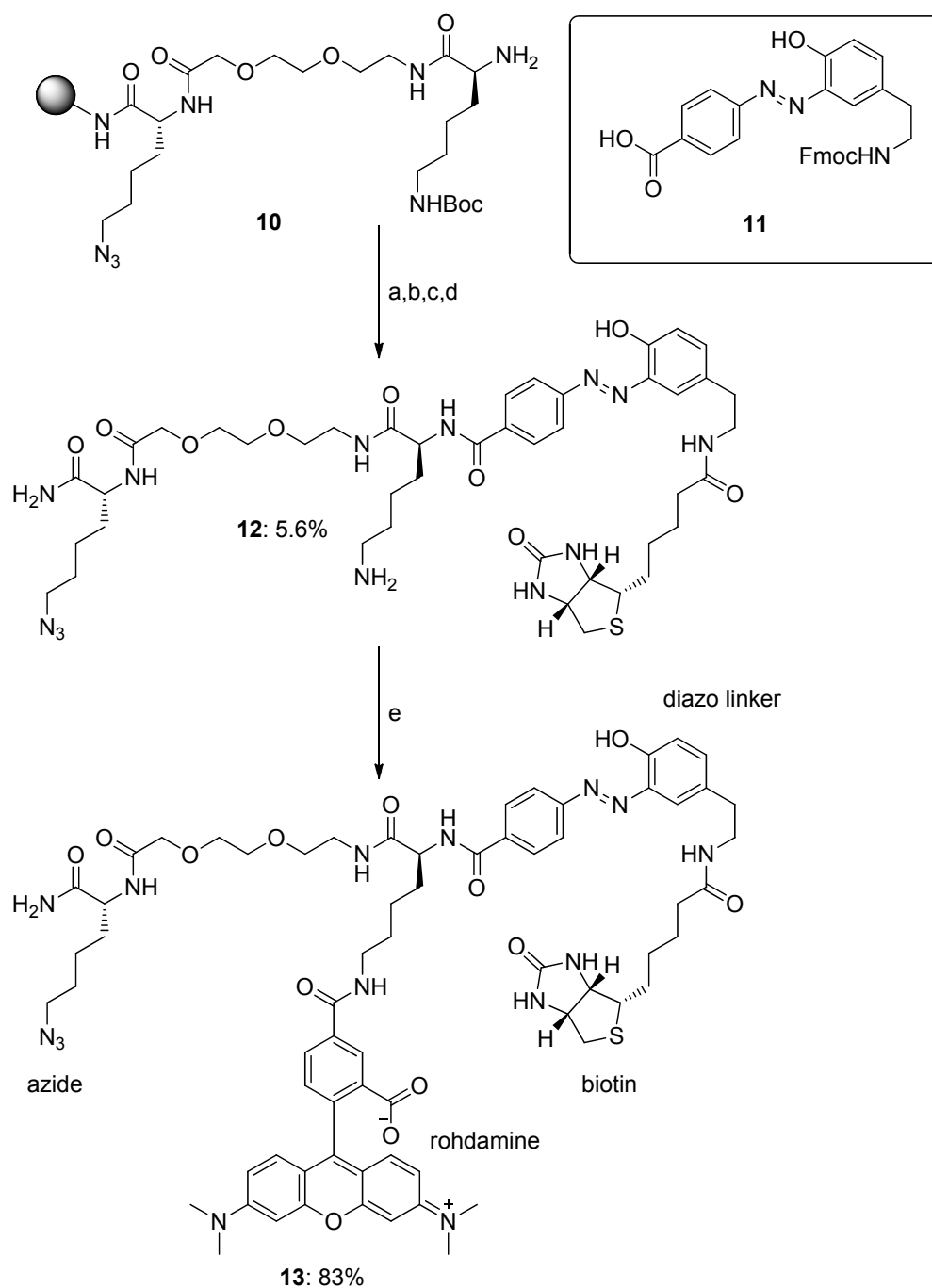
Figure 4. Labeling experiments of *S. aureus* NCTC 8325 proteome with probe

2 A) Concentration dependent labeling (Δ : Labeling with heat denatured proteome). B) Competitive labeling with 1x, 5x, 10x and 50x excesses of **1** C) Comparative enrichment with Rh-biotin-N₃ and Rh-biotin-diazo-N₃.

To identify the molecular targets that are covalently modified by **2** we attempted an enrichment procedure with a trifunctional rhodamine-biotin-azide linker (Rh-biotin-N₃, Supporting Figure 2, Appendix 2).^[118] This tag was reacted with the probe-modified proteome via click chemistry. Labeled proteins were subsequently enriched via biotin-avidin binding and finally released from

biotin beads via heat treatment at 99 °C. To our surprise only weak protein bands could be visualized based on fluorescent SDS gel analysis (Figure 4C). A closer inspection on the heat stability of probe **2** revealed a likely explanation for this result. At a temperature of 99 °C **2** decomposes within 10 minutes as determined by HPLC experiments and therefore results in a detachment of the fluorescent label from the modified protein (Supporting Figure 4, Appendix 2). In order to avoid decomposition of **2** and subsequent loss of labeled protein, we designed and synthesized a diazobenzene based chemical cleavable linker[†] (Rh-biotin-diazo-N₃, **13**) that allows specific cleavage of biotin bound proteins upon treatment with sodium hydrosulfite (Scheme 3).^[119] The synthesis of **13** was performed on a Rink resin according to previously published procedures, which was elongated by Fmoc-SPPS with Fmoc-Lys(N₃)-OH, a PEG spacer, and Fmoc-Lys(Boc)-OH respectively to form resin-bound intermediate **10**, which was then coupled to the diazo-linker building block **11**.^[120] Fmoc-deprotection followed by coupling of biotin and subsequent cleavage from the resin with TFA/TIS/H₂O gave linker **12**. Compound **12** was finally reacted with Rh-NHS to yield the tetra-functional Rh-biotin-diazo-N₃ linker **13**.

[†] This linker has been synthesized and characterized by the co-author Y. Yang.



Scheme 3. Synthesis of Rh-biotin-diazo-N3 (**13**). a) **12**, HBTU, DIEA, DMF; b) 20 % piperidine in DMF; c) Biotin, DIC/HOBt, DMF; d) TFA, TIS, H₂O; e) Rh-NHS, DIEA, DMF.

Using mild reducing conditions for the elution of affinity bound proteins instead of harsh thermal disruption of the avidin-biotin interaction resulted in the selective enrichment of one intense

protein band (Figure 4C). Isolation and in-gel-digestion of this protein band followed by mass spectrometric analysis (LC-MS/MS) revealed peptide fragments that were analyzed via the SEQUEST algorithm to reveal the probabilities for major protein hits. One prominent hit among the listed proteins (Supporting Table 1, Appendix 2) was seryl-tRNA synthetase (STS), the single enzyme in *S. aureus* that is responsible for the loading reaction of seryl-tRNAs with the correct AA. Selective inhibition of this enzyme by **2** would not just reveal the first small molecule inhibitor of STS in *S. aureus* but also offer a plausible explanation of the strong antibacterial activity of this compound. In order to confirm the binding of **1** and **2** to STS as well as to validate their corresponding target inhibition we overexpressed and purified *S. aureus* STS in *E. coli* cells. The recombinant protein was labeled with probe **2** in *E. coli* lysates which revealed a strong fluorescent band only in the induced sample. Heat denaturation of the lysate prior to probe addition again led to a disappearance of the signal and thus confirmed the specificity of probe interaction with the active and folded target (Figure 5 A, Supporting Figure 5, Appendix 2).

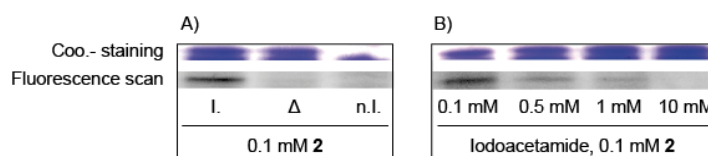


Figure 5. Fluorescence labeling with **2** and coomassie (coo.) staining of recombinant seryl-tRNA-synthetase in *E. coli* proteome. A) Labeling with induced (I.) and non-induced (n.I.) proteome. (Δ: Labeling with heat denatured proteome). B) Competitive labeling with 1x, 5x, 10x and 100x excesses of iodoacetamide.

STS is a homodimeric class II AARS that specifically charges cognate tRNAs with serine. Classification is based on the architecture of AARS catalytic domains.^[101] Class I synthetases share a characteristic Rossman dinucleotide binding fold with two short consensus AA motifs (HIGH and KMSKS), that are involved in ATP binding and amino acid activation.^[121] In comparison class II AARS catalytic domains have an unusual antiparallel β -sheet and three consensus motifs for ATP, AA and tRNA recognition and dimerization.^[122] To verify if labeling of STS is accompanied by inhibition of the catalytic activity in seryl-tRNA-synthetase we

determined the IC_{50} value for compound **2**. Several assay procedures are reported to monitor catalytic activities of AARS.^[123-126] One common approach is based on the radioactive ATP-AMP turnover. Incubation of STS with serine, [α - ^{32}P]-ATP and *E. coli* total tRNA results in the formation of [^{32}P]-AMP that can be quantified following TLC separation. A commercial [^{32}P]-AMP sample was used as a standard to localize and identify the reaction product AMP on the TLC plate (Supporting Figure 6-7, Appendix 2). As shown in the dose response curve in Figure 6 the addition of **2** inhibits the catalytic activity of STS with an IC_{50} of 23.8 μM .

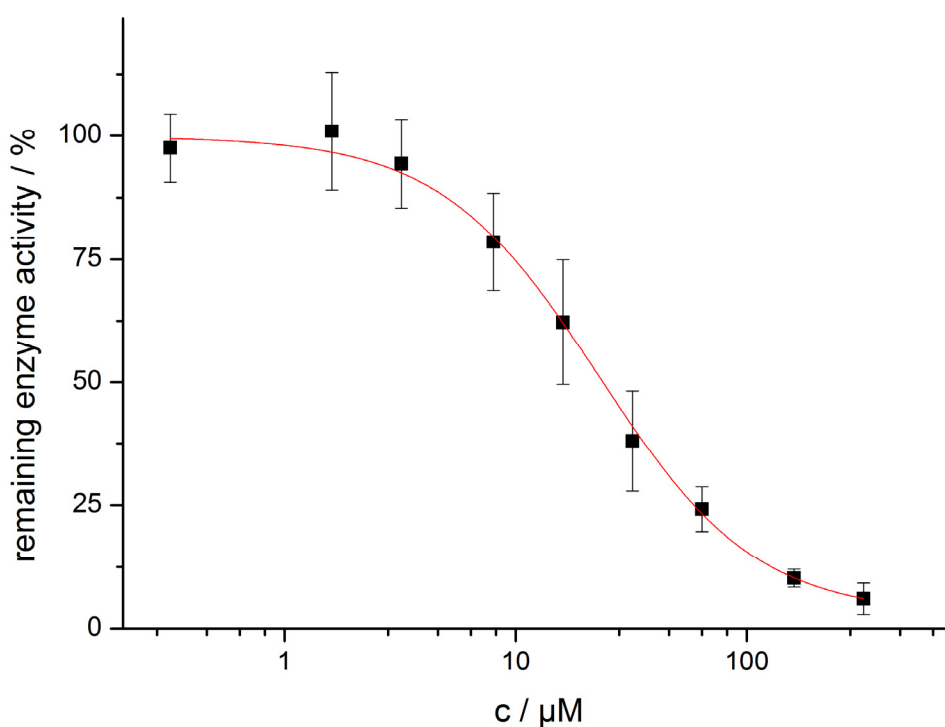


Figure 6. Dose-response curve for **2** against *S. aureus* seryl-tRNA-Synthetase. The data points and the error bars show the means and the standard deviations of four independent experiments.

To gain more information about the nature of the covalent interaction between **2** and STS we performed several downstream experiments and focused on the putative amino acid residue that might be involved in binding. One recent study by Cravatt and co-workers emphasized the

presence of nucleophilic cysteines in some AARS^[127] and since **2** exhibits an electrophilic Michael acceptor system it was likely that a cysteine residue of STS is involved in the nucleophilic attack. Thiols are known to covalently interact with α,β -unsaturated ketones^[46, 128] and in order to validate this hypothesis for STS we pre-incubated the STS expression lysate with various excesses of iodoacetamide, a chemical alkylation reagent for thiols. Interestingly, an only 5-fold excess of iodoacetamide over **2** showed a strong reduction of band intensities and indeed emphasized the preference of **2** towards cysteine residues in STS (Figure 5B).

STS contains five cysteines, however none of those has been reported to be essential for catalysis. As probe **2** could potentially react with all of the five residues (or even with more than one) we individually substituted all five cysteine residues by alanine and purified the mutant enzymes. For identification of the probe binding site, equal amounts of each purified STS mutant (5 μ M final) were reacted with 10 μ M **2** and subsequently compared to the wild type enzyme via fluorescent gel analysis. Except minor changes in the fluorescence intensities all five mutants were still labeled by probe **2** suggesting that indeed more than one cysteine is involved in binding (Figure 7).

In a next step we applied intact protein MS analysis to determine the stoichiometry of STS and bound probe **2**. After the incubation of 200 μ M **2** with 20 μ M STS the protein was loaded on the MS and the resulting spectra showed the attachment of up to two molecules compared to the unmodified protein control (Figure 8). In addition to the mutant labeling studies, this result suggests the presence of two reactive cysteines within STS. However, all our attempts to determine the site of alkylation by MS/MS sequencing failed due to a low ionization of cysteine containing peptides.

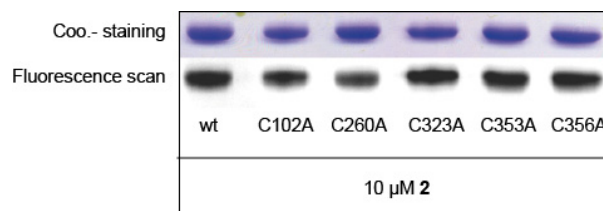


Figure 7. Fluorescence labeling of purified C to A mutants and wt with probe **2**
(wt: wild type).

As all our results suggested that cysteine residues were the site of probe attachment we addressed the question if a cysteine modification mechanism could explain the inhibition of STS. We thus individually investigated the catalytic activities of the five C to A mutants in comparison with the wild type enzyme. Interestingly, all five mutant enzymes displayed no catalytic activity emphasizing that a perturbation of one of the cysteines is already sufficient to directly interfere with the amino acylation of tRNAs by STS (Supporting Figure 8, Appendix 2). Further structural studies by X-ray crystallography are necessary to elucidate the nature of the cysteine network and its direct or indirect role in STS catalysis.

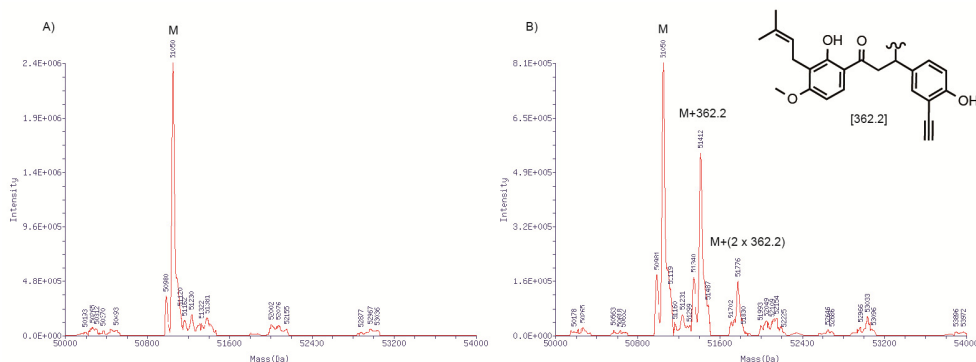


Figure 8. Full length MS experiment for recombinant STS before (A) and after
(B) incubation with probe **2**.

Conclusion

Chalcones represent privileged structures that are present in many natural products. Their potent bioactivities against tumor cells as well as pathogenic bacteria make them interesting candidates for pharmacological studies. We here utilized a chemical-proteomic strategy in order to characterize 4-HD in terms of its antibacterial activity as well as possible modes of action. As 4-HD is heat sensitive we utilized a chemical cleavable linker that is not only essential for 4-HD enrichment and cleavage but also useful for the implementation as a standard proteomic tool that facilitates the analysis of other labile molecules of natural or synthetic origin. Our studies suggest that 4-HD directly inhibits STS activity by the alkylation of essential cysteine residues within the enzyme and thus may induce cell death by the attenuation of bacterial protein biosynthesis. Although STS represents a prominent hit for the 4-HD derived probe **2** we cannot exclude that the compound binds reversibly or irreversibly to other cellular targets as well. However, as tRNA synthetases represent validated antibacterial targets we believe that the chalcone core motif will be useful for future optimization studies and be a suitable chemical tool e.g. for co-crystallization to determine the mode of inhibition.

Acknowledgements

We thank Mona Wolf and Katja Bäuml for excellent scientific support of this project. In addition we also thank Prof. Buchner, Dr. Haslbeck and Edgar Boczek for supporting the radioactive assays. S.A.S. was supported by the Deutsche Forschungsgemeinschaft, SFB749, SFB1035, FOR1406, an ERC starting grant and the Center for Integrated Protein Science, Munich (CIPSM). O.A.B thanks the TUM graduate school for financial support. S.H.L.V. is supported by the CIPSM and the Emmy Noether program of the Deutsche Forschungsgemeinschaft. Y.Y. is a recipient of a fellowship by the Chinese Scholarship Council.

Experimental

General Methods - Reagents and solvents were of reagent grade and used without further purification as obtained from commercial sources. Reactions sensitive to air and moisture were carried out under an inert atmosphere. Column chromatography was performed on Merck silica gel (Geduran Si 60, 0.040-0.063 mm). HPLC analysis was performed on a Waters 2695 separation module, a Waters PAD 2996 and a Waters XBridge C18 column (4.6 x 100 mm). For preparative scale HPLC separation, a Waters 2545 quaternary gradient module in combination with a Waters PAD 2998 and a Waters XBridge C18 (30 x 150 mm) or a YMC Triart C18 (10 x 250 mm) column was used. Mobile phase: water, 0.1% (v/v) TFA and acetonitrile, 0.1% (v/v) TFA unless otherwise noted. ¹H NMR and ¹³C NMR spectra were recorded at rt on Bruker Avance 360, Avance 500 and Avance III 500 spectrometers and were calibrated to the residual proton and carbon signal of the deuterated solvent. Mass spectra were obtained on a Thermo Scientific DFS High Resolution GC/MS (EI) and a LTQ FT Ultra (ESI).

S. aureus strain NCTC 8325 was cultured in BHB-medium consisting of 17.5 g/L brain heart infusion, 2.5 g/L Na₂HPO₄, 2.0 g/L Glucose, 10.0 g/L Peptone, 5.0 g/L NaCl, final pH 7.5. *E. coli* was cultured in LB-medium: 10.0 g/L Peptone, 5 g/L NaCl, 5 g/L yeast extract, final pH 7.5. All strains were grown at 37 °C unless otherwise noted. For selective growth, media with the following final antibiotic concentrations were used: ampicillin 100 µg/mL, kanamycin 25 µg/mL, chloramphenicol 10 µg/mL. Primers for mutagenesis and PCR were purchased from Eurofins MWG Operon. For all biochemistry applications of **1**, DMSO stock solutions were prepared to keep the final DMSO concentrations ≤ 2% unless reported otherwise. PCR reactions were performed using the Phusion® High-Fidelity PCR Kit (NEB) with a C1000 Thermal Cycler (BioRad) following the standard manufacturers-protocols. DNA- bands on agarose were purified with an Omega gel extraction kit and plasmids were isolated from overnight cultures using the Omega plasmid mini kit. DNA and protein concentrations were measured with a TECAN Infinite M200 PRO. Plasmid sequencing was done by GATC Biotech AG. Gene expression was induced with 0.1 mM anhydrotetracyclin. For protein purification an ÄKTApurifier (P900, UPC900, Frac950) was used.

3-Bromo-4-(methoxymethoxy)benzaldehyde (4) - Compound **4** was prepared according to the method of Chi et al. The spectral data matched with those reported in the literature. ^[114]

1-(4-Methoxy-2-((3-methylbut-2-en-1-yl)oxy)phenyl)ethanone (7) - Compound **9** was prepared according to the method of Matsui et al. The spectral data matched with those reported in the literature. ^[113]

4-(Methoxymethoxy)-3-((trimethylsilyl)ethynyl)benzaldehyde (5) - To a solution of **4** (3.0 g, 12 mmol) in piperidine (100 mL) was added PPh₃ (42 mg, 0.3 mmol), CuI (23 mg, 0.1 mmol) and trimethylsilylacetylene (7 mL, 48.8 mmol) under inert atmosphere. The solution was degassed and PdCl₂ (42 mg, 0.3 mmol) was added. The mixture was refluxed for 24 h, concentrated to dryness and purified by column chromatography to yield **5** (1.9 g, 7.2 mmol, 59%) as a colourless solid. ¹H NMR (500 MHz, CDCl₃) δ 0.30 (s, 9H), 3.56 (s, 3H), 5.35 (s, 2H), 7.23 (d, *J* = 8.6 Hz, 1H), 7.81 (dd, *J* = 2.0, 8.6 Hz, 1H), 7.99 (d, *J* = 2.0 Hz, 1H), 9.89 (s, 1H). ¹³C NMR (125 MHz, CDCl₃) δ -0.1, 56.6, 94.7, 99.5, 100.1, 114.4, 114.6, 130.3, 131.3, 136.1, 162.6, 190.3. HRMS (EI): [M]⁺ C₁₄H₁₈O₃²⁸Si calcd 262.1020, found 262.1013. R_f (20% EtOAc/hexanes) = 0.6.

(E)-3-(3-Ethynyl-4-(methoxymethoxy)phenyl)-1-(4-methoxy-2-((3-methylbut-2-en-1-yl)oxy)phenyl)prop-2-en-1-one (8) - A solution of **5** (1.9 g, 7.3 mmol), **7** (2.0 g, 8.7 mmol) and 3 M NaOH (24 mL) in EtOH (50 mL) was stirred for 16 h at rt. The solution was adjusted to pH = 2 with 1 M HCl and extracted with EtOAc. The solvent was removed under reduced pressure and the crude product was purified by HPLC to yield **8** (1.1 g, 2.7 mmol, 37%) as a yellow solid. ¹H NMR (500 MHz, CDCl₃) δ 1.78 (s, 3H), 1.82 (s, 3H), 3.33 (s, 1H), 3.55 (s, 3H), 3.89 (s, 3H), 4.61 (d, *J* = 6.8 Hz, 2H), 5.32 (s, 2H), 5.57 (t, *J* = 6.7 Hz, 1H), 6.52 (d, *J* = 2.1 Hz, 1H), 6.59 (dd, *J* = 2.2, 8.7 Hz, 1H), 7.16 (d, *J* = 8.7 Hz, 1H), 7.51 (dd, *J* = 2.1, 8.7 Hz, 1H), 7.61 (d, *J* = 3.1 Hz, 2H), 7.73 (d, *J* = 2.1 Hz, 1H), 7.86 (d, *J* = 8.7 Hz, 1H). ¹³C NMR (125 MHz, CDCl₃) δ 18.3, 25.9, 55.6, 56.4, 65.5, 79.5, 81.5, 94.7, 99.6, 105.5, 112.9, 114.8, 118.9, 122.1, 126.7, 129.4, 130.7,

133.2, 133.4, 139.1, 139.9, 159.4, 160.1, 164.3, 189.8. HRMS (ESI): $[M + H]^+$ $C_{25}H_{27}O_5$ calcd 407.1853, found 407.1852.

(E)-3-(3-ethynyl-4-(methoxymethoxy)phenyl)-1-(2-hydroxy-4-methoxy-3-(3-methylbut-2-en-1-yl)phenyl)prop-2-en-1-one (9) - A suspension of **8** (1.4 g, 3.4 mmol) and montmorillonite K10 (1.4 g) in CH_2Cl_2 was stirred for 1.5 h at 0 °C. Solids were removed by filtration. The solvent was removed under reduced pressure and the crude product was purified by HPLC to yield **9** (430 mg, 1.1 mmol, 31%) as a yellow solid. 1H NMR (500 MHz, $CDCl_3$) 1.71 (s, 3H), 1.83 (s, 3H), 3.36 (s, 1H), 3.42 (d, $J = 7.0$ Hz, 2H), 3.56 (s, 3H), 3.94 (s, 3H), 5.26 (t, $J = 7.1$ Hz, 1H), 5.34 (s, 2H), 6.53 (d, $J = 9.0$ Hz, 1H), 7.22 (d, $J = 8.7$ Hz, 1H), 7.52 (d, $J = 15.4$ Hz, 1H), 7.59 (dd, $J = 2.1, 8.7$ Hz, 1H), 7.78 7.85 (m, 3H). ^{13}C NMR (125 MHz, $CDCl_3$) δ 17.9, 21.7, 25.9, 55.8, 56.5, 79.2, 81.8, 94.7, 102.1, 113.0, 114.6, 114.9, 117.6, 119.6, 122.0, 128.6, 129.2, 131.0, 132.0, 133.8, 142.6, 159.9, 163.0, 163.3, 192.0. HRMS (ESI): $[M + H]^+$ $C_{25}H_{27}O_5$ calcd 407.1853, found 407.1853.

(E)-3-(3-ethynyl-4-hydroxyphenyl)-1-(2-hydroxy-4-methoxy-3-(3-methylbut-2-en-1-yl)phenyl)prop-2-en-1-one (2) - To a solution of **9** (224 mg, 0.6 mmol) in MeOH was added p-TsOH (105 mg, 0.6 mmol) and the mixture was stirred for 3 d at 30 °C. The solvent was removed under reduced pressure and the crude product was purified by HPLC to yield **2** (122 mg, 0.3 mmol, 62%) as a yellow solid. 1H NMR (500 MHz, $CDCl_3$) 1.71 (s, 3H), 1.83 (s, 3H), 3.41 (d, $J = 7.0$ Hz, 2H), 3.56 (s, 1H), 3.94 (s, 3H), 5.25 (d, $J = 7.1$ Hz, 1H), 6.53 (d, $J = 9.0$ Hz, 1H), 7.04 (d, $J = 8.6$ Hz, 1H), 7.50 (d, $J = 15.4$ Hz, 1H), 7.62 (dd, $J = 2.1, 8.6$ Hz, 1H), 7.72 (d, $J = 2.1$ Hz, 1H), 7.77 7.83 (m, 2H). ^{13}C NMR (125 MHz, $CDCl_3$) δ 17.9, 21.7, 25.9, 55.8, 77.4, 85.3, 102.1, 109.2, 114.6, 115.6, 117.6, 119.1, 122.0, 127.6, 129.2, 131.4, 132.0, 132.4, 142.8, 159.1, 163.0, 163.3, 192.0. HRMS (ESI): $[M + H]^+$ $C_{23}H_{24}O_4$ calcd 363.1591, found 363.1580.

4-Hydroxyderricin (1) - Compound **1** was prepared according to the method of Matsui et al. The spectral data matched with those reported in the literature. ^[113]

(E)-4-((5-(2-(((9H-fluoren-9-yl)methoxy)carbonyl)amino)ethyl)-2-

hydroxyphenyl)diazonyl)benzoic acid (11) - The diazobenzene building block **11** was synthesized following literature procedures.^[120]

Biotin-diazo-N₃ linker 12 - The synthesis of click-cleavable linker **12** was performed on Rink resin. Fmoc-Lys(azide)-OH, Fmoc-PEG-OH and Fmoc-Lys(Boc)-OH were coupled via DIC/HOBt (3 eq. with respect to resin loading). The Fmoc group of Fmoc-Lys(Boc) was removed on the resin by treatment with 20 % piperidine in DMF (20min). The diazobenzene cleavable building block **11** (1.5 eq.), HBTU and DIEA were reacted with the resin overnight. After Fmoc-deprotection biotin (1.5 eq.) was coupled using DIC/HOBt overnight. The resin-bound building block was cleaved by incubation with a solution of TFA: TIS: H₂O (95%: 2.5%: 2.5%) for 2 hours. The peptide was precipitated in cold diethyl ether and purified by HPLC yielding an orange solid (10.5 mg, yield 5.6%). ESI-MS: [M+H]⁺ calculated for C₄₃H₆₃N₁₃O₉S 938.4592, found 938.4686.

Rh-biotin-diazo-N₃ linker 13 -Building block **12** (10 mg, 0.011 mmol) was reacted overnight in DMSO (200 µl) with 5-(and 6-)carboxytetramethylrhodamine, succinimidyl ester (4.68 mg, 0.009 mmol) and DIEA (7.6 µL, 0.044 mol). The solution was purified by HPLC to give a red compound (10 mg; yield 83%). ESI-MS: [M+H]⁺ calculated for C₆₈H₈₃N₁₅O₁₃S 1350.6015, found 1350.6502.

Minimum inhibitory concentration assay - MICs were measured in 96 well plates. 99 µL of a diluted overnight culture in fresh medium (final OD₆₀₀ = 0.01) were supplemented with 1 µL of DMSO probe stocks with various concentrations. Plates were incubated at 37 °C with shaking at 220-250 rpm for 14-16 h. All experiments were conducted in triplicate in at least three independent experiments. Reported MICs represent the lowest concentrations of probe where no bacterial growth was visible.

In vitro labeling – *S. aureus* NCTC 8325 was grown in BHB medium as described above. One hour after reaching stationary phase they were harvested by centrifugation, washed and lysed under ice cooling using a Bandelin Sonopuls HD 2070 (3x20 sec, 80% power) in PBS buffer. Insoluble components were separated by centrifugation (30 min 9000 rpm) and discarded. The

protein concentration of the soluble fraction was measured via Bradford assay and adjusted to 1 mg/mL by dilution in PBS. For heat controls the proteome was denatured with 2% SDS at 98 °C for 10 min. Competitive labeling experiments were performed with proteome that was pre-incubated (20 min) with iodoacetamide or **1**. Then probe **2** was added to the final concentrations reported and mixtures were incubated at rt. After 1 h click reagents were added to the final concentrations of 200 µM rhodamine-azide (Rh-N₃), 1.2 mM tris(2-carboxyethyl)phosphine (TCEP), 96 µM tris[(1-benzyl-1H-1,2,3-triazol-4-yl)methyl]amine (TBTA) ligand and 1 mM CuSO₄ with a final volume of 50 µL. After 1 h at rt 2x BME loading buffer (63 mM Tris-HCl, 10% glycerin, 0.0025% bromphenolblue, 2% SDS, 5% β-mercaptoethanol, pH = 8.3) was added. Samples were separated by SDS-PAGE and analyzed by fluorescence recorded with a Fujifilm LAS-4000 luminescent image analyzer (Fujinon VRF43LMD3 lens, 575DF20 filter). Total protein expression levels were compared subsequently by Coomassie staining.

Enrichment strategies - Preparative labeling experiments were based on the described analytical protocol with the following amounts: protein concentration 6 mg/mL, 200 µM **1**, 10 µM linker (Rh-biotin-N₃ or Rh-biotin-diazo-N₃) with a 1 mL total reaction volume. Previous to click chemistry proteins were precipitated with an equal volume of pre-cooled acetone, washed with methanol and resuspended in PBS to remove excess of probe. Click reagents were added and after 1 h at rt proteins were again precipitated with acetone. The pellet was washed three times with methanol, resuspended in 0.2 % SDS-PBS and incubated with avidin-agarose beads (Sigma-Aldrich, 50 µL) with gentle mixing. This enrichment protocol was also performed with a control lacking **1** to compare the results of the biotin-avidin-enrichment with the background of unspecific protein binding on avidin-agarose beads. After 1 h beads were washed three times with 0.2 % SDS-PBS, twice with 6 M urea and again three times with 0.2 % SDS-PBS. For thermal elution beads were incubated for 6 min with 50 µL BME buffer at 95 °C. For chemical elution beads were 3x incubated for 15 min with 20 µL of elution buffer (100 mM ammonium hydrogen carbonate, 25 mM sodium hydrosulfite).^[119] Released proteins were applied to a preparative SDS-PAGE and fluorescent bands were isolated, washed and digested by trypsin as described previously.^[112]

Mass Spectrometry and Bioinformatics ^[129] ESI-MS spectra were recorded by a Thermo LTQ Orbitrap XL coupled to a Dionex UltiMate 3000 RSLC nano. The peptides were loaded on a Dionex Acclaim® PepMap 100 75 μm \times 2 cm, C18 (3 μm) and subsequently eluted and separated by a Dionex Acclaim® PepMap RLSC 75 μm \times 15 cm, C18 (2 μm). Mass spectrometry data was searched against the corresponding databases via the software Proteome Discoverer 1.3 (Thermo Scientific) using the SEQUEST algorithm. The search was limited to only tryptic peptides, two missed cleavage sites, precursor mass tolerance of 10 ppm and fragment mass tolerance of 0.8 Da. Filters were set to further refine the search results. The X_{corr} vs. charge state filter was set to X_{corr} values of 1.5, 2.0, 2.25 and 2.5 for charge states +1, +2, +3 and +4, respectively. The number of different peptides had to be ≥ 2 and the peptide confidence filter was set to at least medium. These filter values are similar to others previously reported for SEQUEST analysis. X_{corr} values (Score) of each run, the peptide spectrum matches (PSM) as well as the total number of obtained peptides and unique peptides are reported in Supporting Table 1, Appendix2.

Overexpression and purification of Strep-tagged *S. aureus* NCTC 8325 wild type enzymes in *E. coli* BL21 (DE3) – Recombinant expression in *E. coli* was performed using the Invitrogen Gateway protocols. Genes were amplified from genomic DNA with Gateway primers from Supporting Table 2, Appendix 2. The purified *attB*-PCR products were cloned with the Gateway BP Clonase II Mix into the entry-vector pDONOR201 (Invitrogen) for amplification in XL1-Blue Competent Cells (Agilent Technologies) using kanamycin selection. The purified and sequenced plasmid was then used in the LR reaction (Gateway LR Clonase II Enzyme Mix) for recombination with the destination vector pDest007. After transformation into chemically competent BL21 (DE3) cells (NEB) recombinant Strep-tag clones were grown in LB_{amp} medium at 37 °C until OD₆₀₀ ~0.6. Target gene expression was induced with anhydrotetracyclin at 18 °C overnight. Purification of the soluble lysate fraction was carried out with Strep-Tactin Superflow Plus columns (Qiagen) and concentrated using Amicon® Ultra-4 Centrifugal Filter Units NMWL 10,000 (Millipore). Desalted stock solutions were stored in 10 mM Tris buffer (pH 7.5) at -80 °C.

Site-directed mutagenesis - Cysteine to alanine mutations were introduced by fusion PCR using primers in Supporting Table 2 and Supporting Table 3, appendix 2. Single fragments were amplified from plasmid DNA, purified by agarose gel electrophoresis and subsequently used in the fusion reaction. Cloning and overexpression were performed as described above. The mutations were verified by sequence analysis.

Aminoacylation Assay and IC₅₀ determination – Inhibition of the seryl-tRNA-synthetase was measured by formation and separation of [α -³²P]-AMP from [α -³²P]-ATP by thin layer chromatography.^[130] DMSO solutions of **1** (1 μ L) were placed in reaction tubes and diluted with 16 μ L assay buffer (100 mM HEPES (pH 7.2), 10 mM MgCl₂, 30 mM KCl). One tube with 1 μ L DMSO was used as positive control for 100% enzyme activity determination. 1 μ L of purified enzyme was added (1 μ L assay buffer as no enzyme control for background subtraction) and the enzyme/inhibitor-mixtures were pre-incubated for 20 min at rt. The reaction was started by addition of a 7 μ L reaction mixture resulting in final concentrations of 5 μ M ATP, 50 nM [α -³²P]-ATP (Hartmann Analytic) 1 mM serine, 4 mg/mL *E. coli* total tRNA (Roche) and 320 nM enzyme.^[126] After incubation at 37 °C for 1 h the reaction was stopped by spotting 1 μ L volumes per reaction on polyethylenimine-cellulose plates (Merck Bioscience). The plates were developed with a mobile phase of 0.5 M LiCl in 2 N formic acid. Spot intensities were determined with a Typhoon 9200 Variable Mode Imager using Image Quant for Quantification (GE Healthcare). All measurements were performed in triplicates in at least 4 independent trials. AMP spot identities were validated with commercial [α -³²P]-AMP (Hartmann Analytic). Inhibition-values were corrected for background hydrolysis (no enzyme reaction), normalized and plotted against the concentrations of **2**.

D SUMMARY

α -Pyrones and pyrimidones as photoaffinity probes

Natural products are privileged structures for the interaction with proteins. In combination with attached reporter groups these molecules are useful tools for the labeling of target proteins. Identification of these proteins relies on covalent probe binding for visualization and purification.

The covalent labeling of target proteins by natural product based probes with intrinsic photoreactivity could be initiated by irradiation with UV light to form a reactive species for the crosslinking reaction. In comparison to probes with introduced photoreactive groups no additional structural elements have to be added, allowing for more “native” binding to be examined.

α -Pyrones and pyrimidones are well known for their photo-chemistry and elements of many natural products. An application that utilizes this reactivity in covalent protein labeling events has not been yet reported in the literature. Within this thesis α -pyrone- and pyrimidone-containing probes have been used to investigate their intrinsic crosslinking potential in protein labeling experiments. Irradiation experiments with these probes in the presence of a suitable nucleophile were used to validate the known photoreactivity of these building blocks and to tune the experimental settings. Synthesized probes were then successfully used in proteome labeling experiments to confirm our hypothesis of photo induced protein-crosslinking capabilities.

A major limitation of this approach concerns a lack of specificity for probes without a strong binding constant for their target structures. Although most of the probes have been designed to mimic biologically active scaffolds with an expected unique labeling pattern, only the application of a vancomycin-derived α -pyrone photo-probe showed a specific light induced labeling of known vancomycin-targets.

Two major prerequisites for photo-crosslinking groups are a high reactivity and a short lifetime of the reactive species to prevent unspecific labeling. The generation of a relatively stable reactive species after irradiation of α -pyrones and pyrimidone structures might explain the unspecific labeling of low affinity probes. This would limit the application of this concept to molecules with a very high binding constant as shown by the vancomycin-probe. Nevertheless the reported data

clearly indicate that the activation of these photo reactive scaffolds facilitate covalent protein labeling. Further studies will expand this concept to other high affinity-binding natural products that already contain a α -pyrone or pyrimidone moiety.

Synthesis of a benzophenone-alkyne tag for affinity based protein profiling

The investigation of interactions between reversible inhibitors and their target-structures suffers from the necessity of at least two additional elements that have to be introduced into the native structure: one reactive group for the photoinduced covalent crosslinking and a reporter group for visualization or identification. Usually both groups are independently introduced at different positions of the parent compound. But in many cases the structure of the parent compound does not provide adequate functionalities for multiple chemoselective modifications without changing the biological profile.

Pseudopterosin A (PsA) is a natural product isolated from the soft coral *Pseudopterogorgia elisabethae* in the Caribbean region. The mechanism of the antibacterial activity of this compound is unknown and likely is caused by non-covalent interactions with its binding partners. A probe design therefore has to consider the addition of additional photoreactive and reporter groups into the PsA structure. To minimize the disruption of the biological activity by addition of these groups we designed a universal applicable benzophenone based tool that combines photocrosslinking capabilities with an alkyne handle for click-chemistry-based tag attachment. The tool was designed for integration into natural product structures by a substitution reaction via a spacer. This spacer connects the natural product with the bifunctional tag and retains a suitable conformational flexibility for efficient crosslinking. Successful synthesis of this tool enabled the exemplary modification of PsA and provided an ABPP probe for subsequent labeling experiments.

Although intentionally designed to limit structure perturbations, the determination of growth inhibition of *S. aureus* revealed a complete loss of the antibacterial activity of the PsA probe compared to the natural product. In addition, initial UV-labeling experiments in *S. aureus* lysates

did not specifically mark any complementary binding partners and could not verify the benefits of the designed tag.

However since the selected modification of PsA might prevent any specific interactions, the experimental data does not yet enable an estimate of the tags versatility. Additional studies will be necessary to examine the tags advantages in different applications.

Target profiling of 4-hydroxyderricin in *S. aureus*

The separation and identification of the natural product extracts from the plant *Angelica keiskei* revealed the chalcone 4-hydroxyderricin (4-HD) to possess interesting antibacterial activities against *S. aureus*. Although a variety of previous studies confirm the antibacterial potential of this natural product, the biological targets and mode of action in bacterial systems were still unknown. The reported electrophilicity of the central Michael system towards thiols is a strong indication for a covalent modification of its target structures. This makes this compound an ideal starting point for the design of a molecular probe with intrinsic protein reactivity. Based on the available structure-activity relationship (SAR) data, a 4-HD probe with an alkyne reporting group was designed and synthesized to unravel the molecular mechanism by activity based protein profiling.

The comparison of the growth inhibition of *S. aureus* by the natural product and the derived probe demonstrated that the introduction of the alkyne tag did not change the antibacterial properties. Both compounds exhibited minimal inhibitory concentrations (MIC) below 5 μ M.

Initial incubation experiments of the designed probe with soluble fractions of *S. aureus* lysates illustrated several protein bands after click chemistry mediated introduction of a rhodamine dye and analysis by SDS-PAGE and in-gel fluorescence scanning. The competitive labeling with the natural product as well as incubation experiments with heat denatured proteomes confirmed the probes selectivity for the same active sites as the natural product and for just correctly folded protein structures.

An especially designed chemical cleavable linker was used for biotin enrichment of labeled proteins to avoid probe decomposition by heat treatment. Subsequent analysis by mass spectrometry (LC MS/MS) unraveled *S. aureus* seryl-tRNA synthetase (STS) as a major protein hit. This class of enzymes is essential for the translation of the genetic code into the amino acid sequences of proteins. The inhibition of this important cellular function adjourns protein biosynthesis and represents an interesting target that could explain the antibacterial activity of 4-HD.

Target validation by selective labeling of overexpressed and purified *S. aureus* STS as well as inhibition of the catalytic activity with an IC_{50} of 23.8 μ M additionally support the hypothesis of a covalent probe modification of this important enzyme.

The strong reduction of labeling intensities after pre-incubation of STS with the thiol alkylating agent iodoacetamide suggested the preference of the probes' Michael acceptor for reactive cysteines. Unfortunately, labeling experiments with all five C to A point mutations of STS could not identify the reactive cysteine but suggested a covalent modification of more than one cysteine. Although full-length MS determination experiments of STS before and after the incubation with our probe confirm this assumption the exact identification of the reactive cysteines by MS/MS analysis failed due to low ionization of cysteine containing peptides.

Determination of the catalytic activities of the five C to A mutants compared to the wild type enzyme showed that the substitution of each single C by A entirely disturbs the amino acylation reaction of STS. These results strongly support an inhibition mechanism based on the covalent modification of reactive STS cysteines by the Michael acceptor system and could explain the mode of action of this antibacterial natural product.

E ZUSAMMENFASSUNG

α -Pyrone und Pyrimidone als Photoaffinitätssonden

Naturstoffe sind privilegierte Strukturen für die Interaktion mit Proteinen. In Kombination mit geeigneten Reportergruppen sind diese Moleküle nützliche Werkzeuge, um durch selektive Wechselwirkung Zielproteine zu markieren. Basierend auf einer kovalenten Bindung können wichtige Proteintargets durch Visualisierung und Aufreinigung identifiziert werden.

Naturstoffe mit intrinsischer Photoreaktivität können durch die Bestrahlung mit UV-Licht kovalent an ihre Protein-Targets binden. Im Gegensatz zu artifiziellen Photosonden sind Strukturveränderungen der Naturstoffe in diesen Fällen durch zusätzliche Photocrosslinker unnötig. Eine Veränderung des biologischen Profils durch die Modifikation des Naturstoffs kann daher vermieden werden.

α -Pyrone und Pyrimidone sind wichtige Bausteine vieler Naturstoffe und bekannt für ihre Photochemie. Im Rahmen dieser Arbeit wird erstmals die Anwendung dieser intrinsischen Reaktivität in Bezug auf die kovalente Proteinmarkierung beschrieben. Bestrahlungsexperimente mit α -Pyrone und Pyrimidon Sonden wurden durchgeführt, um die bekannte Photoreaktivität dieser Bausteine gegenüber geeigneten Nucleophilen zu validieren und die optimalen experimentellen Bedingungen zu ermitteln. Die erfolgreiche Anwendung dieser Parameter in der lichtinduzierten Proteinmarkierung bestätigte unsere Hypothese und belegt erstmals die Proteinreaktivität von α -Pyrone- und Pyrimidon-Photosonden.

Eine wesentliche Einschränkung dieser Anwendung besteht in der geringen Selektivität von Sonden mit nur geringer Target-Affinität. Obwohl das Design der meisten Sonden in dieser Arbeit auf die Nachahmung von biologisch aktiven Verbindungen mit einem erwarteten einzigartigen Markierungsprofil abzielte, zeigte nur die Anwendung einer Vancomycin- α -Pyrone-Sonde eine lichtabhängige Markierung von bekannten Vancomycin-Targets.

Zwei wesentliche Voraussetzungen für die Anwendung einer photoreaktiven Gruppe in der Proteinmarkierung sind eine hohe Reaktivität und eine kurze Lebensdauer der durch Licht aktivierten Spezies. Die Bildung einer relativ stabilen „reaktiver Spezies“ durch die Bestrahlung von α -Pyrone- und Pyrimidon-Strukturen könnte die unspezifische Markierung von Sonden mit

geringer Affinität erklären und die Anwendung dieser Photoreaktivität auf Moleküle mit sehr hohen Bindungskonstanten beschränken. Dennoch belegen die experimentellen Daten die UV-lichtabhängige Proteinreaktivität dieser Photosonden und begründen die Erweiterung dieses Konzepts auf α -Pyron- und Pyrimidon-Naturstoffe mit hoher Target-Affinität.

Synthese eines Benzophenon-Alkin-Tags für das affinity based protein profiling

Strukturen reversibler Inhibitoren müssen für die kovalente Modifikation ihrer Targets und deren Charakterisierung durch zwei zusätzliche Struktureinheiten erweitert werden: eine reaktive Gruppe für die lichtinduzierte kovalente Verknüpfungsreaktion und eine Reporter-Gruppe für die Visualisierung und Identifikation. Gewöhnlich werden dieses Tags an verschiedenen Positionen der bioaktiven Verbindung installiert. In vielen Fällen stellt die zugrundeliegende Struktur jedoch keine ausreichenden Funktionalitäten für zwei chemoselektive Modifikationen zur Verfügung ohne die biologische Aktivität zu verändern.

Pseudopterosin A (PsA) ist ein Naturstoff, der aus den Extrakten der karibischen Koralle *Pseudopterogorgia elisabethae* isoliert werden kann. Der Mechanismus dieser antibakteriellen Verbindung ist sehr wahrscheinlich auf nicht-kovalente Wechselwirkungen mit ihren Targets zurückzuführen. Das Design einer Sonde muss daher die Implementierung einer photoreaktiven Gruppe und eines Reportertags berücksichtigen. Um Änderungen der biologischen Aktivität zu minimieren wurde daher im Rahmen dieser Arbeit ein universell anwendbares Benzophenon-Derivat entwickelt, das Photoreaktivität mit einem Alkin für die Einführung eines Reportertags via Klick-Chemie vereinigt. Zusätzlich wurde für die Verknüpfung mit dem Naturstoff durch eine Substitutionsreaktion ein Spacer installiert. Dieser Arm verbindet nach der Einführung den Naturstoff mit dem bifunktionalen Tag und gewährleistet eine ausreichende konformationelle Flexibilität. Die erfolgreiche Synthese dieses Tools ermöglichte die exemplarische Integration in die PsA Struktur und lieferte eine ABPP Sonde für die Anwendung in der Proteinmarkierung.

Obwohl das Design des Tags eine Änderung des biologischen Profils der Sonde im Vergleich zu der Ausgangsverbindung vermeiden sollte, hat die Modifikation des Naturstoffs in diesem Fall einen Verlust der antibakteriellen Aktivität verursacht. Zusätzlich haben erste UV-labeling Experimente in *S. aureus* Lysaten zu keiner selektiven Markierung komplementärer Proteine geführt. Aufgrund der Datenlage und der gewählten Naturstoff-Modifikation kann daher davon ausgegangen werden, dass dieses PsA System durch den Verlust der biologischen Aktivität keine angemessene Beurteilung der Funktionalität dieses Tags erlaubt. Vor diesem Hintergrund müssen erst zusätzliche Anwendungen mit alternativen Naturstoffen die Vorteile dieses Tags belegen.

Target-Identifizierung von 4-Hydroxyderricin in *S. aureus*

4-Hydroxyderricin (4-HD) ist ein Chalkon isoliert aus der Pflanze *Angelika keiskei* mit interessanten antibakteriellen Eigenschaften gegen *S. aureus*. Obwohl zahlreiche Studien die Aktivität dieses Naturstoffs belegen sind die biologischen Targets und der Wirkungsmechanismus bisher nicht untersucht.

Die bekannte Reaktivität des elektrophilen Michael-Systems dieser Verbindung gegenüber Thiol-Gruppen weist auf einen kovalenten Inhibitionsmechanismus hin und macht diese Verbindung zu einem interessanten Startpunkt für das Design einer ABPP-Sonde. Im Rahmen dieser Arbeit wurde daher basierend auf bekannten SAR Daten ein 4-HD-Derivat mit einer Alkin-Reporter-Gruppe entworfen und synthetisiert, um die antibakteriellen Mechanismen dieser Verbindung in *S. aureus* zu untersuchen.

Der Vergleich der Wachstumsinhibition von *S. aureus* durch den Naturstoff und die ABPP-Sonde konnte zeigen, dass die Modifikation der Grundstruktur durch ein Alkin zu keiner Änderung der antibakteriellen Aktivität führt. Beide Verbindungen haben einen MIC unter 5 μ M.

Durch die Anwendung dieser Sonde in der Markierung von Ziel-Proteinen in *S. aureus* Lysaten wurden durch Einführung eines Rhodamin-Farbstoffs und die Analyse durch SDS PAGE und Fluoreszenz-Scanning erste potentielle Targets abgebildet. Kompetitives Labeling mit dem Naturstoff als auch Markierungsexperimente mit hitzedenaturierten Proteomen bestätigten die

Selektivität der Sonde für dieselben Targets wie der Naturstoff und nur für intakte Proteinstrukturen.

Für die notwendige Biotin-Anreicherung von markierten Proteinen wurde ein speziell synthetisierter chemische spaltbarer Linker verwendet, um die Zersetzung der Sonde durch thermische Einwirkung zu vermeiden.

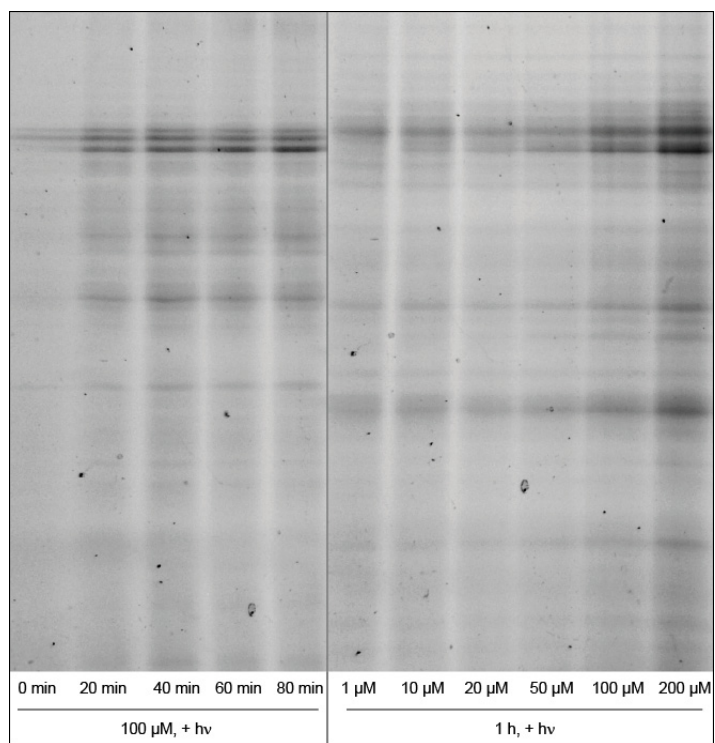
Die Analyse der isolierten Proteine durch Massenspektrometrie (LC MS/MS) identifizierte die essentielle *S. aureus* Seryl-tRNA Synthetase (STS) als wahrscheinlichstes Target. Die Gruppe dieser Enzyme katalysiert die Translation des genetischen Codes in Proteinprimärsequenzen. Die Inhibition dieser wichtigen Funktion unterbricht die Proteinbiosynthese und repräsentiert ein interessantes Target, das die antibakterielle Aktivität von 4-HD erklären könnte.

Targetvalidierung erfolgte durch die selektive Markierung und Inhibition der katalytischen Aktivität von rekombinanter *S. aureus* STS (IC_{50} 23.8 μ M).

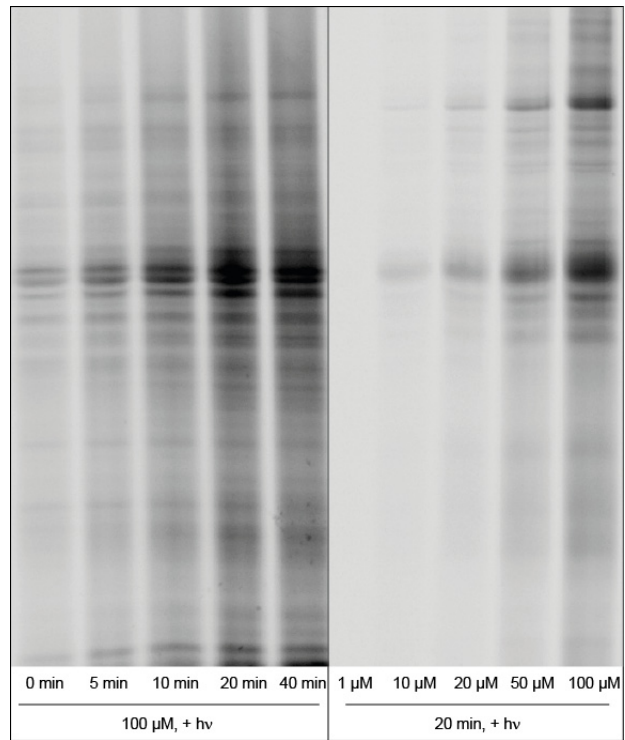
Durch kompetitive Markierungsexperimente mit dem Thiol-Alkylierungsreagenzien Iodacetamid konnte die Annahme einer kovalenten Bindung des Michael-Systems über reaktive Cysteine bestätigt werden. Das Labeling mit einzelnen C zu A STS-Punktmutaten ermöglichte jedoch keine eindeutige Identifikation der beteiligten Cysteine. In Kombination mit Volllänge-MS-Daten von STS vor und nach der Sondeninkubation deuteten diese Resultate vielmehr auf die Beteiligung von mehr als einem Cystein hin. Die genaue Charakterisierung dieser reaktiven Cysteine durch MS/MS Analyse konnte jedoch aufgrund der ungenügenden Ionisierung entscheidender Peptide nicht erreicht werden.

Dennoch zeigte die Untersuchung der fünf STS-Punktmutaten, dass jede einzelne C zu A Substitution zum vollständigen Verlust der katalytischen Aktivität führt. Diese Ergebnisse bestätigen daher die Hypothese einer Inhibition durch kovalente Bindung des Michael-Systems an reaktive Cysteine und können zu einer plausiblen Erklärung für die antibakteriellen Eigenschaften dieses Naturstoffs beitragen.

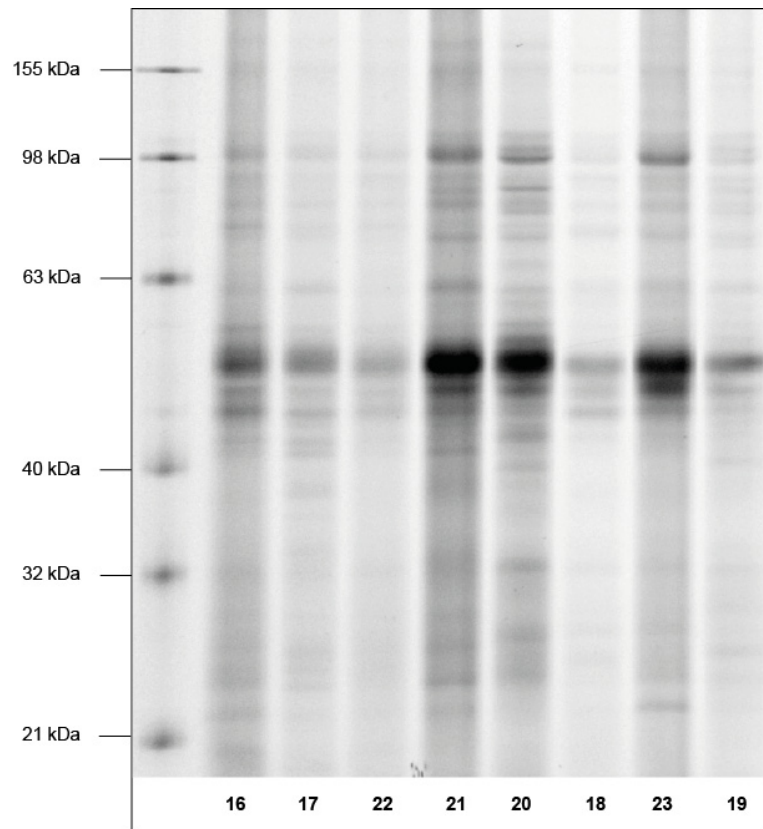
F APENDIX 1



Supporting Figure 1. Time and concentration dependent labeling of *S. aureus* Mu50 cytosol crude cellular lysate with **17**.

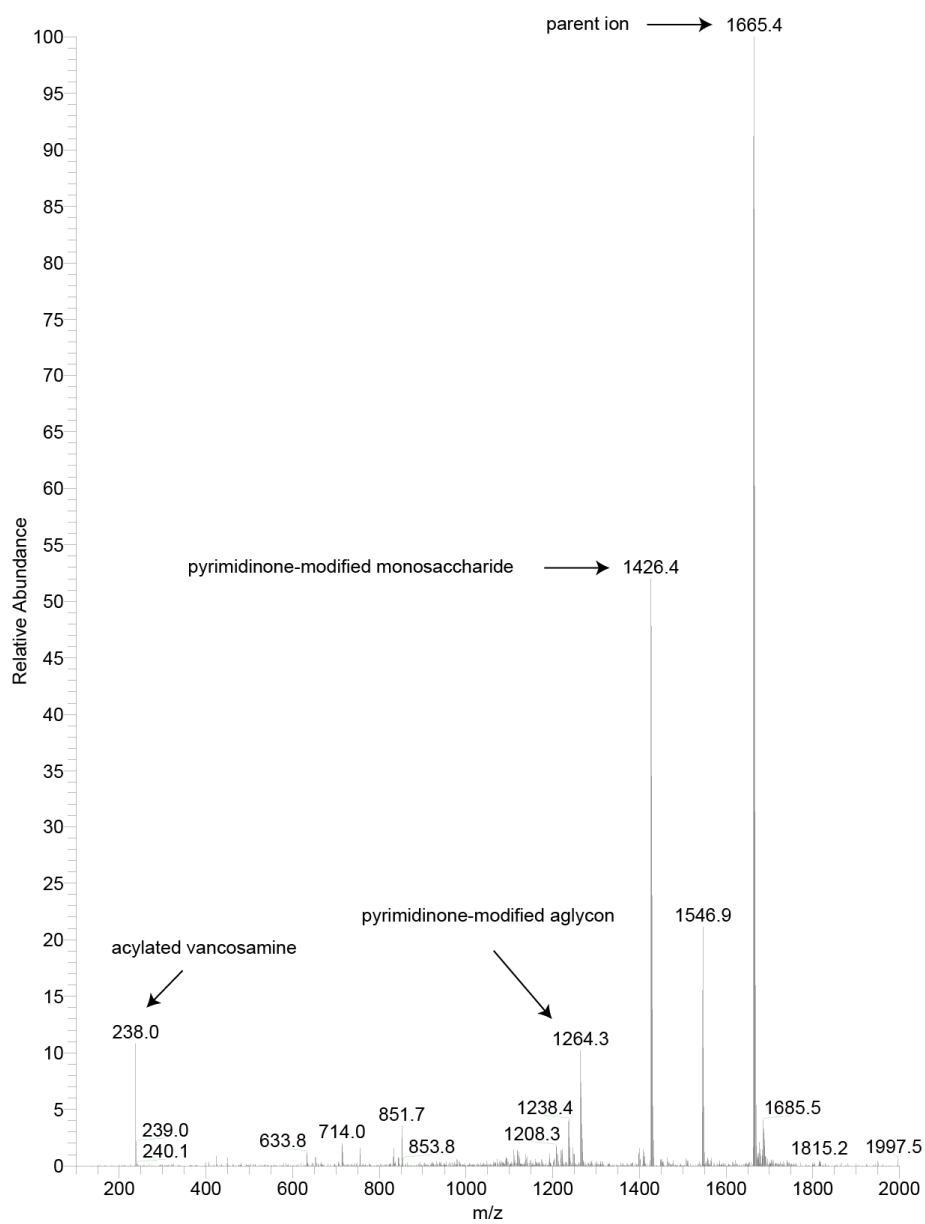


Supporting Figure 2. Time and concentration dependent labeling of *E. coli* cytosol crude cellular lysate with **20**.



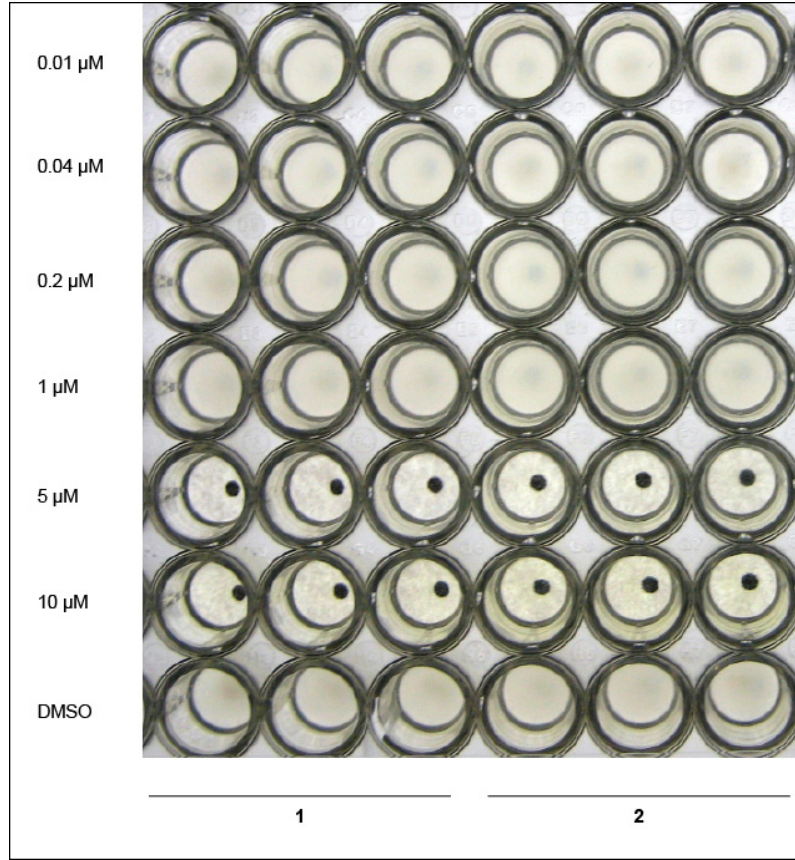
Supporting Figure 3. Labeling of *E. coli* crude cell lysate with probes **16-23**.

ob19454 #10-16 RT: 0.24-0.38 AV: 7 NL: 1.67E7
T: + c ESI Full ms [100.00-2000.00]

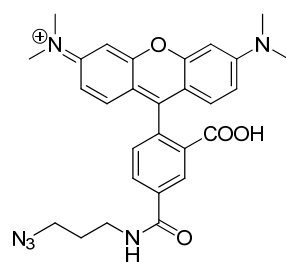


Supporting Figure 3. LR-ESI-MS of 55.

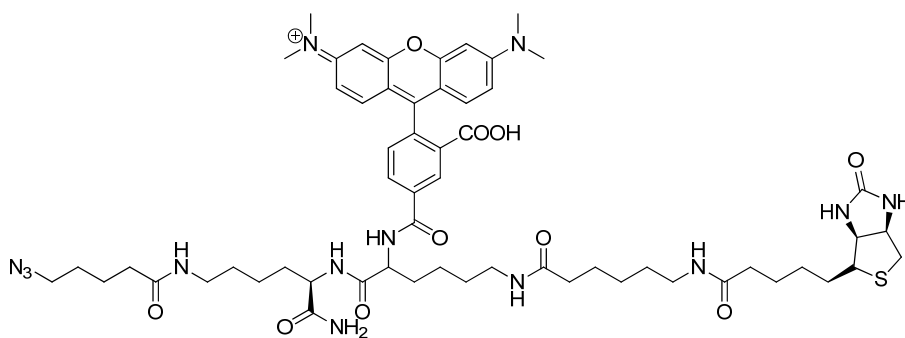
G APENDIX 2



Supporting Figure 1. Comparative MIC of **1** and **2** in *S. aureus* NCTC 8325.

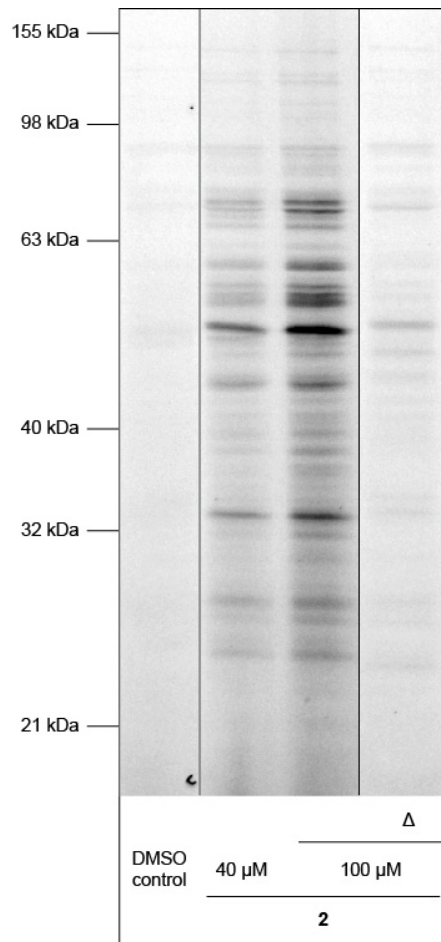


Rh-N₃

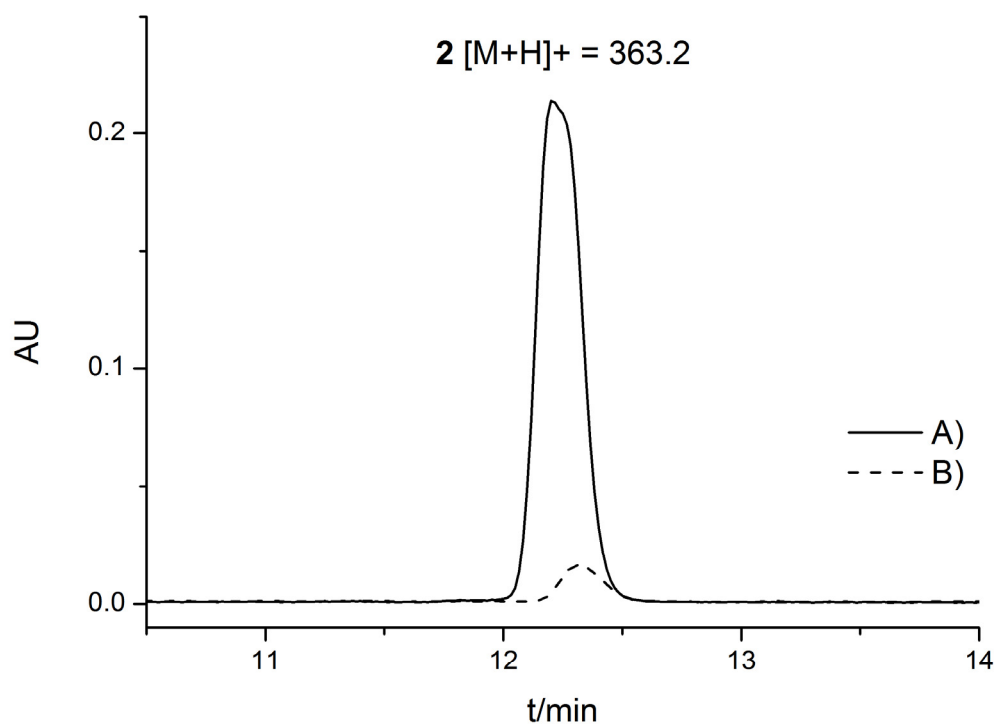


Rh-biotin-N₃

Supporting Figure 2. Structures of rhodamine azide Rh-N₃ and trifunctional rhodamine-biotin-N₃.^[118]



Supporting Figure 3. Concentration dependent labeling experiments of *S. aureus* NCTC 8325 proteome with probe **2** (Δ : Labeling with heat denatured proteome).



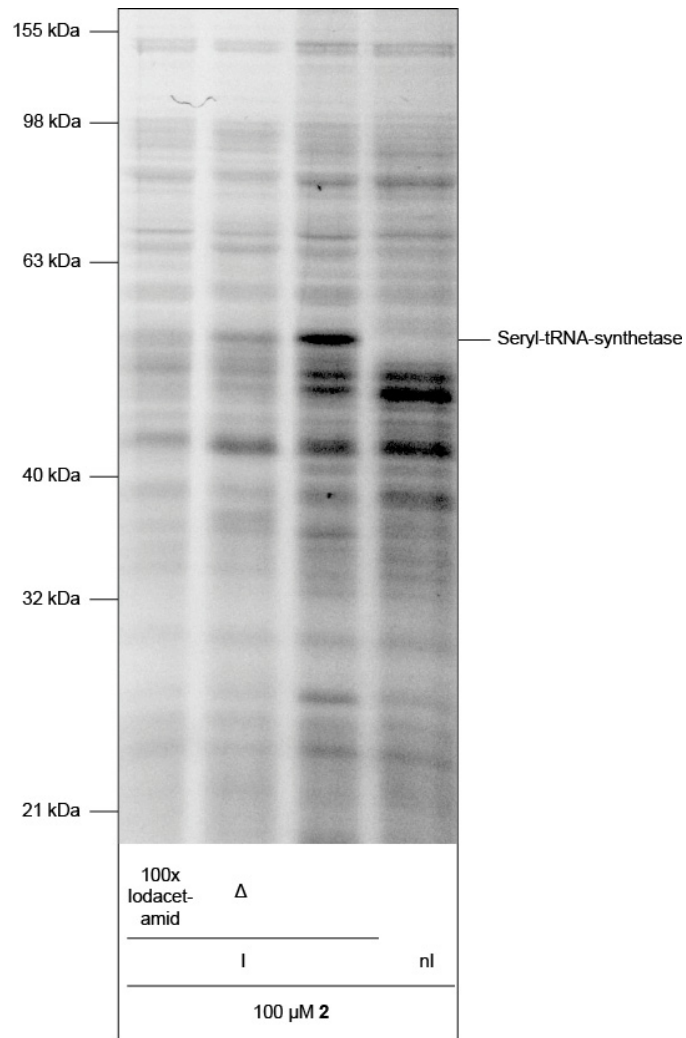
Supporting Figure 4. UV absorption of **2** at 363 nm: A) before and B) after heat decomposition in water at 99 °C for 20 min.

| Protein | Protein ID | MW [kD] | Exp. # | Score | # Peptides | # Unique Peptides | PSM |
|------------------------|------------|---------|--------|--------|------------|-------------------|-----|
| Seryl-tRNA synthetase | P95689 | 48,6 | 1 | 7,99 | 2 | 2 | 2 |
| | | | 2 | 5,65 | 2 | 2 | 2 |
| | | | 3 | 37,18 | 9 | 9 | 12 |
| | | | 4 | - | - | - | - |
| | | | 5 | - | - | - | - |
| Glycyl-tRNA synthetase | Q2FY08 | 53,6 | 1 | 12,05 | 4 | 4 | 4 |
| | | | 2 | 72,31 | 16 | 16 | 22 |
| | | | 3 | 71,07 | 15 | 15 | 21 |
| | | | 4 | 41,81 | 10 | 10 | 13 |
| | | | 5 | - | - | - | - |
| Enolase | Q2G028 | 47,1 | 1 | 8,60 | 3 | 3 | 3 |
| | | | 2 | 46,24 | 10 | 10 | 13 |
| | | | 3 | 55,76 | 12 | 12 | 16 |
| | | | 4 | 68,37 | 13 | 13 | 20 |
| | | | 5 | 5,94 | 2 | 2 | 2 |
| Elongation factor Tu | Q2G0N0 | 43,1 | 1 | 83,09 | 9 | 9 | 25 |
| | | | 2 | 197,96 | 17 | 17 | 61 |
| | | | 3 | 247,81 | 17 | 17 | 77 |
| | | | 4 | 247,02 | 17 | 17 | 73 |
| | | | 5 | 18,84 | 3 | 3 | 6 |

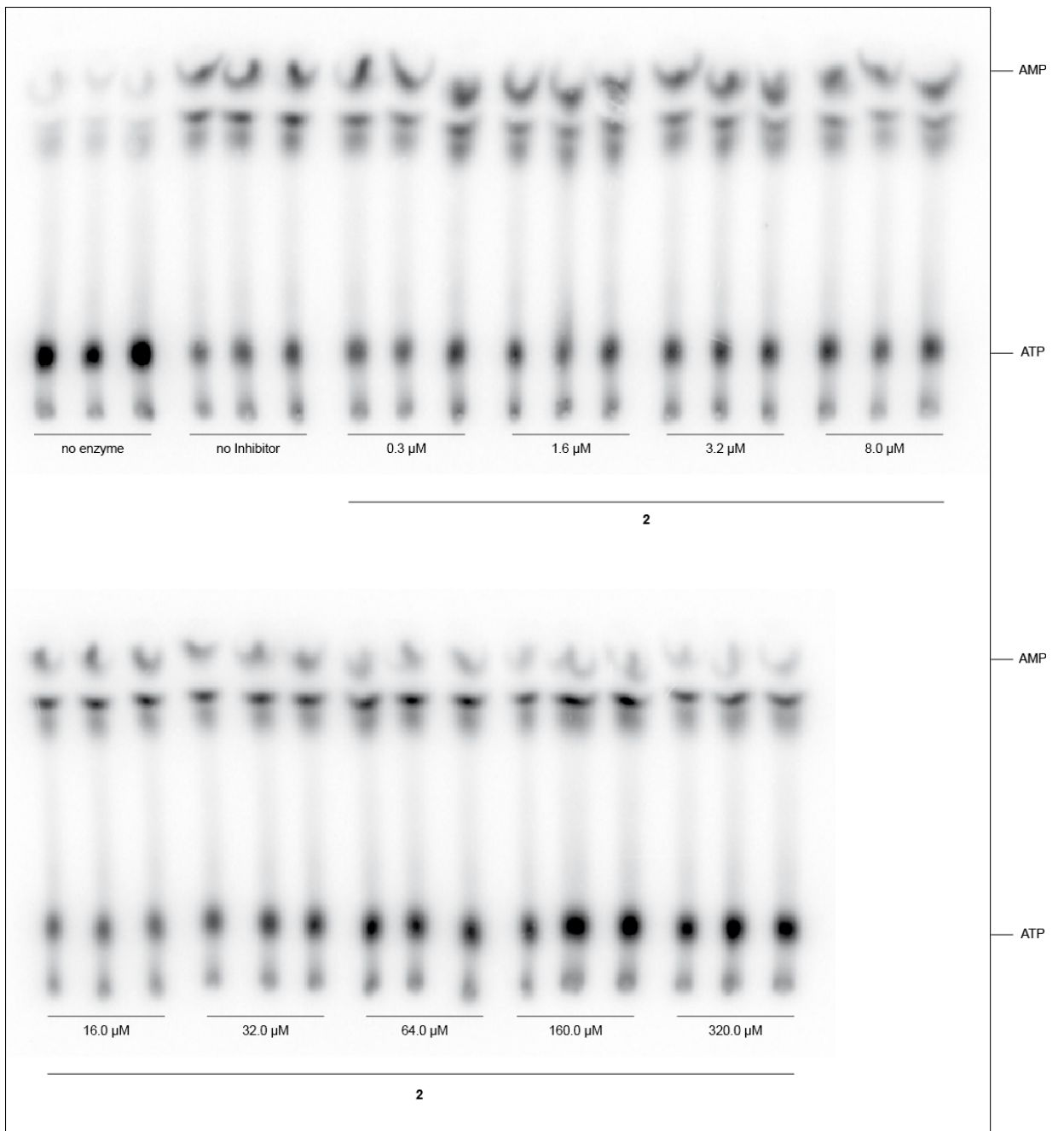
Supporting Table 1. Probabilities for protein hits identified by MS in three independent enrichment experiments (Exp. 1-3) in comparison with two DMSO control experiments (Exp. 4-5) in *S. aureus*.

| Gene, organism | Forward primer | Reverse primer |
|--|---|--|
| Seryl-tRNA synthetase (P95689), <i>S. aureus</i> NCTC 8325 | 5'-GGG GAC AAG TTT GTA CAA AAA AGC AGG CTT TAT GTT AGA CAT TAG ATT AT TC | 5'-GGG GAC CAC TTT GTA CAA GAA AGC TGG GTG TTA TTT AAC TGG TTT TGA AAT TT |

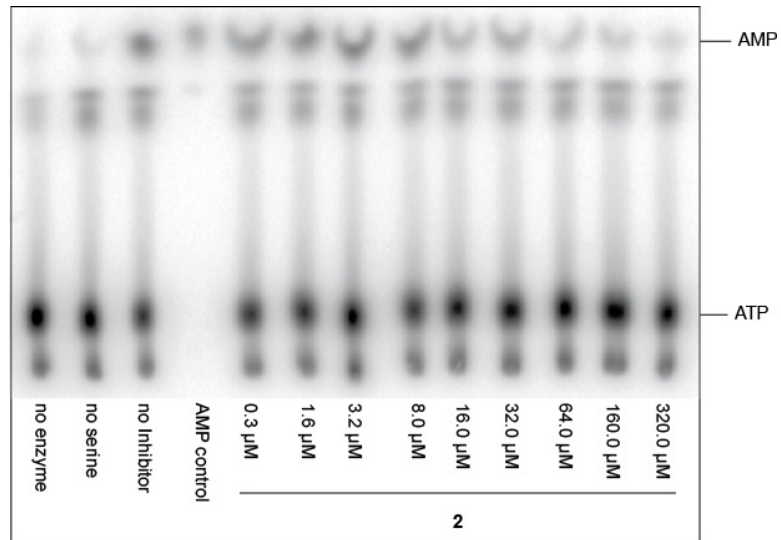
Supporting Table 2. Gateway PCR primers.



Supporting Figure 5. Labeling of recombinant Seryl-tRNA synthetase in *E. coli* proteome. I: induced nl: non-induced.



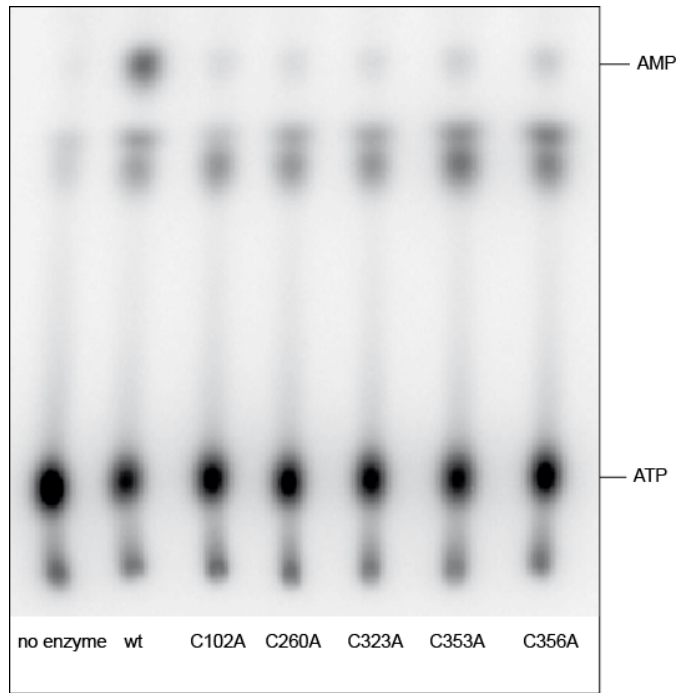
Supporting Figure 6. TLC read out for Seryl-tRNA-Synthetase catalyzed AMP quantification.



Supporting Figure 7. TLC read out for Seryl-tRNA-Synthetase catalyzed AMP quantification with “no serine” and AMP control.

| Seryl-tRNA synthetase (P95689), <i>S. aureus</i> NCTC 8325 mutants | Forward primer | Reverse primer |
|--|--|--|
| C102A | 5'-TAA ATG AAA TTG ATA ATA AAA TGA CAG GTA TCC TTG CTC GTA TTC CAA ATT TAA TAA GTG ATG A | 5'-TCA TCA CTT ATT AAA TTT GGA ATA CGA GCA AGG ATA CCT GTC ATT TTA TTA TCA ATT TCA TTT A |
| C260A | 5'-ATT CAC TGG TCA ATC TGC AGC TTT CCG TAG TGA AGC AGG A | 5'-TCC TGC TTC ACT ACG GAA AGC TGC AGA TTG ACC AGT GAA T |
| C323A | 5'-GTT AGG TTT ACC ATA CCG TCG TGT TAT TTT AGC TAC AGG TGA TAT TGG AT | 5'-ATC CAA TAT CAC CTG TAG CTA AAA TAA CAC GAC GGT ATG GTA AAC CTA AC |
| C353A | 5'-TAC AAT GAT TAT AAA GAA ATT AGT TCA GCC TCA AAC TGT ACG GAT TTC CAA GC | 5'-GCT TGG AAA TCC GTA CAG TTT GAG GCT GAA CTA ATT TCT TTA TAA TCA TTG TA |
| C356A | 5'-AAA TTA GTT CAT GCT CAA ACG CTA CGG ATT TCC AAG CGC GTC | 5'-GAC GC GCT TGG AAA TCC GTA GCG TTT GAG CAT GAA CTA ATT T |

Supporting Table 3. Mismatch primers for cysteine to alanine mutations.



Supporting Figure 8. TLC activity read out for STS wt and STS C to A mutants.

H BIBLIOGRAPHY

- [1] E. E. Carlson, *ACS Chemical Biology* **2010**, *5*, 639-653.
- [2] J. Krysiak, R. Breinbauer, *Vol. 324* (Ed.: S. A. Sieber), Springer Berlin / Heidelberg, **2012**, pp. 43-84.
- [3] D. J. Newman, G. M. Cragg, *Journal of Natural Products* **2007**, *70*, 461-477.
- [4] R. Breinbauer, I. R. Vetter, H. Waldmann, *Angewandte Chemie International Edition* **2002**, *41*, 2878-2890.
- [5] M. A. Azad, G. D. Wright, *Bioorg Med Chem* **2012**, *20*, 1929-1939.
- [6] N. Li, H. S. Overkleeft, B. I. Florea, *Curr Opin Chem Biol* **2012**, *16*, 227-233.
- [7] M. Nodwell, S. Sieber, in *Activity-Based Protein Profiling, Vol. 324* (Ed.: S. A. Sieber), Springer Berlin Heidelberg, **2012**, pp. 1-41.
- [8] M. J. Evans, B. F. Cravatt, *Chemical Reviews* **2006**, *106*, 3279-3301.
- [9] M. Fonovic, M. Bogyo, *Curr Pharm Des* **2007**, *13*, 253-261.
- [10] J. E. Hein, V. V. Fokin, *Chem Soc Rev* **2010**, *39*, 1302-1315.
- [11] C. D. Hein, X. M. Liu, D. Wang, *Pharm Res* **2008**, *25*, 2216-2230.
- [12] T. Böttcher, M. Pitscheider, S. A. Sieber, *Angewandte Chemie International Edition* **2010**, *49*, 2680-2698.
- [13] C. Drahl, B. F. Cravatt, E. J. Sorensen, *Angewandte Chemie International Edition* **2005**, *44*, 5788-5809.
- [14] N. Jessani, S. Niessen, B. Q. Wei, M. Nicolau, M. Humphrey, Y. Ji, W. Han, D. Y. Noh, J. R. Yates, 3rd, S. S. Jeffrey, B. F. Cravatt, *Nat Methods* **2005**, *2*, 691-697.
- [15] M. Gersch, J. Kreuzer, S. A. Sieber, *Nat Prod Rep* **2012**, *29*, 659-682.
- [16] A. Fleming, *Bull World Health Organ* **2001**, *79*, 780-790.
- [17] R. R. Yocum, J. R. Rasmussen, J. L. Strominger, *Journal of Biological Chemistry* **1980**, *255*, 3977-3986.
- [18] I. Staub, S. A. Sieber, *J Am Chem Soc* **2008**, *130*, 13400-13409.

- [19] C. Drahl, B. F. Cravatt, E. J. Sorensen, *Angew Chem Int Ed Engl* **2005**, *44*, 5788-5809.
- [20] T. Akihisa, T. Motoi, A. Seki, T. Kikuchi, M. Fukatsu, H. Tokuda, N. Suzuki, Y. Kimura, *Chem Biodivers* **2012**, *9*, 318-330.
- [21] H. P. Ávila, E. d. F. A. Smânia, F. D. Monache, A. Smânia Júnior, *Bioorg. Med. Chem.* **2008**, *16*, 9790-9794.
- [22] L. Luo, R. Wang, X. Wang, Z. Ma, N. Li, *Food Chemistry* **2012**, *131*, 992-998.
- [23] X. Zhang, L. Luo, Z. Ma, *Analytical and Bioanalytical Chemistry* **2011**, *400*, 3463-3471.
- [24] P. P. Geurink, L. M. Prely, G. A. van der Marel, R. Bischoff, H. S. Overkleeft, *Top Curr Chem* **2012**, *324*, 85-113.
- [25] S. A. Fleming, *Tetrahedron* **1995**, *51*, 12479-12520.
- [26] K. A. Kalesh, H. Shi, J. Ge, S. Q. Yao, *Organic & Biomolecular Chemistry* **2010**, *8*, 1749-1762.
- [27] E. L. Vodovozova, *Biochemistry (Mosc)* **2007**, *72*, 1-20.
- [28] Y. Tanaka, M. R. Bond, J. J. Kohler, *Mol Biosyst* **2008**, *4*, 473-480.
- [29] F. Kotzyba-Hibert, I. Kapfer, M. Goeldner, *Angewandte Chemie International Edition in English* **1995**, *34*, 1296-1312.
- [30] G. W. J. Fleet, R. R. Porter, J. R. Knowles, *Nature* **1969**, *224*, 511-512.
- [31] Y. Z. Li, J. P. Kirby, M. W. George, M. Poliakoff, G. B. Schuster, *Journal of the American Chemical Society* **1988**, *110*, 8092-8098.
- [32] K. L. Buchmueller, B. T. Hill, M. S. Platz, K. M. Weeks, *J Am Chem Soc* **2003**, *125*, 10850-10861.
- [33] R. J. Bergeron, J. B. Dionis, M. J. Ingeno, *The Journal of Organic Chemistry* **1987**, *52*, 144-149.
- [34] J. V. Staros, H. Bayley, D. N. Standring, J. R. Knowles, *Biochemical and Biophysical Research Communications* **1978**, *80*, 568-572.
- [35] R. A. Smith, J. R. Knowles, *J Am Chem Soc* **1973**, *95*, 5072-5073.
- [36] J. Brunner, H. Senn, F. M. Richards, *Journal of Biological Chemistry* **1980**, *255*, 3313-3318.

- [37] M. Platz, A. S. Admasu, S. Kwiatkowski, P. J. Crocker, N. Imai, D. S. Watt, *Bioconjugate Chemistry* **1991**, *2*, 337-341.
- [38] R. E. Galardy, L. C. Craig, M. P. Printz, *Nat New Biol* **1973**, *242*, 127-128.
- [39] G. Dorman, G. D. Prestwich, *Biochemistry* **1994**, *33*, 5661-5673.
- [40] P. J. A. Weber, A. G. Beck-Sickinger, *The Journal of Peptide Research* **1997**, *49*, 375-383.
- [41] C. Dalhoff, M. Hüben, T. Lenz, P. Poot, E. Nordhoff, H. Köster, E. Weinhold, *Chembiochem* **2010**, *11*, 256-265.
- [42] J. J. Tate, J. Persinger, B. Bartholomew, *Nucleic Acids Research* **1998**, *26*, 1421-1426.
- [43] M. J. Evans, B. F. Cravatt, *Chem Rev* **2006**, *106*, 3279-3301.
- [44] M. Fonovic, M. Bogyo, *Expert Rev Proteomics* **2008**, *5*, 721-730.
- [45] W. P. Heal, T. H. Dang, E. W. Tate, *Chem Soc Rev* **2011**, *40*, 246-257.
- [46] T. Bottcher, S. A. Sieber, *J Am Chem Soc* **2010**, *132*, 6964-6972.
- [47] P. P. Geurink, B. I. Florea, G. A. Van der Marel, B. M. Kessler, H. S. Overkleeft, *Chem Commun (Camb)* **2010**, *46*, 9052-9054.
- [48] P. R. Kym, K. E. Carlson, J. A. Katzenellenbogen, *Bioconjug Chem* **1995**, *6*, 115-122.
- [49] A. Blencowe, W. Hayes, *Soft Matter* **2005**, *1*, 178-205.
- [50] G. Dorman, G. D. Prestwich, *Biochemistry* **1994**, *33*, 5661-5673.
- [51] C. Grenot, A. de Montard, T. Blachere, M. R. de Ravel, E. Mappus, C. Y. Cuilleron, *Biochemistry* **1992**, *31*, 7609-7621.
- [52] X. D. Qian, W. T. Beck, *J Biol Chem* **1990**, *265*, 18753-18756.
- [53] D. C. Chiara, A. K. Hamouda, M. R. Ziebell, L. A. Mejia, G. Garcia, 3rd, J. B. Cohen, *Biochemistry* **2009**, *48*, 10066-10077.
- [54] J. D. Young, S. M. Jarvis, M. J. Robins, A. R. Paterson, *J Biol Chem* **1983**, *258*, 2202-2208.
- [55] I. J. AP, G. J. Menkveld, K. H. Thedinga, *Biochim Biophys Acta* **1989**, *979*, 153-156.
- [56] P. E. Linnett, A. D. Mitchell, M. D. Osselton, L. J. Mulheirn, R. B. Beechey, *Biochem J* **1978**, *170*, 503-510.
- [57] P. S. Steyn, F. R. van Heerden, *Nat Prod Rep* **1998**, *15*, 397-413.

- [58] Y. Hirata, H. Nakata, K. Yamada, K. Okuhara, T. Naito, *Tetrahedron* **1961**, *14*, 252-274.
- [59] C. Altomare, G. Perrone, M. C. Zonno, A. Evidente, R. Pengue, F. Fanti, L. Polonelli, *J Nat Prod* **2000**, *63*, 1131-1135.
- [60] G. R. Madhavan, R. Chakrabarti, R. K. Vikramadithyan, R. N. Mamidi, V. Balraju, B. M. Rajesh, P. Misra, S. K. Kumar, B. B. Lohray, V. B. Lohray, R. Rajagopalan, *Bioorg Med Chem* **2002**, *10*, 2671-2680.
- [61] L. Zhou, X. Cheng, B. A. Connolly, M. J. Dickman, P. J. Hurd, D. P. Hornby, *J Mol Biol* **2002**, *321*, 591-599.
- [62] W. H. Pirkle, L. H. McKendry, *J Am Chem Soc* **1969**, *91*, 1179-1186.
- [63] J. P. Guthrie, C. L. McIntosh, P. DeMayo, *Canadian Journal of Chemistry* **1969**, *48*, 237-242.
- [64] C. T. Bedford, W. H. Pirkle, T. Money, *Canadian Journal of Chemistry* **1970**, *48*, 2645-2650.
- [65] E. J. Corey, W. H. Pirkle, *Tetrahedron Letters* **1967**, 5255-5256.
- [66] H. Rostkowska, A. Khvorostov, R. Fausto, M. J. Nowak, *J Phys Chem A* **2003**, *107*, 5913-5919.
- [67] T. Nishio, *Liebigs Ann Chem* **1992**, 71-73.
- [68] A. D. Allen, T. T. Tidwell, *The Journal of Organic Chemistry* **1998**, *64*, 266-271.
- [69] J. Andraos, A. J. Kresge, *Journal of the American Chemical Society* **1992**, *114*, 5643-5646.
- [70] B. R. Arnold, C. E. Brown, J. Luszytk, *Journal of the American Chemical Society* **1993**, *115*, 1576-1577.
- [71] P. J. Lillford, D. P. N. Satchell, *Journal of the Chemical Society B: Physical Organic* **1967**, *0*, 360-365.
- [72] M. C. Pannone, C. W. Macosko, *Journal of Applied Polymer Science* **1987**, *34*, 2409-2432.
- [73] M. Meldal, C. W. Tornoe, *Chem Rev* **2008**, *108*, 2952-3015.
- [74] V. V. Rostovtsev, L. G. Green, V. V. Fokin, K. B. Sharpless, *Angew Chem Int Ed Engl* **2002**, *41*, 2596-2599.

- [75] A. E. Speers, G. C. Adam, B. F. Cravatt, *J Am Chem Soc* **2003**, *125*, 4686-4687.
- [76] H. Vorbruggen, G. Hofle, *Chem Ber* **1981**, *114*, 1256-1268.
- [77] H. Vorbruggen, B. Bennua, *Chem Ber* **1981**, *114*, 1279-1286.
- [78] X. Ariza, J. Vilarrasa, *J Org Chem* **2000**, *65*, 2827-2829.
- [79] S. R. M. Bushby, G. H. Hitchings, *Br J Pharmac Chemother* **1968**, 72-90.
- [80] S. C. Zammit, A. J. Cox, R. M. Gow, Y. Zhang, R. E. Gilbert, H. Krum, D. J. Kelly, S. J. Williams, *Bioorg Med Chem Lett* **2009**, *19*, 7003-7006.
- [81] S. A. Snyder, S. P. Breazzano, A. G. Ross, Y. Lin, A. L. Zografos, *J Am Chem Soc* **2009**, *131*, 1753-1765.
- [82] V. Aucagne, J. Berna, J. D. Crowley, S. M. Goldup, K. D. Hanni, D. A. Leigh, P. J. Lusby, V. E. Ronaldson, A. M. Slawin, A. Viterisi, D. B. Walker, *J Am Chem Soc* **2007**, *129*, 11950-11963.
- [83] I. J. Fairlamb, L. R. Marrison, J. M. Dickinson, F. J. Lu, J. P. Schmidt, *Bioorg Med Chem* **2004**, *12*, 4285-4299.
- [84] L. R. Marrison, J. M. Dickinson, R. Ahmed, I. J. Fairlamb, *Tetrahedron Letters* **2002**, *43*, 8853-8857.
- [85] M. S. Islam, M. Kitagawa, M. Imoto, T. Kitahara, H. Watanabe, *Biosci Biotechnol Biochem* **2006**, *70*, 2523-2528.
- [86] S. M. Efange, E. M. Alessi, H. C. Shih, Y. C. Cheng, T. J. Bardos, *J Med Chem* **1985**, *28*, 904-910.
- [87] R. G. Vaswani, A. R. Chamberlin, *J Org Chem* **2008**, *73*, 1661-1681.
- [88] J. E. Oh, K. H. Lee, *Bioorg Med Chem* **1999**, *7*, 2985-2990.
- [89] R. K. Dieter, J. R. Fishpaugh, *Journal of Organic Chemistry* **1987**, *52*, 923-926.
- [90] X. Zhang, M. McLaughlin, R. Munoz, P. Lizeth, R. P. Hsung, J. Wang, *Synthesis* **2007**, 749-753.
- [91] D. A. Matthews, J. T. Bolin, J. M. Burridge, D. J. Filman, K. W. Volz, B. T. Kaufman, C. R. Beddell, J. N. Champness, D. K. Stammers, J. Kraut, *J Biol Chem* **1985**, *260*, 381-391.

- [92] A. M. Brzozowski, A. C. Pike, Z. Dauter, R. E. Hubbard, T. Bonn, O. Engstrom, L. Ohman, G. L. Greene, J. A. Gustafsson, M. Carlquist, *Nature* **1997**, 389, 753-758.
- [93] N. Foy, E. Stephan, A. Vessieres, E. Salomon, J. M. Heldt, M. Huche, G. Jaouen, *Chembiochem* **2003**, 4, 494-503.
- [94] J. Eirich, R. Orth, S. A. Sieber, *Journal of the American Chemical Society* **2011**, 133, 12144-12153.
- [95] H. Correa, F. Aristizabal, C. Duque, R. Kerr, *Marine Drugs* **2011**, 9, 334-344.
- [96] A. Ata, H. Y. Win, D. Holt, P. Holloway, E. P. Segstro, G. S. Jayatilake, *Helvetica Chimica Acta* **2004**, 87, 1090-1098.
- [97] K. Uehara, C. B. Wagner, T. Vogler, H. Luftmann, A. Studer, *Angewandte Chemie International Edition* **2010**, 49, 3073-3076.
- [98] M. W. B. McCulloch, B. Haltli, D. H. Marchbank, R. G. Kerr, *Marine Drugs* **2012**, 10, 1711-1728.
- [99] O. A. Battenberg, M. B. Nodwell, S. A. Sieber, *The Journal of Organic Chemistry* **2011**, 76, 6075-6087.
- [100] O. A. Battenberg, Y. Yang, S. H. L. Verhelst, S. A. Sieber, *Molecular BioSystems* **2013**, 9, 343-351.
- [101] J. G. Hurdle, A. J. O'Neill, I. Chopra, *Antimicrobial Agents and Chemotherapy* **2005**, 49, 4821-4833.
- [102] U. A. Ochsner, X. Sun, T. Jarvis, I. Critchley, N. Janjic, *Expert Opinion on Investigational Drugs* **2007**, 16, 573-593.
- [103] D. Hoepfner, C. W. McNamara, C. S. Lim, C. Studer, R. Riedl, T. Aust, S. L. McCormack, D. M. Plouffe, S. Meister, S. Schuierer, U. Plikat, N. Hartmann, F. Staedtler, S. Cotesta, E. K. Schmitt, F. Petersen, F. Supek, R. J. Glynn, J. A. Tallarico, J. A. Porter, M. C. Fishman, C. Bodenreider, T. T. Diagana, N. R. Movva, E. A. Winzeler, *Cell Host Microbe* **2012**, 11, 654-663.
- [104] R. L. Jarvest, J. M. Berge, V. Berry, H. F. Boyd, M. J. Brown, J. S. Elder, A. K. Forrest, A. P. Fosberry, D. R. Gentry, M. J. Hibbs, D. D. Jaworski, P. J. O'Hanlon, A. J. Pope, S.

- Rittenhouse, R. J. Sheppard, C. Slater-Radosti, A. Worby, *Journal of Medicinal Chemistry* **2002**, *45*, 1959-1962.
- [105] T. L. Keller, D. Zocco, M. S. Sundrud, M. Hendrick, M. Edenius, J. Yum, Y. J. Kim, H. K. Lee, J. F. Cortese, D. F. Wirth, J. D. Dignam, A. Rao, C. Y. Yeo, R. Mazitschek, M. Whitman, *Nat Chem Biol* **2012**, *8*, 311-317.
- [106] F. L. Rock, W. Mao, A. Yaremchuk, M. Tukalo, T. Crepin, H. Zhou, Y. K. Zhang, V. Hernandez, T. Akama, S. J. Baker, J. J. Plattner, L. Shapiro, S. A. Martinis, S. J. Benkovic, S. Cusack, M. R. Alley, *Science* **2007**, *316*, 1759-1761.
- [107] S. Shibata, J. R. Gillespie, A. M. Kelley, A. J. Napuli, Z. Zhang, K. V. Kovzun, R. M. Pefley, J. Lam, F. H. Zucker, W. C. Van Voorhis, E. A. Merritt, W. G. Hol, C. L. Verlinde, E. Fan, F. S. Buckner, *Antimicrob Agents Chemother* **2011**, *55*, 1982-1989.
- [108] I. A. Critchley, C. L. Young, K. C. Stone, U. A. Ochsner, J. Guiles, T. Tarasow, N. Janjic, *Antimicrobial Agents and Chemotherapy* **2005**, *49*, 4247-4252.
- [109] T. Akihisa, H. Tokuda, M. Ukiya, M. Iizuka, S. Schneider, K. Ogasawara, T. Mukainaka, K. Iwatsuki, T. Suzuki, H. Nishino, *Cancer Letters* **2003**, *201*, 133-137.
- [110] Y. Inamori, K. Baba, H. Tsujibo, M. Taniguchi, K. Nakata, M. Kozawa, *Chem Pharm Bull (Tokyo)* **1991**, *39*, 1604-1605.
- [111] K. Sugamoto, C. Kurogi, Y. Matsushita, T. Matsui, *Tetrahedron Letters* **2008**, *49*, 6639-6641.
- [112] S. A. Sieber, S. Niessen, H. S. Hoover, B. F. Cravatt, *Nat Chem Biol* **2006**, *2*, 274-281.
- [113] K. Sugamoto, Y.-i. Matsusita, K. Matsui, C. Kurogi, T. Matsui, *Tetrahedron* **2011**, *67*, 5346-5359.
- [114] H. J. Lee, J. W. Seo, B. H. Lee, K. H. Chung, D. Y. Chi, *Bioorganic & Medicinal Chemistry Letters* **2004**, *14*, 463-466.
- [115] M. Meldal, C. W. Tornøe, *Chemical Reviews* **2008**, *108*, 2952-3015.
- [116] V. V. Rostovtsev, L. G. Green, V. V. Fokin, K. B. Sharpless, *Angewandte Chemie* **2002**, *114*, 2708-2711.
- [117] A. E. Speers, G. C. Adam, B. F. Cravatt, *J. Am. Chem. Soc.* **2003**, *125*, 4686-4687.

- [118] J. Eirich, J. L. Burkhart, A. Ullrich, G. C. Rudolf, A. Vollmar, S. Zahler, U. Kazmaier, S. A. Sieber, *Molecular Biosystems* **2012**, *8*, 2067-2075.
- [119] M. Fonovic, S. H. L. Verhelst, M. T. Sorum, M. Bogyo, *Mol Cell Proteomics* **2007**, *6*, 1761-1770.
- [120] S. H. L. Verhelst, M. Fonovic, M. Bogyo, *Angew Chem Int Ed Engl* **2007**, *46*, 1284-1286.
- [121] M. Ibba, D. Soll, *Annu Rev Biochem* **2000**, *69*, 617-650.
- [122] H. Belrhali, A. Yaremchuk, M. Tukalo, C. Berthet-Colominas, B. Rasmussen, P. Bosecke, O. Diat, S. Cusack, *Structure* **1995**, *3*, 341-352.
- [123] J. Gilbert, C. R. Perry, B. Slocombe, *Antimicrob Agents Chemother* **1993**, *37*, 32-38.
- [124] S. Hati, B. Ziervogel, J. Sternjohn, F. C. Wong, M. C. Nagan, A. E. Rosen, P. G. Siliciano, J. W. Chihade, K. Musier-Forsyth, *J Biol Chem* **2006**, *281*, 27862-27872.
- [125] C. Vincent, F. Borel, J. C. Willison, R. Leberman, M. Hartlein, *Nucleic Acids Res* **1995**, *23*, 1113-1118.
- [126] Y. Zeng, H. Roy, P. B. Patil, M. Ibba, S. Chen, *Antimicrobial Agents and Chemotherapy* **2009**, *53*, 4619-4627.
- [127] E. Weerapana, C. Wang, G. M. Simon, F. Richter, S. Khare, M. B. Dillon, D. A. Bachovchin, K. Mowen, D. Baker, B. F. Cravatt, *Nature* **2010**, *468*, 790-795.
- [128] M. B. Nodwell, H. Menz, S. F. Kirsch, S. A. Sieber, *Chembiochem* **2012**, *13*, 1439-1446.
- [129] J. M. Krysiak, J. Kreuzer, P. Macheroux, A. Hermetter, S. A. Sieber, R. Breinbauer, *Angew Chem Int Ed Engl* **2012**, *51*, 7035-7040.
- [130] L. Sun, F. T. Edelman, C. J. O. Kaiser, K. Papsdorf, A. M. Gaiser, K. Richter, *Plos One* **2012**, *7*, e33980.

I PUBLICATIONS

O. A. Battenberg, M. B. Nodwell, S. A. Sieber, *The Journal of Organic Chemistry* **2011**, 76, 6075-6087.

O. A. Battenberg, Y. Yang, S. H. L. Verhelst, S. A. Sieber, *Molecular BioSystems* **2013**, 9, 343-351.

J CURICULUM VITAE

Oliver Alexander Battenberg

geb. 19. Oktober 1983 in Marburg

Akademischer Werdegang

Seit 10/2009

Ludwig Maximilian Universität / Technische Universität München

Promotion am Lehrstuhl für organische Chemie II - Prof. Dr. Stephan A. Sieber:

Naturstoffderivate als molekulare Sonden im Activity Based Protein Profiling.

10/2003 - 12/2008

Philipps-Universität Marburg

Studium der Chemie, Abschluss Dipl. Chem.

Diplomarbeit am Lehrstuhl für organische Chemie – Dr. Markus Oberthür:

Synthese von Fluoreszenz- und Biotin-markierten Echinocandin-derivaten.

Schulausbildung

6/2003

Elisabethschule Marburg

Abitur